

UVM ScholarWorks

Impact of Subarachnoid Hemorrhage on Astrocyte Calcium Signaling: Implications for Impaired Neurovascular Coupling

Item Type	dissertation;article
Authors	Pappas, Anthony Christ
Download date	2026-06-17 00:56:07
Link to Item	https://hdl.handle.net/20.500.14849/4439

IMPACT OF SUBARACHNOID HEMORRHAGE ON ASTROCYTE CALCIUM
SIGNALING: IMPLICATIONS FOR IMPAIRED NEUROVASCULAR COUPLING

A Dissertation Presented

by

Anthony C. Pappas

to

The Faculty of the Graduate College

of

The University of Vermont

In Partial Fulfillment of the Requirements
for the Degree of Doctor of Philosophy
Specializing in Neuroscience

January, 2016

Defense Date: October 23, 2015
Dissertation Examination Committee:

George C. Wellman, Ph.D., Advisor
Jeffrey L. Spees, Ph.D., Chairperson
Victor May, Ph.D.
Joseph E. Brayden, Ph.D.
Mark T. Nelson, Ph.D.
Cynthia J. Forehand, Ph.D., Dean of the Graduate College

Abstract

Deficits within the brain microcirculation contribute to poor patient outcome following aneurysmal subarachnoid hemorrhage (SAH). However, the underlying pathophysiology is not well understood. Intra-cerebral (parenchymal) arterioles are encased by specialized glial processes, called astrocyte endfeet. Ca^{2+} signals in the endfeet, driven by the ongoing pattern of neuronal activity, regulate parenchymal arteriolar diameter and thereby influence local cerebral blood flow. In the healthy brain, this phenomenon, called neurovascular coupling (NVC), matches focal increases in neuronal activity with local arteriolar dilation. This ensures adequate delivery of oxygen and other nutrients to areas of the brain with increased metabolic demand. Recently, we demonstrated inversion of NVC from vasodilation to vasoconstriction in brain slices obtained from SAH model animals. This pathological change, which would restrict blood flow to active brain regions, was accompanied by an increase in the amplitude of spontaneous Ca^{2+} events in astrocyte endfeet. It is possible that the emergence of higher amplitude endfoot Ca^{2+} events shifts the polarity of NVC after SAH by elevating levels of vasoactive agents (e.g. K^+ ions) within the perivascular space. *In the first aim of this dissertation we tested whether altered endfoot Ca^{2+} signaling underlies the inversion of NVC after SAH.*

Brain injury is often associated with increased levels of extracellular purine nucleotides (e.g. ATP). A recent study found that ATP levels in the cerebrospinal fluid of aneurysmal SAH patients were roughly 400-fold higher than that of non-SAH controls. Astrocytes express a variety of purinergic (P2) receptors that, when activated, could trigger a spike in intra-cellular Ca^{2+} . It is possible that enhanced signaling via astrocyte P2 receptors underlies the change in endfoot Ca^{2+} signaling after SAH. *In the second aim of this dissertation we determined the role of purinergic signaling in the generation of high-amplitude spontaneous endfoot Ca^{2+} events after SAH.*

Parenchymal arteriolar diameter and endfoot Ca^{2+} dynamics were recorded simultaneously in fluo-4-loaded rat brain slices using combined infrared-differential interference contrast and multi-photon fluorescence microscopy. We report that SAH led to a time-dependent emergence of spontaneous endfoot high-amplitude Ca^{2+} signals (eHACSs) that were only present in brain slices exhibiting inversion of NVC. Depletion of intracellular Ca^{2+} stores abolished spontaneous endfoot Ca^{2+} signals, including eHACSs, and restored arteriolar dilation in SAH brain slices to two downstream elements in the NVC signaling cascade, (1) increased endfoot Ca^{2+} and (2) elevated extracellular K^+ . We next tested the role of purinergic signaling in the generation of SAH-induced eHACSs by recording endfoot activity before and after treatment with the broad-spectrum purinergic receptor antagonist, suramin. Remarkably, suramin selectively abolished eHACSs and restored vasodilatory NVC in SAH brain slices. Desensitization of Ca^{2+} -permeable ionotropic purinergic (P2X) receptors had no effect on eHACSs after SAH. However, eHACSs were selectively blocked using a cocktail of inhibitors targeting G_q -coupled purinergic (P2Y) receptors. Collectively, our results support a model in which SAH leads to an emergence of P2Y receptor-mediated eHACSs that cause inversion of NVC. Further, we identify the FDA-approved drug, suramin, as a potential therapy to be used in the treatment of aneurysmal SAH.

Citations

Material from this dissertation has been published in the following form:

Pappas, A.C., Koide, M., Wellman, G.C.. (2015) Astrocyte Ca^{2+} signaling drives inversion of neurovascular coupling after subarachnoid hemorrhage. J Neurosci, 35,13375-13384.

Material from this dissertation has been submitted for publication to the Journal of Cerebral Blood Flow and Metabolism on (Dec. 5th 2015) in the following form:

Pappas, A.C., Koide, M., Wellman, G.C.. (2015) Purinergic signaling triggers endfoot high-amplitude Ca^{2+} signals and causes inversion of neurovascular coupling after subarachnoid hemorrhage. J Cereb Blood Flow Metab (*submitted*).

Acknowledgements

Without a doubt, I owe a debt of gratitude to my advisor, Dr. George C. Wellman. He welcomed me into his lab in 2011 and has since guided me patiently through the years encouraging my best work along the way. I sincerely appreciate all of his effort and council. Dr. Wellman's high standard for excellence in science is extremely admirable and I am proud to leave here carrying that tradition onto my next step.

I would like to acknowledge the members of my dissertation committee: Drs. Spees, May, Brayden and Nelson, as well as the members of my qualifying exam committee: Drs. Jaworski and Cipolla. Collectively, their experimental and professional guidance have been an invaluable asset. My development as a scientist would have really been stifled without their input. Along these lines, I am extremely fortunate to have had the chance to work and train with Dr. Masayo Koide. She is a brilliant scientist that brings an unbelievably thorough perspective to the table. Watching Dr. Koide's mind analyze a problem has provided me with a first-rate example of scientific excellence. I consider my time spent with her a truly advantageous gift.

Lastly, I wish to express my gratitude to Drs. Nishi and Eckenstein for the influential role they played in directing the course of my life. In 2008 I had almost closed the door on neuroscience, but ended up joining Dr. Eckenstein's lab as a student in the SNURF program. My experiences in his lab instilled in me a sense of confidence and purpose. At the end of the program, Dr. Nishi offered me a full-time position in her lab. This provided me with the experience I needed to be accepted into a graduate program and undoubtedly put me on me on my current path. Thank you both so much.

Table of Contents

Citations	ii
Acknowledgements.....	iii
List of Figures.....	vi
List of Tables	vii
Chapter 1: Comprehensive Literature Review.....	1
Cerebral Blood Flow	1
Anatomy of the Cerebral Vasculature	1
Mechanisms Regulating Cerebral Blood Flow.....	2
Astrocytes and their Relationship to Intra-Cerebral Blood Vessels.....	4
Astrocyte Involvement in Neurovascular Coupling	5
Stroke	11
Definition and Classifications	11
Aneurysmal Subarachnoid Hemorrhage (SAH).....	11
Impact of SAH on the Intra-Cerebral Vasculature	13
Animal Models to Understand SAH Pathology	14
Astrocyte Ca ²⁺ signaling	18
Evoked vs Spontaneous Ca ²⁺ Signaling	18
Origin of Spontaneous Ca ²⁺ Signals in Astrocytes.....	20
Astrocyte Ca ²⁺ Signaling in Disease	22
Purinergic Signaling.....	25
Purine and Pyrimidine Nucleotides and their Receptors.....	25
Astrocyte Purinergic Signaling in Disease	26
References	31
Chapter 2: Astrocyte Ca ²⁺ signaling drives inversion of neurovascular coupling after subarachnoid hemorrhage.....	43
Abstract	44
Introduction	46
Materials and Methods	48
Results	53

The emergence of high-amplitude spontaneous Ca ²⁺ events in astrocyte endfeet (eHACSs) after SAH	53
The inversion of NVC parallels the emergence of eHACSs after SAH.....	55
Abolition of eHACSs restores vasodilatory responses in brain slices from SAH animals.....	57
Asymmetrical enlargement of perivascular astrocyte endfeet after SAH	59
Discussion	60
References	66
Chapter 3: Purinergic signaling triggers endfoot high-amplitude Ca ²⁺ signals and causes inversion of neurovascular coupling after subarachnoid hemorrhage	84
Abstract	85
Introduction	86
Materials and Methods	88
Results	90
Purinergic receptor inhibition abolishes SAH-induced eHACSs	90
Suramin restores vasodilatory NVC after SAH.....	91
P2Y receptors mediate SAH-induced eHACSs.....	92
Activation of P2Y receptors in brain slices from control animals mimics SAH.....	93
SAH-induced eHACSs occur independent of neurotransmitter release	94
Discussion	95
References	99
Chapter 4: Discussion and Future Directions	114
References	122
Comprehensive Bibliography	125

List of Figures

Figure 1-1. Two potential pathways driving neurovascular coupling.	28
Figure 1-2. Schematic depicting a mechanism whereby the increased amplitude of spontaneous endfoot Ca^{2+} events could lead to inversion of neurovascular coupling after SAH.	30
Figure 2-1. Emergence of endfoot high-amplitude Ca^{2+} signals (eHACS) following SAH	72
Figure 2-2. The inversion of NVC parallels the emergence of eHACSs in brain slices from SAH model animals.	74
Figure 2-3. The presence of eHACSs is associated with inversion of NVC.	76
Figure 2-4. Abolishing eHACSs restores arteriolar dilation in brain slices from SAH animals.....	78
Figure 2-5. Astrocyte endfeet with asymmetrical hypertrophy encase parenchymal arterioles following SAH.....	80
Figure 3-1. Inhibition of purinergic signaling with suramin selectively blocks SAH-induced eHACSs.....	105
Figure 3-2. Blocking eHACSs restores vasodilatory NVC after SAH.....	107
Figure 3-3. P2Y receptors mediate SAH-induced eHACSs.....	109
Figure 3-4. Activation of P2Y receptors in brain slices from control animals mimics SAH.....	111
Figure 3-5. Local neurotransmission is not involved in the generation of SAH-induced eHACSs.....	113

List of Tables

Table 2-1. Impact of SAH on spontaneous Ca ²⁺ events in astrocyte endfeet	81
Table 2-2. Impact of SAH on NVC	83

Chapter 1: Comprehensive Literature Review

Cerebral Blood Flow

Anatomy of the Cerebral Vasculature

Given its high metabolic demand and extremely limited energy reserves, the brain is one of the most highly perfused organs in the body. It is continually supplied with oxygen and nutrients by a dense network of capillaries and micro-vessels which, in humans, total about 400 miles in length (Begley and Brightman, 2003). In order to reach these rich capillary beds, oxygenated-blood from the heart is first pumped into the brain via two pairs of large arteries: the left and right internal carotid arteries, and the left and right vertebral arteries. The former diverge to become the left and right middle cerebral arteries (MCAs) and anterior cerebral arteries (ACA), respectively, whereas the latter converge on the surface of the pons to form the basilar artery. The vertebral-basilar system feeds the brainstem, cerebellum and posterior portions of the cerebrum. Collectively, the vertebral-basilar network comprises the posterior circulation of the brain, whereas the left and right MCAs and ACAs comprise the anterior circulation and supply the remaining neural tissue. Although blood flow between the anterior and posterior circulations is normally kept separate, there is a large anastomosis called the Circle of Willis located at the ventral surface of the brain which physically links the two networks.

There are some important differences between the arteries coursing over the brain surface and their penetrating branches that feed the underlying neurons. Firstly, the walls of brain surface (pial) arteries are comprised of multiple layers of circumferentially-

oriented vascular smooth muscle cells (Cipolla 2009). Even the smallest pial arteries and arterioles have from 2-3 layers of vascular smooth muscle. In contrast, penetrating and parenchymal arterioles have just a single layer of vascular smooth muscle. Another important contrast is that the walls of pial arteries and arterioles are innervated extrinsically by the peripheral nervous system (Baeres and Moller 2004; Hamel 2006). This innervation is lost as the brain-penetrating branches become parenchymal arterioles deep to the Virchow-Robin space (Cipolla et al., 2004; Cipolla 2009). Accordingly, the responsiveness of MCA-derived parenchymal arterioles to neurotransmitters such as serotonin and noradrenaline is significantly blunted when compared to the effects of these transmitters directly on the MCA (Cipolla et al., 2004). Perhaps the most profound distinction between pial and parenchymal arterioles is the near complete investment of parenchymal arterioles by astrocyte endfeet (McCaslin et al., 2011). The endfoot sheath surrounding parenchymal arterioles plays a very important role in regulating arteriolar diameter and thus, local cerebral blood flow (Filosa et al., 2015; Kim et al., 2015).

Mechanisms Regulating Cerebral Blood Flow

Continuous perfusion of the brain is essential for the maintenance of neuronal homeostasis and function. Two key mechanisms are in place to ensure that the brain remains adequately perfused under a variety of conditions: cerebral auto-regulation and neurovascular coupling (also known as functional hyperemia). Cerebral auto-regulation refers to the intrinsic property of the arterial wall to maintain constant blood flow by responding to increases and decreases in intraluminal pressure by constricting and dilating, respectively. This remarkable property, called myogenic tone, was first

described over a hundred years ago by the English physiologist, William Bayliss (Bayliss, 1902), and the mechanisms by which this occurs in the brain have only recently begun to be elucidated. Currently, the prevailing theory is that pressure-induced stretch activates G-coupled purinergic receptors (in the case of parenchymal arterioles) on the smooth muscle membrane leading to Na^+ influx via transient receptor potential melastatin 4 (TRPM4) channels (Brayden et al., 2013; Li et al., 2014). The activation of TRPM4 causes smooth muscle depolarization, Ca^{2+} influx through voltage-dependent Ca^{2+} channels (VDCCs) and activation of the contractile apparatus. This cerebral auto-regulatory mechanism ensures constant blood flow over a range of physiologic pressures and also serves to protect downstream capillaries from drastic changes in blood flow which would occur in the absence of myogenic tone.

Aside from cerebral auto-regulation, the brain possesses the unique ability to redirect blood flow according to ongoing changes in neuronal metabolic demand. Interestingly, this process, called neurovascular coupling, was first noted by Roy and Sherrington (1890) well before the auto-regulatory phenomenon had been observed. In their classic study, Roy and Sherrington (1890) measured volume expansion of the canine brain during peripheral nerve stimulation, and reported that brief stimulation of the sciatic nerve reliably evoked an immediate increase in cerebral volume. This transient expansion of the brain paralleled a rise in arterial pressure suggesting that increased neuronal activity was tightly coupled to increased cerebral blood flow. Notably, the evoked cerebral volume expansion was observed under a variety of conditions including stimulation of the medulla oblongata and spinal cord. It was even evident during volitional movement of the lightly anesthetized animal. Although this rudimentary study

was unable to address the mechanistic pathway involved, it succeeded in advancing the notion that neuronal activity and cerebral blood flow are functionally linked. Importantly, this study helped lay the groundwork for a concept (i.e. neurovascular coupling) which would later form the basis of functional magnetic resonance imaging (fMRI).

Astrocytes and their Relationship to Intra-Cerebral Blood Vessels

Investment of local synapses as well as the intra-cerebral vasculature by cortical astrocytes was first described over a century ago by the renowned neuroanatomist, Santiago Ramon y Cajal (Navaerrete and Araque, 2014). This structural arrangement between astrocyte endfeet and nearby blood vessels has since been confirmed using more conventional methods, such as transmission electron microscopy and *in vivo* multiphoton imaging (Mathiisen et al., 2010; McCaslen et al., 2011). Interestingly, early analyses of astrocyte biophysical properties suggested that the functional significance of this arrangement served to protect neuronal elements by shunting the increase in extracellular K^+ ions that accompanies enhanced synaptic transmission to distant areas with lower K^+ levels (Trachtenburg and Pollen, 1970). Later work by Newman (1984) expanded on this theme by demonstrating substantial K^+ conductance in astrocyte endfeet which could be stimulated by an elevation of extracellular K^+ at distal cellular processes. Remarkably, the evoked K^+ conductance exhibited by the endfeet was roughly 10-fold higher than that of the rest of the cell (Newman, 1986). These observations ultimately led the investigators to pose the question of whether the K^+ released from astrocyte

endfeet in response to enhanced neurotransmission plays a role in the regulation of local cerebral blood flow (Paulson and Newman, 1987).

Unfortunately, however, this concept was ahead of its time. Before the matter was directly addressed in the study by Filosa et al. (2006) a number of important observations were made which helped bolster our understanding of the signaling dynamics between neurons and astrocytes. The first major discovery was that of intra- and inter-cellular Ca^{2+} waves in cultured astrocyte networks exposed to the excitatory neurotransmitter, glutamate (Cornell-Bell et al., 1990). The observation that glutamate evoked astrocyte Ca^{2+} waves that often spread between cells, was the first indication that local synaptic activity could elicit long-range signaling in nearby astrocytes. Importantly, this concept was confirmed by subsequent work demonstrating similar Ca^{2+} elevations in hippocampal astrocytes *in situ* following brief stimulation of the Schaffer collaterals (Porter and McCarthy, 1996); the principle excitatory input to the hippocampus. The elevation of astrocyte Ca^{2+} in these studies was suggested to be due to spillover of glutamate from the synaptic cleft activating ionotropic and metabotropic glutamate receptors on astrocyte processes. This possibility was supported by the later work of Shelton and McCarthy (1999) who showed that astrocyte Ca^{2+} elevations could be evoked by treating brain slices with the group I/II metabotropic glutamate receptor agonist, t-ACPD.

Astrocyte Involvement in Neurovascular Coupling

Considering the anatomical arrangement of astrocytes, with some processes enveloping neuronal synapses and others wrapping around the intra-cerebral vasculature

(i.e. endfeet), it was only natural to ask whether a link existed between neuronal activity-evoked astrocyte Ca^{2+} elevations and the regulation of local cerebral blood flow. Taking advantage of the *ex vivo* brain slice preparation, which preserves the unique architecture of astrocytes, Zonta et al (2002) clearly demonstrated that neuronal stimulation triggered astrocyte endfoot Ca^{2+} elevations which preceded vasodilation of the underlying arteriole. Further, consistent with previous studies, treatment of brain slices with a metabotropic glutamate receptor antagonist, MPEP, significantly blunted the neurally-evoked endfoot Ca^{2+} elevations as well as arteriolar dilation. Conversely, application of the metabotropic glutamate receptor agonist, t-ACPD, triggered a rise in endfoot Ca^{2+} that preceded arteriolar dilation. Expanding on this work, Winship et al. (2007) confirmed these results *in vivo* by demonstrating rapid, neuronal activity-dependent Ca^{2+} signals in cortical astrocytes which preceded the hyperemic response. Together, these studies comprised the first demonstration of an essential role for astrocyte Ca^{2+} signaling in linking neuronal activity with increased local cerebral blood flow. However, it should be noted that in the decades prior to these studies, the prevailing theory behind neurovascular coupling was that direct innervation of the vascular wall contributed to the coordination of local blood flow with neuronal function (Reinhard et al., 1979; Vaucher and Hamel, 1995; Krimer et al., 1998). While this theory has lost support over the years, the existence of a neuronal component to neurovascular coupling cannot be totally ruled out.

To this day there is dissent as to the vasoactive factor(s) that are released from the endfeet during neurovascular coupling. Generally speaking, there are 2 major Ca^{2+} -dependent pathways which could be recruited in the endfeet following neuronal activation (Fig. 1). The first of these pathways, which gained popularity early on,

involves Ca^{2+} -dependent cleavage of arachidonic acid (AA) from the endfoot membrane by phospholipase A₂ (PLA₂) (Koehler et al, 2009). Early work using primary cultures of astrocytes obtained from 3-day-old rat pups showed that exposure to glutamate mobilized AA and resulted in the release of one of its metabolites, epoxyeicosatrienoic acids (EETS) (Alkayed et al., 1997). EETs are potent dilators of brain surface arteries and exert their effect by enhancing K^+ efflux from vascular smooth muscle cells (Gebremedhin et al., 1992). Formation of EETs from AA requires the action of cytochrome P-450 (P-450) 2C11, an enzyme which has been shown to be expressed by cortical astrocytes (Alkayed et al., 1996). Interestingly, treatment of pial arteries with another AA metabolite, 20-hydroxyeicosatetraenoic acid (20-HETE), caused vasoconstriction by inhibiting smooth muscle K^+ channel activity (Harder et al., 1994). Contrary to EETs, the generation of 20-HETE from AA occurs via the action of P-450 4-A. Harder et al (1994) demonstrated functional expression of P-450 4-A in cerebral vascular smooth muscle cells isolated from cats. In a perplexing, yet high-profile study by Mulligan and MacVicar (2004), elevation of astrocyte endfoot Ca^{2+} by photolysis of caged- Ca^{2+} (uncaging) caused vasoconstriction of the underlying blood vessel. Based on their pharmacologic approach, the investigators concluded that the endfoot Ca^{2+} elevation activated Ca^{2+} -sensitive PLA₂ leading to the release of AA from the endfoot membrane. According to their model, the liberated AA then diffused across the perivascular space entering the vascular wall where it was metabolized into the vasoconstrictor, 20-HETE, by P-450 4-A. It is important here to mention that the brain slices used in these studies were not pretreated with a vasoconstrictive agent. Thus, as the vasculature in their preparation was unpressurized, it

is likely that the vessels were maximally dilated at baseline. This complicates things, as the only response that could be measured, based on their conditions, is vasoconstriction.

There is yet a third class of vasoactive AA metabolites which has been suggested to play a role in neurovascular coupling; the prostaglandins (Haydon and Carmignoto 2006). In a study by Zonta et al (2003) it was discovered that the glutamate-induced elevation of intracellular Ca^{2+} elevation led to the release of prostaglandin E_2 (PGE_2) from astrocytes *in vitro*. Astrocytes express the cyclooxygenase-2 (COX-2) enzyme which is responsible for the conversion of AA to PGE_2 (Hirst et al., 1999). Interestingly, despite the attention and recognition PGE_2 has received for its alleged vasodilatory influence during neurovascular coupling (Attwell et al., 2010), recent work demonstrated that PGE_2 actually constricts parenchymal arterioles isolated from the rodent brain (Dabertrand et al., 2013). This would argue against the involvement of astrocyte-derived PGE_2 in linking neuronal activity to increased local cerebral blood flow.

Given the confounding results and complex mechanism(s) by which astrocyte-derived AA is thought to impact the local intra-cerebral vasculature during neurovascular coupling, it is difficult to reconcile this pathway with the rapid and highly reproducible vasodilatory responses exhibited by parenchymal arterioles *in vivo* (Winship et al., 2007).

The second Ca^{2+} -dependent pathway which could be recruited into neurovascular coupling brings us back to the original proposition by Paulson and Newman (1987). That is, astrocyte-mediated K^+ release establishes the link between increased neuronal activity and enhanced local cerebral blood flow. Cerebral arteries are extremely sensitive to changes in the extracellular K^+ concentration. Modest increases in extracellular K^+ (≤ 20 mM) dilate cerebral arteries and parenchymal arterioles by activating inward rectifier K^+

(Kir) channels on vascular smooth muscle (Knot et al., 1996; Zaritsky et al., 2000; Filosa et al., 2006; Girouard et al., 2010). Conversely, larger increases in extracellular K^+ (> 20 mM) depolarize the smooth muscle membrane leading to enhanced Ca^{2+} influx through VDCCs and vasoconstriction. Large-conductance Ca^{2+} -activated K^+ (BK) channels are enriched in the endfoot membrane abutting parenchymal arteriolar smooth muscle (Price et al., 2002). Astrocytes express the $\beta 4$ subunit which confers profound Ca^{2+} sensitivity to the BK channels (Horrigan and Aldrich, 2002; Bai et al., 2011; Seidel et al., 2011). As parenchymal arteriolar dilation occurs within seconds of an evoked rise in endfoot Ca^{2+} (Takano et al., 2006), Filosa et al. (2006), tested whether endfoot BK channels are recruited into the neurovascular coupling signaling cascade. Using on-cell patch clamp electrophysiology, Filosa et al. (2006) clearly demonstrated robust iberiotoxin-sensitive BK currents in the endfeet following neuronal activation. Thus, during neurovascular coupling, BK-dependent K^+ efflux could conceivably impact blood vessel diameter by directly affecting the smooth muscle membrane potential. This would be consistent with the rapid responses of parenchymal arterioles (1-2 second latency) to increased endfoot Ca^{2+} (Takano et al., 2006).

Elevation of extracellular K^+ can cause either dilation or constriction depending on the concentration (Knot et al., 1996). In a clever study demonstrating the duality of arteriolar responses to elevated K^+ , Girouard et al. (2010) showed that evoking a modest rise in endfoot Ca^{2+} (300-400 nM) caused the anticipated vasodilation, whereas evoking larger increases in endfoot Ca^{2+} (> 700 nM) caused vasoconstriction. Interestingly, Girouard et al (2010) also showed that arteriolar constriction could be evoked by raising endfoot Ca^{2+} modestly (300-400 nM) in the presence of artificially elevated extracellular

K^+ . Importantly, both the evoked dilations and constrictions were abolished in the presence of the BK channel blocker, paxilline. These data not only highlight endfoot-derived K^+ as a key mediator of neurovascular coupling, they also show that polarity of the arteriolar response depends on the amount of K^+ released (i.e. the amplitude of the endfoot Ca^{2+} transient).

At present, the pathways involved in neurovascular coupling are still under scrutiny. For example, the identity of the vasoactive agent released from the endfeet during neurovascular coupling continues to be debated. Further, recent advances in genetic manipulation techniques (e.g. knock-outs and designer receptors exclusively activated by designer drugs [DREADS]) have shaken the field and questioned the role of astrocyte Ca^{2+} signaling in mediating neurovascular coupling (Nizar et al., 2013; Bonder and McCarthy, 2014). Despite these setbacks, however, it seems that even in a mouse model in which astrocytes allegedly lack inositol 1,4,5-trisphosphate (IP_3) dependent Ca^{2+} signals, both endfoot Ca^{2+} signaling and neurovascular coupling are retained (Srinivasan et al., 2015). Currently, the field of neurovascular coupling is also even beginning to explore the potential role of the vascular endothelium in mediating the upstream arteriolar dilation (Chen et al., 2014). It is possible that endothelial Kir channels sense ongoing changes in local K^+ and send a hyperpolarizing electrical signal through the capillary network to dilate upstream arterioles (Longden and Nelson, 2015). Importantly, it is likely that for such a critical phenomenon as neurovascular coupling, there will be multiple, redundant pathways to ensure adequate delivery of oxygen-rich blood to areas of the brain with increased metabolic demand.

Stroke

Definition and Classifications

Strokes, often referred to as cerebrovascular accidents, occur following a pathological disruption of blood flow to the brain that results in neuronal cell death. Broadly, strokes are classified into two subtypes: ischemic and hemorrhagic. In the case of ischemic strokes, blood flow to the brain, or parts of the brain, is disrupted by a physical barrier, often a blood clot. Ischemic strokes are the most common form of stroke and recent work has actually demonstrated a reduction in age-standardized mortality rates over the past two decades for ischemic stroke patients (Bennett et al., 2009). Conversely, hemorrhagic strokes, which include both intra-cerebral hemorrhage (ICH) and subarachnoid hemorrhage (SAH), are much less prevalent (~ 10-27% of all strokes) yet both have 30-day mortality rates at nearly 50% (Feigin et al., 2009; Krishnamurthi et al., 2014).

Hemorrhagic strokes, as the name implies, involve massive bleeding following the rupture of a cerebral blood vessel. This bleeding can occur within the brain parenchyma, in the case of ICH, or within the subarachnoid space, as in SAH. For the purposes of this dissertation, we will focus primarily on SAH.

Aneurysmal Subarachnoid Hemorrhage (SAH)

The rupture of a “saccular” cerebral aneurysm, an acquired vascular abnormality causing protrusion of the arterial wall, accounts for 80-85% of spontaneous, non-traumatic SAH strokes (Jakubowski and Kendall, 1978). Cerebral aneurysms typically form at the base of the brain near branch points close to the Circle of Willis (Ajiboye et

al., 2015). The incidence of cerebral aneurysms in adults is estimated between 1-5% (Mocco et al., 2004), yet aneurysm rupture is quite rare; affecting only about 30,000 people annually in the United States (Peters et al., 2001). Following aneurysmal rupture, high-pressure arterial blood is released into the subarachnoid space (i.e. SAH) where it can spread over the brain surface. As mentioned, this form of stroke carries a relatively high mortality rate and only about half of long-term survivors regain independence for daily life (Passier et al., 2012).

A major hurdle affecting survival and functional outcome after aneurysmal SAH is the development of delayed cerebral ischemia (DCI) days to weeks after the initial bleed (Al-Khindi et al., 2010; Ostergaard et al., 2013). DCI presents either as cerebral infarction within a single territory close to the site of aneurysm rupture, multiple independent lesions scattered throughout the brain, or a combination of both (Dreier et al., 2002; Rabinstein et al., 2005; Weidauer et al., 2008). Historically, the prolonged, blood-induced constriction of large-diameter pial arteries (i.e. vasospasm) was thought to underlie the development of DCI after SAH (Pluta et al., 2009). This is largely because the development of SAH-induced vasospasm, occurring 3-8 days post-stroke, often coincides with the onset of DCI (Weir et al., 1978). However, recent clinical trials using the endothelin receptor inhibitor, Clazosentan, have demonstrated effective prevention of vasospasm, yet failed to significantly improve patient outcome (Macdonald et al., 2011; Macdonald et al., 2012). Importantly, this indicates that vasospasm is not the sole cause of DCI after SAH. Further, these negative results have redirected the focus of SAH research to other mechanisms that could conceivably play a role in the development of DCI.

Impact of SAH on the Intra-Cerebral Vasculature

Currently, the prevailing theory is that a disruption of blood flow within the brain parenchyma after SAH contributes to the development of DCI by restricting O₂ delivery to discrete brain territories. This idea is attractive; as it is consistent with the fact that angiographic vasospasm often fails to predict the pattern of subsequent brain infarction in SAH patients (Rabinstein et al., 2005; Weidauer et al., 2008). Further, the arterial networks on the brain surface exhibit substantial anastomoses and redundancy which are protective in case of small vessel occlusion (Vander Eecken and Adams, 1953). In contrast, parenchymal arterioles lack such collateral flow (Nishimura et al., 2010). Each arteriole feeds a specific domain within the cortex and there is little overlap in the territories supplied by neighboring vessels. Thus, disruption of blood flow through one or more adjacent parenchymal arterioles would be predicted to cause a spatially-defined focal infarct, similar to what is observed in the human brain following SAH (Dreier et al., 2002; Rabinstein et al., 2005; Weidauer et al., 2008).

The idea that blood flow through distal arterioles (in relation to brain surface arteries) is hemodynamically important after SAH is not necessarily new. Descriptions of this concept can be found in early reports of altered cerebral blood flow almost 50 years ago (Zingesser et al., 1968; Heilbrun et al., 1972). Heilbrun et al. (1972) even suggested that auto-regulatory dysfunction in the small-diameter arterioles could lead to focal ischemia after SAH by reducing blood flow beyond some critical threshold. Interestingly, more recent work implicates impairment in metabolically-driven changes in intra-cerebral blood flow (i.e. functional hyperemia, or neurovascular coupling) in aneurysmal SAH patients (Dreier et al., 2009). In this study, the investigators

simultaneously measured brain electrical activity and regional cerebral blood flow using direct current-electrocorticography and laser Doppler flowmetry, respectively. The authors found that cortical spreading depolarizations (CSDs), which involve a mass neuronal depolarization followed by a quiescent recovery period, were sometimes accompanied by a physiologic hemodynamic response (i.e. increased blood flow and tissue hyperoxia) or an inverse hemodynamic response (decreased blood flow and tissue hypoxia). Importantly, clusters of prolonged CSDs, which were associated with inverse hemodynamic responses, occurred in regions exhibiting neuronal damage. These data indicate a possible link between inverse hemodynamic responses (i.e. neuronal activity-dependent vasoconstriction) and the development of focal brain injury in patients following aneurysmal SAH.

Animal Models to Understand SAH Pathology

Understanding the impact of SAH on intra-cerebral hemodynamics is difficult given the technical limitations for human studies. However, the use of animal models has provided a great advantage in our ability to discern the mechanisms leading to vascular dysfunction and the development of DCI following SAH. The breadth of animal models ranges from rodents to non-human primates. For the purposes of this dissertation, we will focus primarily on the rat intra-cisternal double injection SAH model. Although this model has been modified from the original (Solomon et al., 1985) by including a second SAH induction (usually following a 24-48 hour recovery period), it is frequently used as it reliably recapitulates the delayed vasospasm observed in SAH patients (Vatter et al., 2006). Briefly, autologous arterial blood is introduced into the subarachnoid space of

anesthetized animals by way of the cisterna magna. Typically, the animals are then allowed to recover for 24 to 48 hours, after which the procedure is repeated. One limitation is that this model does not mimic the arterial wall damage accompanying a ruptured aneurysm. However, it is still preferred over vascular perforation models as the blood volume entering the subarachnoid space is under the experimenter's control.

Using experimental models of SAH, such as the ones described above, we now know that the presence of subarachnoid blood has a profound impact on parenchymal arteriolar function. *Ex vivo* studies using animal models of SAH have demonstrated enhanced myogenic tone and decreased sensitivity to endothelial-derived vasodilators in isolated parenchymal arterioles (Park et al., 2009; Nystoriak et al., 2011). Given that brain parenchymal arterioles account for roughly 40% of the total cerebrovascular resistance (Faraci and Heistad, 1990), the enhanced tone in these blood vessels after SAH could significantly limit cerebral perfusion on a global scale. This interpretation would be consistent with the early observations by Heilbrun et al. (1972), who noted a decrease in global cerebral blood flow in SAH patients even in the absence of angiographic vasospasm.

It is possible that extravasated blood components, such as oxyhemoglobin, could cause enhanced tone after SAH by altering expression of key ion channels on parenchymal arteriolar myocytes. Acute exposure of pial arteries to oxyhemoglobin led to enhanced pressure-dependent constriction by suppressing voltage-dependent K^+ (K_v) channels on vascular smooth muscle (Ishiguro et al., 2006). Further, culturing pial arteries for five days in the presence of the blood component, oxyhemoglobin, resulted in functional expression of the R-type VDCC (Link et al., 2008). Importantly, upregulation

of the R-type VDCC contributed to the myogenic tone of these arteries. Although the studies above addressed SAH-induced changes in brain surface arteries, they have helped pave the way for elucidating the impact of SAH on parenchymal arterioles. Accordingly, studies have shown that parenchymal arteriolar myocytes isolated from SAH model animals exhibit suppression of K_v channels (Koide and Wellman, 2013). Importantly, K_v suppression in parenchymal arterioles appears to involve the same oxyhemoglobin-mediated endocytic pathway causing K_v suppression in pial artery myocytes (Koide et al., 2007). To date, however, it remains to be determined whether parenchymal arteriolar myocytes express R-type VDCCs after SAH.

The above mechanisms, which affect parenchymal arteriolar auto-regulation, would be expected to negatively impact blood flow in the brain on a global level by increasing the total cerebrovascular resistance. However, as mentioned previously, blood flow through parenchymal arterioles is also regulated extrinsically by surrounding astrocyte endfeet in a phenomenon called, neurovascular coupling. Human studies have already provided evidence demonstrating an inverse coupling between neuronal activity and local cerebral blood flow after SAH (Dreier et al., 2009). Importantly, this deficit is also present in the rat double injection SAH model. Recent work demonstrated inversion of neurovascular coupling from vasodilation to vasoconstriction in brain slices obtained from SAH model animals (Koide et al., 2012). As mentioned, neurovascular coupling is dependent on neurally-evoked elevation of endfoot Ca^{2+} causing release of vasoactive agents (such as K^+ ions) into the perivascular space (Straub and Nelson, 2007). Importantly, Koide et al. (2012) demonstrated that the opposing vascular responses between control and SAH animals (i.e. dilation and constriction) were both abrogated in

the presence of the BK channel blocker, paxilline. This suggests that elevation of extracellular K^+ mediates both the dilation in control animals and the constriction after SAH. Further, this study demonstrated that the dilation and constriction were retained even when endfoot Ca^{2+} was elevated experimentally by photolysis of caged- Ca^{2+} ; a technique that bypasses neuronal activation. This indicates that the inversion of neurovascular coupling after SAH reflects abnormal signaling between the astrocyte endfeet and underlying parenchymal arterioles.

The investigators made another interesting observation in this study; an increase in the amplitude of spontaneous Ca^{2+} events in astrocyte endfeet surrounding parenchymal arterioles. Importantly, the increased amplitude of spontaneous Ca^{2+} events after SAH was suggested to cause an abnormal elevation of perivascular K^+ that, when combined with K^+ efflux stimulated by neuronal activity or endfoot Ca^{2+} uncaging, raised perivascular K^+ beyond the dilation/constriction threshold (Fig. 2). This interpretation would be consistent with previous work by Girouard et al. (2010) which showed that artificially raising the pre-existing K^+ concentration resulted in a reversal of neurovascular coupling from vasodilation to vasoconstriction in brain slices from healthy control animals. Further, this interpretation is significant because the concept of a functional change in astrocytes leading to a vascular deficit after SAH had not been previously considered. Determining the role of spontaneous astrocyte Ca^{2+} signaling in mediating a disturbance in local cerebral blood flow will profoundly impact our understanding of the adverse events following SAH. *The first aim of this dissertation is to determine whether altered Ca^{2+} signaling in astrocyte endfeet underlies SAH-induced inversion of neurovascular coupling.*

Astrocyte Ca²⁺ signaling

Evoked vs Spontaneous Ca²⁺ Signaling

Astrocytes are incapable of firing action potentials, but rather, they signal to neighboring cells using a special form of Ca²⁺ excitability (Verkhratsky et al., 1998). Astrocyte Ca²⁺ signaling can be triggered by a variety of manipulations including: exposure to endogenous ligands (e.g. glutamate, histamine, and ATP) (Cornell-Bell et al., 1990; Kirischuk et al., 1995; Shelton and McCarthy, 2000), electrical stimulation (Nedergaard, 1994), and mechanical stretch (Newman and Zahs, 1997). The responsiveness of astrocytes to these environmental signals highlights their role in sensing and maintaining CNS homeostasis.

Shortly after the discovery that neurotransmitters such as glutamate evoke astrocyte Ca²⁺ elevations (Cornell-Bell et al., 1990), it was discovered that astrocytes in culture exhibit spontaneous fluctuations in intra-cellular Ca²⁺ in the absence of neuronal input (Fatatis and Russell, 1992). This early work sparked considerable interest in determining the nature and functional consequences of spontaneous astrocyte Ca²⁺ signaling. In their now classic study, Parri et al. (2001) first proposed the concept that astrocytes not only sense ongoing neurotransmission, but that they can also act as generators of neuronal activity through spontaneous fluctuations in intracellular Ca²⁺. By combining patch clamp electrophysiology with brain slice Ca²⁺ imaging, the investigators demonstrated that asynchronous, spontaneous (i.e. non-stimulated) intra- and inter-cellular astrocyte Ca²⁺ waves triggered NMDA receptor-mediated currents in adjacent

neurons. A similar approach by Fiacco and McCarthy (2004) demonstrated astrocyte Ca^{2+} signal-dependent AMPA receptor currents in adjacent neurons. These thought-provoking studies sparked a massive interest in linking spontaneous astrocyte Ca^{2+} signaling to neuronal physiology. As a result, we now know that astrocyte spontaneous Ca^{2+} signaling contributes to synaptic plasticity (Henneberger et al. 2010; Navarrete et al., 2012; Chen et al., 2013), neurotransmitter release (Perea and Araque, 2007), and network activity (Angulo et al., 2004). Further, it is likely that the same astrocyte-to-neuron signaling pathways, which were largely explored in rodent brains, are relevant to the human condition. Using biopsies from human epileptic patients, Navarrete et al. (2013) showed convincing evidence that astrocyte Ca^{2+} signals could increase the frequency of NMDA receptor-mediated currents in neighboring cortical or hippocampal neurons.

While the bulk of the work has examined spontaneous Ca^{2+} signaling in astrocyte somata or perisynaptic processes, it should be noted that astrocyte endfeet also exhibit spontaneous Ca^{2+} events in the absence of neuronal stimulation (Koide et al., 2012; Dunn et al., 2013; Shigetomi et al., 2013). Currently, there is little known about these spontaneous endfoot Ca^{2+} oscillations. However, it is possible that endfoot Ca^{2+} signaling could influence neurovascular coupling by altering levels of vasoactive substances (e.g. K^+ ions) within the restricted perivascular space, as was suggested to occur following SAH (Koide et al., 2012).

Ca^{2+} -permeable TRP Vanilloid 4 (TRPV4) channels are functionally expressed on astrocyte endfeet (Benfenati et al., 2007). Dunn et al. (2013) demonstrated that pharmacologic activation of endfoot TRPV4 channels resulted in a transient increase in

the frequency and amplitude of spontaneous endfoot Ca^{2+} events *in situ*. Interestingly, pharmacologic inhibition of endfoot TRPV4 activity abrogated neurovascular coupling responses (both endfoot Ca^{2+} elevation and arteriolar dilation) *in situ* and *in vivo*. These data suggest a possible role for endfoot TRPV4 channels during neurovascular coupling in healthy control animals. To determine whether aberrant TRPV4 activity contributed to the increased amplitude of spontaneous endfoot Ca^{2+} events and inversion of neurovascular coupling after experimental SAH, Koide and Wellman (2015) recorded these phenomena in brain slices obtained from SAH animals before and after treatment with a selective TRPV4 inhibitor. The investigators found no effect of TRPV4 inhibition on the altered Ca^{2+} signals or inverted neurovascular coupling responses after SAH.

To date, the studies by Dunn et al. (2013) and Koide and Wellman (2015) represent the only attempts to elucidate the role of spontaneous endfoot Ca^{2+} signaling on local blood flow regulation in brain cortex. Thus, determining whether the increased amplitude of spontaneous endfoot Ca^{2+} events drives inversion of neurovascular coupling after SAH will not only resolve a potential pathway involved in SAH pathology, it may also identify another role for endogenous astrocyte Ca^{2+} signaling in the brain.

Origin of Spontaneous Ca^{2+} Signals in Astrocytes

Astrocyte Ca^{2+} signals, whether evoked or spontaneous, are generally appreciated to result from the release of Ca^{2+} from subcellular IP_3 -dependent ER stores (Cornell-Bell et al., 1990; Shao and McCarthy, 1995; Nett et al., 2002; Parri and Crunelli, 2003; Straub et al., 2006). Astrocytes express a multitude of Ca^{2+} -permeable ion channels (e.g. TRPV4) and G_q -coupled receptors that, when activated, could trigger Ca^{2+} release from

the ER. Early studies examining spontaneous astrocyte Ca^{2+} signaling in the developing ventrobasal thalamus attributed a Ca^{2+} -induced Ca^{2+} release (CICR) pathway involving Ca^{2+} influx through voltage-dependent Ca^{2+} channels (VDCCs) triggering subsequent Ca^{2+} release through subcellular IP_3 receptors (IP_3Rs) (Parri et al., 2001; Parri and Crunelli, 2003). However, the expression of VDCCs in astrocytes is controversial. Currently, the only evidence for VDCC expression in astrocytes comes from studies examining cultured cells (MacVicar, 1984; MacVicar et al., 1991; Latour et al., 2003). Aside from the few studies examining astrocytes of the developing thalamus (Parri et al., 2001; Parri and Crunelli, 2003), there is no evidence of VDCCs in hippocampal or cortical astrocytes *in situ* (Carmignoto et al., 1998). It is possible that VDCC expression in astrocytes is location-specific and/or developmentally regulated. We learned earlier that activation of TRPV4 channels could transiently increase the amplitude and frequency of spontaneous endfoot Ca^{2+} events (Dunn et al., 2013). This effect was mediated by CICR in the endfeet. However, inhibition of TRPV4 channels did not block the basal events suggesting that spontaneous endfoot Ca^{2+} activity occurs independent of TRPV4 channels.

A thorough characterization of the mechanism underlying the generation of spontaneous astrocyte Ca^{2+} signals was provided in an early study by Nett et al. (2002). These investigators ruled out the possibility that basal neuronal activity contributed to the generation of astrocyte Ca^{2+} events by recording astrocyte Ca^{2+} activity in the presence of tetrodotoxin (TTX) or Bafilomycin A1. TTX blocks the generation of neuronal action potentials by inhibiting fast Na^+ channels on neurons. Bafilomycin prevents the filling of synaptic vesicles with neurotransmitter by inhibiting the vacuolar H^+ -ATPase pump

(Zhou et al., 2000). In both cases, spontaneous astrocyte Ca^{2+} signals persisted in the absence of neurotransmitter release arguing against a role for neuronal input in the generation of astrocyte Ca^{2+} signals. To examine the possibility that ambient levels of extracellular glutamate or ATP could trigger these apparently endogenous glial Ca^{2+} signals, Nett et al. (2002) recorded astrocyte Ca^{2+} activity before and after treatment with a cocktail of antagonists targeting metabotropic glutamatergic and purinergic receptors. As mentioned, both glutamate and ATP had been shown previously to trigger Ca^{2+} increases in astrocytes (Cornell-Bell et al., 1990; Kirischuk et al., 1995). Interestingly, bath application of these inhibitors had no effect on spontaneous astrocyte Ca^{2+} events. Based on these data, the authors concluded that the generation of spontaneous Ca^{2+} signals represents an intrinsic property of astrocytes that may function to modulate local neuronal activity. It should be noted here that the authors focused primarily on events within astrocyte somata and perisynaptic processes. There was no mention of spontaneous activity in perivascular endfeet.

Astrocyte Ca^{2+} Signaling in Disease

Given the role of spontaneous astrocyte Ca^{2+} signaling in modulating neurophysiology in the healthy brain, it stands to reason that aberrant astrocyte Ca^{2+} signals may be causally linked to brain dysfunction after injury or disease. This concept is heavily supported by the literature. Rodent models of epilepsy, Alzheimer's disease and SAH have all reported changes in astrocyte Ca^{2+} signaling which are thought to contribute to the pathogenesis of their respective diseases. For example, in a study measuring paroxysmal depolarization (PDS) of hippocampal neurons *in situ*, a

phenomenon involved in triggering epileptiform discharges, Tian et al. (2005) demonstrated strong evidence that aberrant astrocyte Ca^{2+} signaling preceded the generation of PDS in nearby clusters of neurons. The authors subsequently confirmed this finding *in vivo* by simultaneously measuring astrocyte Ca^{2+} signals and extracellular field potentials in anesthetized animals. Going one step further, the investigators then showed that pre-treatment of animals with antiepileptic drugs suppressed astrocyte Ca^{2+} oscillations and reduced seizure-like events.

The early stages of Alzheimer's disease (AD) is accompanied by an impairment in neuronal activity-dependent vasodilation (i.e. neurovascular coupling) (Farkas and Luiten, 2001; Takano et al., 2007). Consistent with a role for astrocyte endfoot Ca^{2+} signaling mediating local blood flow changes during neurovascular coupling, Takano et al. (2007) found that young (2-4 months old) AD model mice exhibiting such vascular instability also showed an increased frequency of spontaneous Ca^{2+} oscillations in cortical astrocytes. Deposition of amyloid β along the walls of intra-cerebral microvessels occurs early in AD model mice (Davis et al., 2004). Takano et al. (2007) showed that treatment of mice with amyloid β caused a time-dependent increase in astrocyte Ca^{2+} signaling. A more recent study expanded on these findings and demonstrated that the hyperactive Ca^{2+} signaling phenotype exhibited by astrocytes in AD could be normalized by inhibition of the G_q -coupled metabotropic purinergic receptor, P2Y_1 (Delekate et al., 2014). Based on these data, it would appear that early deposition of amyloid β causes P2Y_1 -mediated enhancement of astrocyte Ca^{2+} signaling and disrupted neurovascular coupling. It is likely that these deleterious changes subsequently lead to neurodegeneration and cognitive decline; the hallmarks of AD.

In a rat model of aneurysmal SAH, Koide et al. (2012) found both an increase in the amplitude of spontaneous Ca^{2+} events in perivascular astrocyte endfeet and inversion of neurovascular coupling from vasodilation to vasoconstriction. Although a causal link between these two phenomena has yet to be established, the functional consequences observed in the SAH model (increased amplitude of spontaneous Ca^{2+} events and inversion of neurovascular coupling) bear a striking resemblance to that which occurs early in AD. Thus, it is possible that pathological changes in spontaneous astrocyte Ca^{2+} signaling precede the disruption of cerebral hemodynamics following SAH.

Astrocytes typically respond to CNS injury by undergoing a characteristic hypertrophy and hyperplasia, called reactive gliosis (Sofroniew, 2009; Burda and Sofroniew, 2014). Reactive astrocytes can be observed in each of the disease models mentioned above (Wetherington et al., 2008; Heneka et al., 2005; Murakami et al., 2011; Delekate et al., 2014). However, given the heterotypic responses of individual astrocytes to environmental signals following CNS perturbation, it would be difficult to determine whether reactive gliosis itself is accompanied by a predictable change in spontaneous astrocyte Ca^{2+} signaling. Brain injury triggers a multi-cellular response and leads to the release of numerous factors, such as ATP, $\text{TNF-}\alpha$ and thrombin, that could conceivably impact astrocyte Ca^{2+} signaling (Shirawaka et al., 2010; Santello et al., 2011; Agulhon et al., 2012; Pascual et al., 2012; Burda and Sofroniew, 2014).

Purinergic Signaling

Purine and Pyrimidine Nucleotides and their Receptors

Purine and pyrimidine nucleotides (e.g. ATP, ADP, adenosine, and UTP, UDP, respectively) contribute to a variety of cellular functions within the cytosol. However, receptors for extracellular purine and pyrimidine nucleotides are found throughout the body and activation of these receptors leads to the transduction of a wide range of biological signals. Drury and Szent-Gyorgin (1929) first proposed a role for extracellular signaling via purine nucleotides nearly a century ago when they discovered the cardiovascular effects of intravenous administration of adenosine. Subsequent work by Gillespie (1934) demonstrated opposing actions of ATP and adenosine on intestinal smooth muscle contractility, indicating that these nucleotides may be signaling through different receptors. Currently, we know there are two families of purine receptors: P1, which are activated by adenosine, and P2, which are activated by ATP, ADP, UTP, and UDP (Ralevic and Burnstock, 1998). For the purposes of this dissertation, we will focus primarily on the P2 receptor family.

Purinergic P2 receptors can be subdivided into Ca^{2+} -permeable (P2X) ion channels, or metabotropic G protein-coupled (P2Y) receptors. There are seven P2X receptor subtypes (P2X₁-P2X₇) all of which are activated by extracellular ATP. P2Y receptors, on the other hand, have eight different subtypes (P2Y₁, P2Y₂, P2Y₄, P2Y₆, P2Y₁₁, P2Y₁₂, P2Y₁₃, and P2Y₁₄) and are activated by a variety of extracellular ligands (ATP, ADP, UTP, and UDP) with varying degrees of affinity (Ralevic and Burnstock, 1998). Different P2Y receptors are coupled to different G proteins. The receptors P2Y₁,_{6,11} are G_q-coupled and trigger an elevation of intracellular Ca^{2+} when activated, whereas

P2Y₁₂₋₁₄ couple to G_{i/o} and reduce activity of adenylate cyclase. The P2 family of receptors is broadly expressed throughout the brain and has been implicated in a variety of neuronal and glial functions in health and disease.

Astrocyte Purinergic Signaling in Disease

Extracellular purine nucleotides are often elevated in the brain following a variety of CNS insults, including aneurysmal SAH (Kasseckert et al., 2013). Damaged and/or dying cells represent one source of elevated ATP following brain injury. However, astrocytes are generally considered to be the principal source of released ATP in the CNS (Franke et al., 2012). Astrocytes can release ATP via Ca²⁺-dependent exocytosis (i.e. vesicular release) or through hemi-channels formed by connexins and pannexins (Montana et al., 2006; Bowser and Khakh, 2007; Kang et al., 2008). Interestingly, astrocyte lysosomes have recently been identified as another potential source of released ATP in the brain, although this has only been observed in cultured cells (Zhang et al., 2007).

Astrocytes express many subtypes of P2X and P2Y receptors whose activation causes a rise in intra-cellular Ca²⁺ (for reviews see: Iles and Alexandre-Ribeiro, 2004, and Franke et al., 2012). These P2 receptors regulate diverse functions such as proliferation/apoptosis (Neary et al., 1996), gliotransmission (Pannicke et al., 2000; Duan et al., 2003), and astrocyte reactivity (Brambilla et al., 1999; Abbracchio et al., 1999). Based largely on immuno-labeling studies, the G_q-coupled P2Y₁, P2Y₂, and P2Y₄ receptors have all been shown to be expressed on perivascular astrocyte endfeet (Simard et al., 2003; Franke et al., 2012). Kasseckert et al. (2013) found that the ATP levels in

cerebrospinal fluid obtained from human SAH patients were roughly 400 times higher than that of non-SAH patients. Under healthy conditions, cerebrospinal fluid is thought to flow into the brain parenchyma along a paravascular pathway between parenchymal arterioles and surrounding astrocyte endfeet (Iloff et al., 2012; Iliff et al., 2013). Thus, it is conceivable that elevated levels of ATP and/or other purine nucleotides in the cerebrospinal fluid after SAH could trigger a pathological change in endfoot Ca^{2+} signaling (i.e. high-amplitude Ca^{2+} events). *The second specific aim of this dissertation is to determine whether purinergic signaling underlies the emergence of high-amplitude spontaneous Ca^{2+} events in astrocyte endfeet following SAH.*

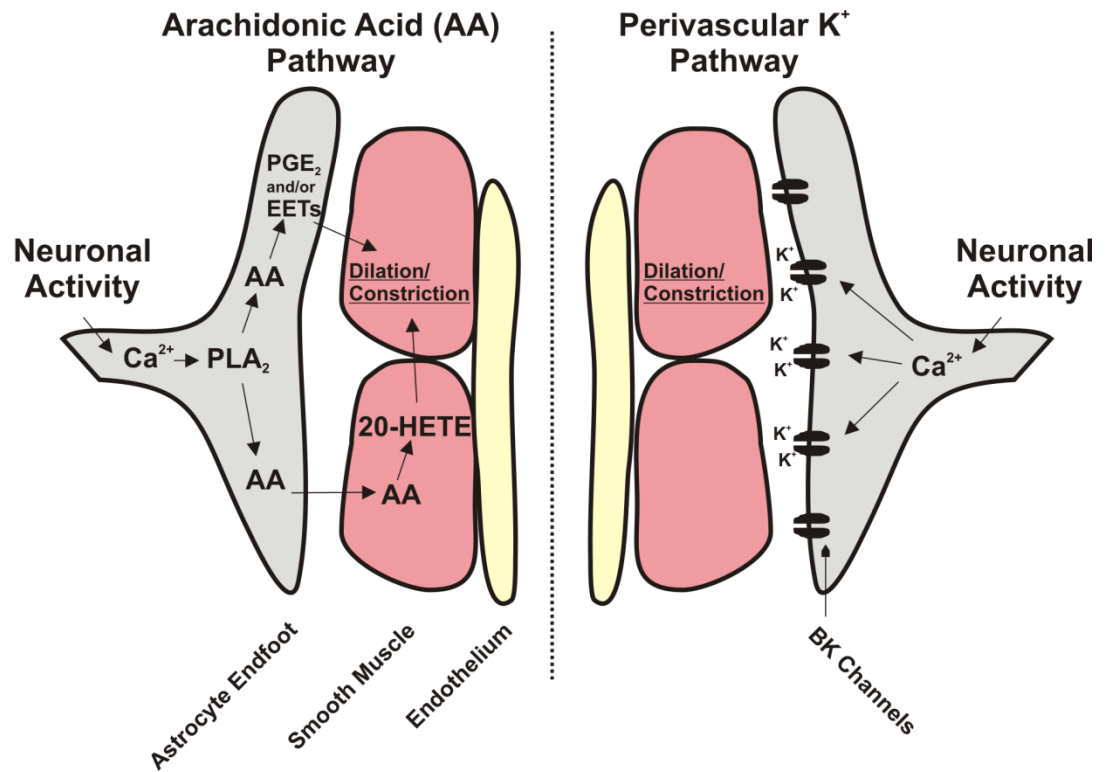


Figure 1-1. Two potential pathways driving neurovascular coupling.

Arachidonic acid (AA) could be released by phospholipase A₂ (PLA₂) following a neuronal activity-dependent elevation of endfoot Ca²⁺ (left of dotted line). Enzymes within the endfoot may metabolize AA into prostaglandin E₂ (PGE₂) and/or epoxyeicosatrienoic acids (EETs) which could impact arteriolar diameter after diffusing across the perivascular space and entering the vascular smooth muscle. However, AA itself may also diffuse across the perivascular space and impact arteriolar diameter after being converted to 20-hydroxyeicosatetraenoic acid (20-HETE) by smooth muscle enzymes. Alternatively, the endfoot Ca²⁺ elevation could open large-conductance Ca²⁺-activated K⁺ (BK) channels (right of dotted line). Increased perivascular K⁺ would rapidly impact arteriolar diameter by directly influencing the smooth muscle membrane potential.

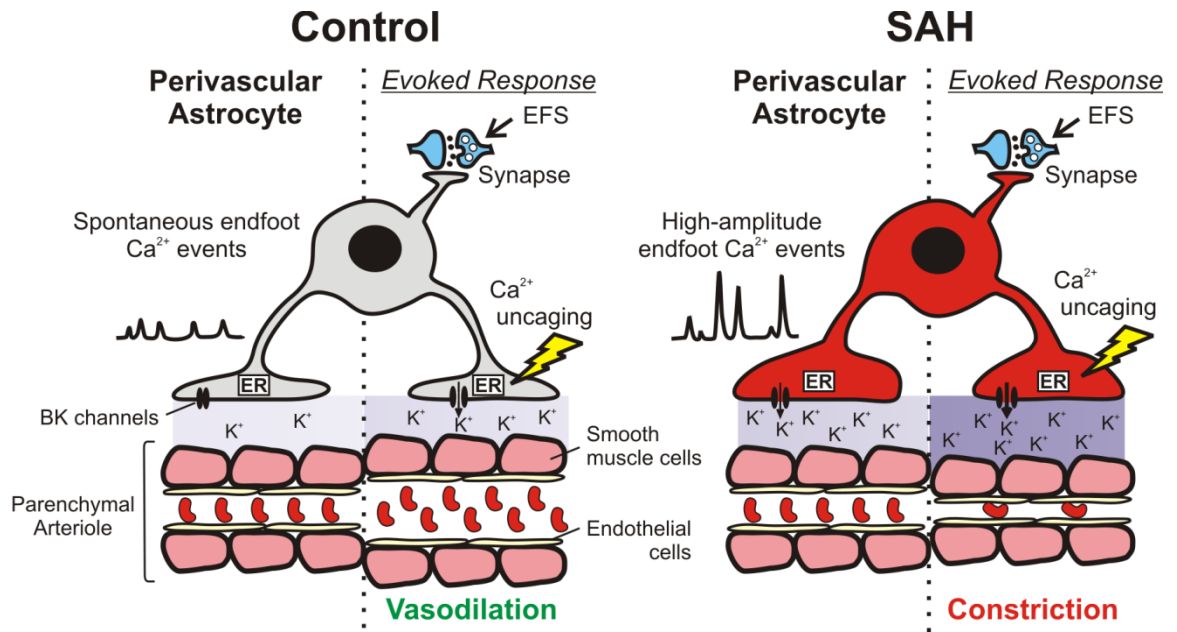


Figure 1-2. Schematic depicting a mechanism whereby the increased amplitude of spontaneous endfoot Ca^{2+} events could lead to inversion of neurovascular coupling after SAH.

In the absence of stimulation (left of dotted lines), perivascular astrocyte endfeet exhibit asynchronous spontaneous Ca^{2+} signaling events. However, there is an increase in the amplitude of these events after SAH. We hypothesize that the high-amplitude Ca^{2+} events in SAH animals cause excessive K^+ efflux through endfoot BK channels leading to an abnormal elevation of perivascular K^+ . Evoking a rise in endfoot Ca^{2+} either by electrical field stimulation (EFS) or Ca^{2+} uncaging (right of dotted lines) causes a modest BK channel-dependent elevation of extracellular K^+ . In healthy control animals, this modest increase in perivascular K^+ hyperpolarizes the vascular smooth muscle and causes arteriolar dilation. In SAH animals, however, the stimulated K^+ efflux could combine with abnormally elevated K^+ levels to bring perivascular K^+ beyond the dilation/constriction threshold.

References

- Abbracchio MP, Brambilla R, Ceruti S, Cattabeni F (1999) Signalling mechanisms involved in P2Y receptor-mediated reactive astrogliosis. *Prog Brain Res* 120:333-342.
- Agulhon C, Sun MY, Murphy T, Myers T, Lauderdale K, Fiocco TA (2012) Calcium Signaling and Gliotransmission in Normal vs. Reactive Astrocytes. *Front Pharmacol* 3:139.
- Ajiboye N, Chalouhi N, Starke RM, Zanaty M, Bell R (2015) Unruptured Cerebral Aneurysms: Evaluation and Management. *Scientific World Journal* 2015:954954.
- Al-Khindi T, Macdonald RL, Schweizer TA (2010) Cognitive and functional outcome after aneurysmal subarachnoid hemorrhage. *Stroke* 41:e519-e536.
- Alkayed NJ, Birks EK, Narayanan J, Petrie KA, Kohler-Cabot AE, Harder DR (1997) Role of P-450 arachidonic acid epoxygenase in the response of cerebral blood flow to glutamate in rats. *Stroke* 28:1066-1072.
- Alkayed NJ, Narayanan J, Gebremedhin D, Medhora M, Roman RJ, Harder DR (1996) Molecular characterization of an arachidonic acid epoxygenase in rat brain astrocytes. *Stroke* 27:971-979.
- Angulo MC, Kozlov AS, Charpak S, Audinat E (2004) Glutamate released from glial cells synchronizes neuronal activity in the hippocampus. *J Neurosci* 24:6920-6927.
- Attwell D, Buchan AM, Charpak S, Lauritzen M, MacVicar BA, Newman EA (2010) Glial and neuronal control of brain blood flow. *Nature* 468:232-243.
- Baeres FM, Moller M (2004) Origin of PACAP-immunoreactive nerve fibers innervating the subarachnoidal blood vessels of the rat brain. *J Cereb Blood Flow Metab* 24:628-635.
- Bai JP, Surguchev A, Navaratnam D (2011) β 4-subunit increases *Slo* responsiveness to physiological Ca^{2+} concentrations and together with β 1 reduces surface expression of *Slo* in hair cells. *Am J Physiol Cell Physiol* 300:C435-C446.
- Bayliss WM (1902) On the local reactions of the arterial wall to changes of internal pressure. *J Physiol* 28:220-231.
- Begley DJ, Brightman MW (2003) Structural and functional aspects of the blood-brain barrier. *Prog Drug Res* 61:39-78.

- Benfenati V, Amiry-Moghaddam M, Caprini M, Mylonakou MN, Rapisarda C, Ottersen OP, Ferroni S (2007) Expression and functional characterization of transient receptor potential vanilloid-related channel 4 (TRPV4) in rat cortical astrocytes. *Neuroscience* 148:876-892.
- Bennett DA, Krishnamurthi RV, Barker-Collo S, Forouzanfar MH, Naghavi M, Connor M, Lawes CM, Moran AE, Anderson LM, Roth GA, Mensah GA, Ezzati M, Murray CJ, Feigin VL (2014) The global burden of ischemic stroke: findings of the GBD 2010 study. *Glob Heart* 9:107-112.
- Bonder DE, McCarthy KD (2014) Astrocytic G_q-GPCR-linked IP₃R-dependent Ca²⁺ signaling does not mediate neurovascular coupling in mouse visual cortex *in vivo*. *J Neurosci* 34:13139-13150.
- Bowser DN, Khakh BS (2007) Vesicular ATP is the predominant cause of intercellular calcium waves in astrocytes. *J Gen Physiol* 129:485-491.
- Brambilla R, Burnstock G, Bonazzi A, Ceruti S, Cattabeni F, Abbracchio MP (1999) Cyclo-oxygenase-2 mediates P2Y receptor-induced reactive astrogliosis. *Br J Pharmacol* 126:563-567.
- Brayden JE, Li Y, Tavares MJ (2013) Purinergic receptors regulate myogenic tone in cerebral parenchymal arterioles. *J Cereb Blood Flow Metab* 33:293-299.
- Burda JE, Sofroniew MV (2014) Reactive gliosis and the multicellular response to CNS damage and disease. *Neuron* 81:229-248.
- Carmignoto G, Pasti L, Pozzan T (1998) On the role of voltage-dependent calcium channels in calcium signaling of astrocytes *in situ*. *J Neurosci* 18:4637-4645.
- Chen BR, Kozberg MG, Bouchard MB, Shaik MA, Hillman EM (2014) A critical role for the vascular endothelium in functional neurovascular coupling in the brain. *J Am Heart Assoc* 3:e000787.
- Chen J, Tan Z, Zeng L, Zhang X, He Y, Gao W, Wu X, Li Y, Bu B, Wang W, Duan S (2013) Heterosynaptic long-term depression mediated by ATP released from astrocytes. *Glia* 61:178-191.
- Cipolla MJ (2009) *The Cerebral Circulation*.
- Cipolla MJ, Li R, Vitullo L (2004) Perivascular innervation of penetrating brain parenchymal arterioles. *J Cardiovasc Pharmacol* 44:1-8.

- Cornell-Bell AH, Finkbeiner SM, Cooper MS, Smith SJ (1990) Glutamate induces calcium waves in cultured astrocytes: long-range glial signaling. *Science* 247:470-473.
- Dabertrand F, Hannah RM, Pearson JM, Hill-Eubanks DC, Brayden JE, Nelson MT (2013) Prostaglandin E2, a postulated astrocyte-derived neurovascular coupling agent, constricts rather than dilates parenchymal arterioles. *J Cereb Blood Flow Metab* 33:479-482.
- Davis J, Xu F, Deane R, Romanov G, Previti ML, Zeigler K, Zlokovic BV, Van Nostrand WE (2004) Early-onset and robust cerebral microvascular accumulation of amyloid β -protein in transgenic mice expressing low levels of a vasculotropic Dutch/Iowa mutant form of amyloid β -protein precursor. *J Biol Chem* 279:20296-20306.
- Delekate A, Fuchtemeier M, Schumacher T, Ulbrich C, Foddis M, Petzold GC (2014) Metabotropic P2Y₁ receptor signalling mediates astrocytic hyperactivity *in vivo* in an Alzheimer's disease mouse model. *Nat Commun* 5:5422.
- Dreier JP, Major S, Manning A, Woitzik J, Drenckhahn C, Steinbrink J, Tolias C, Oliveira-Ferreira AI, Fabricius M, Hartings JA, Vajkoczy P, Lauritzen M, Dirnagl U, Bohner G, Strong AJ (2009) Cortical spreading ischaemia is a novel process involved in ischaemic damage in patients with aneurysmal subarachnoid haemorrhage. *Brain* 132:1866-1881.
- Dreier JP, Sakowitz OW, Harder A, Zimmer C, Dirnagl U, Valdueza JM, Unterberg AW (2002) Focal laminar cortical MR signal abnormalities after subarachnoid hemorrhage. *Ann Neurol* 52:825-829.
- Drury AN, Szent-Gyorgyi A (1929) The physiological activity of adenine compounds with especial reference to their action upon the mammalian heart. *J Physiol* 68:213-237.
- Duan S, Anderson CM, Keung EC, Chen Y, Chen Y, Swanson RA (2003) P2X₇ receptor-mediated release of excitatory amino acids from astrocytes. *J Neurosci* 23:1320-1328.
- Dunn KM, Hill-Eubanks DC, Liedtke WB, Nelson MT (2013) TRPV4 channels stimulate Ca²⁺-induced Ca²⁺ release in astrocytic endfeet and amplify neurovascular coupling responses. *Proc Natl Acad Sci U S A* 110:6157-6162.
- Faraci FM, Heistad DD (1990) Regulation of large cerebral arteries and cerebral microvascular pressure. *Circ Res* 66:8-17.
- Farkas E, Luiten PG (2001) Cerebral microvascular pathology in aging and Alzheimer's disease. *Prog Neurobiol* 64:575-611.

- Fatatis A, Russell JT (1992) Spontaneous changes in intracellular calcium concentration in type I astrocytes from rat cerebral cortex in primary culture. *Glia* 5:95-104.
- Feigin VL, Lawes CM, Bennett DA, Barker-Collo SL, Parag V (2009) Worldwide stroke incidence and early case fatality reported in 56 population-based studies: a systematic review. *Lancet Neurol* 8:355-369.
- Fiacco TA, McCarthy KD (2004) Intracellular astrocyte calcium waves *in situ* increase the frequency of spontaneous AMPA receptor currents in CA1 pyramidal neurons. *J Neurosci* 24:722-732.
- Filosa JA, Bonev AD, Straub SV, Meredith AL, Wilkerson MK, Aldrich RW, Nelson MT (2006) Local potassium signaling couples neuronal activity to vasodilation in the brain. *Nat Neurosci* 9:1397-1403.
- Filosa JA, Morrison HW, Iddings JA, Du W, Kim KJ (2015) Beyond neurovascular coupling, role of astrocytes in the regulation of vascular tone. *Neuroscience*.
- Franke H, Verkhratsky A, Burnstock G, Illes P (2012) Pathophysiology of astroglial purinergic signalling. *Purinergic Signal* 8:629-657.
- Gebremedhin D, Ma YH, Falck JR, Roman RJ, VanRollins M, Harder DR (1992) Mechanism of action of cerebral epoxyeicosatrienoic acids on cerebral arterial smooth muscle. *Am J Physiol* 263:H519-H525.
- Gillespie JH (1934) The biological significance of the linkages in adenosine triphosphoric acid. *J Physiol* 80:345-359.
- Girouard H, Bonev AD, Hannah RM, Meredith A, Aldrich RW, Nelson MT (2010) Astrocytic endfoot Ca^{2+} and BK channels determine both arteriolar dilation and constriction. *Proc Natl Acad Sci U S A* 107:3811-3816.
- Hamel E (2006) Perivascular nerves and the regulation of cerebrovascular tone. *J Appl Physiol* (1985) 100:1059-1064.
- Harder DR, Gebremedhin D, Narayanan J, Jefcoat C, Falck JR, Campbell WB, Roman R (1994) Formation and action of a P-450 4A metabolite of arachidonic acid in cat cerebral microvessels. *Am J Physiol* 266:H2098-H2107.
- Haydon PG, Carmignoto G (2006) Astrocyte control of synaptic transmission and neurovascular coupling. *Physiol Rev* 86:1009-1031.
- Heilbrun MP, Olesen J, Lassen NA (1972) Regional cerebral blood flow studies in subarachnoid hemorrhage. *J Neurosurg* 37:36-44.

- Heneka MT, Sastre M, Dumitrescu-Ozimek L, Dewachter I, Walter J, Klockgether T, Van LF (2005) Focal glial activation coincides with increased BACE1 activation and precedes amyloid plaque deposition in APP[V717I] transgenic mice. *J Neuroinflammation* 2:22.
- Henneberger C, Papouin T, Oliet SH, Rusakov DA (2010) Long-term potentiation depends on release of D-serine from astrocytes. *Nature* 463:232-236.
- Hirst WD, Young KA, Newton R, Allport VC, Marriott DR, Wilkin GP (1999) Expression of COX-2 by normal and reactive astrocytes in the adult rat central nervous system. *Mol Cell Neurosci* 13:57-68.
- Horrigan FT, Aldrich RW (2002) Coupling between voltage sensor activation, Ca²⁺ binding and channel opening in large conductance (BK) potassium channels. *J Gen Physiol* 120:267-305.
- Iloff JJ, Wang M, Liao Y, Plog BA, Peng W, Gundersen GA, Benveniste H, Vates GE, Deane R, Goldman SA, Nagelhus EA, Nedergaard M (2012) A paravascular pathway facilitates CSF flow through the brain parenchyma and the clearance of interstitial solutes, including amyloid β . *Sci Transl Med* 4:147ra111.
- Iloff JJ, Wang M, Zeppenfeld DM, Venkataraman A, Plog BA, Liao Y, Deane R, Nedergaard M (2013) Cerebral arterial pulsation drives paravascular CSF-interstitial fluid exchange in the murine brain. *J Neurosci* 33:18190-18199.
- Illes P, Alexandre RJ (2004) Molecular physiology of P2 receptors in the central nervous system. *Eur J Pharmacol* 483:5-17.
- Ishiguro M, Morielli AD, Zvarova K, Tranmer BI, Penar PL, Wellman GC (2006) Oxyhemoglobin-induced suppression of voltage-dependent K⁺ channels in cerebral arteries by enhanced tyrosine kinase activity. *Circ Res* 99:1252-1260.
- Jakubowski J, Kendall B (1978) Coincidental aneurysms with tumours of pituitary origin. *J Neurol Neurosurg Psychiatry* 41:972-979.
- Kang J, Kang N, Lovatt D, Torres A, Zhao Z, Lin J, Nedergaard M (2008) Connexin 43 hemichannels are permeable to ATP. *J Neurosci* 28:4702-4711.
- Kasseckert SA, Shahzad T, Miqdad M, Stein M, Abdallah Y, Scharbrodt W, Oertel M (2013) The mechanisms of energy crisis in human astrocytes after subarachnoid hemorrhage. *Neurosurgery* 72:468-474.
- Kim KJ, Iddings JA, Stern JE, Blanco VM, Croom D, Kirov SA, Filosa JA (2015) Astrocyte contributions to flow/pressure-evoked parenchymal arteriole vasoconstriction. *J Neurosci* 35:8245-8257.

- Kirischuk S, Moller T, Voitenko N, Kettenmann H, Verkhratsky A (1995) ATP-induced cytoplasmic calcium mobilization in Bergmann glial cells. *J Neurosci* 15:7861-7871.
- Knot HJ, Zimmermann PA, Nelson MT (1996) Extracellular K^+ -induced hyperpolarizations and dilatations of rat coronary and cerebral arteries involve inward rectifier K^+ channels. *J Physiol* 492 (Pt 2):419-430.
- Koehler RC, Roman RJ, Harder DR (2009) Astrocytes and the regulation of cerebral blood flow. *Trends Neurosci* 32:160-169.
- Koide M, Bonev AD, Nelson MT, Wellman GC (2012) Inversion of neurovascular coupling by subarachnoid blood depends on large-conductance Ca^{2+} -activated K^+ (BK) channels. *Proc Natl Acad Sci U S A* 109:E1387-E1395.
- Koide M, Penar PL, Tranmer BI, Wellman GC (2007) Heparin-binding EGF-like growth factor mediates oxyhemoglobin-induced suppression of voltage-dependent potassium channels in rabbit cerebral artery myocytes. *Am J Physiol Heart Circ Physiol* 293:H1750-H1759.
- Koide M, Wellman GC (2013) SAH-induced suppression of voltage-gated K^+ (K_V) channel currents in parenchymal arteriolar myocytes involves activation of the HB-EGF/EGFR pathway. *Acta Neurochir Suppl* 115:179-184.
- Koide M, Wellman GC (2015) Activation of TRPV4 channels does not mediate inversion of neurovascular coupling after SAH. *Acta Neurochir Suppl* 120:111-116.
- Krimer LS, Muly EC, III, Williams GV, Goldman-Rakic PS (1998) Dopaminergic regulation of cerebral cortical microcirculation. *Nat Neurosci* 1:286-289.
- Krishnamurthi RV, Moran AE, Forouzanfar MH, Bennett DA, Mensah GA, Lawes CM, Barker-Collo S, Connor M, Roth GA, Sacco R, Ezzati M, Naghavi M, Murray CJ, Feigin VL (2014) The global burden of hemorrhagic stroke: a summary of findings from the GBD 2010 study. *Glob Heart* 9:101-106.
- Latour I, Hamid J, Beedle AM, Zamponi GW, MacVicar BA (2003) Expression of voltage-gated Ca^{2+} channel subtypes in cultured astrocytes. *Glia* 41:347-353.
- Li Y, Baylie RL, Tavares MJ, Brayden JE (2014) TRPM4 channels couple purinergic receptor mechanoactivation and myogenic tone development in cerebral parenchymal arterioles. *J Cereb Blood Flow Metab* 34:1706-1714.
- Link TE, Murakami K, Beem-Miller M, Tranmer BI, Wellman GC (2008) Oxyhemoglobin-induced expression of R-type Ca^{2+} channels in cerebral arteries. *Stroke* 39:2122-2128.

- Longden TA, Nelson MT (2015) Vascular inward rectifier K⁺ channels as external K⁺ sensors in the control of cerebral blood flow. *Microcirculation* 22:183-196.
- Macdonald RL, Higashida RT, Keller E, Mayer SA, Molyneux A, Raabe A, Vajkoczy P, Wanke I, Bach D, Frey A, Marr A, Roux S, Kassell N (2011) Clazosentan, an endothelin receptor antagonist, in patients with aneurysmal subarachnoid haemorrhage undergoing surgical clipping: a randomised, double-blind, placebo-controlled phase 3 trial (CONSCIOUS-2). *Lancet Neurol* 10:618-625.
- Macdonald RL, Higashida RT, Keller E, Mayer SA, Molyneux A, Raabe A, Vajkoczy P, Wanke I, Bach D, Frey A, Nowbakht P, Roux S, Kassell N (2012) Randomized trial of clazosentan in patients with aneurysmal subarachnoid hemorrhage undergoing endovascular coiling. *Stroke* 43:1463-1469.
- MacVicar BA (1984) Voltage-dependent calcium channels in glial cells. *Science* 226:1345-1347.
- MacVicar BA, Hochman D, Delay MJ, Weiss S (1991) Modulation of intracellular Ca²⁺ in cultured astrocytes by influx through voltage-activated Ca²⁺ channels. *Glia* 4:448-455.
- Mathiisen TM, Lehre KP, Danbolt NC, Ottersen OP (2010) The perivascular astroglial sheath provides a complete covering of the brain microvessels: an electron microscopic 3D reconstruction. *Glia* 58:1094-1103.
- McCaslin AF, Chen BR, Radosevich AJ, Cauli B, Hillman EM (2011) *In vivo* 3D morphology of astrocyte-vasculature interactions in the somatosensory cortex: implications for neurovascular coupling. *J Cereb Blood Flow Metab* 31:795-806.
- Mocco J, Komotar RJ, Lavine SD, Meyers PM, Connolly ES, Solomon RA (2004) The natural history of unruptured intracranial aneurysms. *Neurosurg Focus* 17:E3.
- Montana V, Malarkey EB, Verderio C, Matteoli M, Parpura V (2006) Vesicular transmitter release from astrocytes. *Glia* 54:700-715.
- Mulligan SJ, MacVicar BA (2004) Calcium transients in astrocyte endfeet cause cerebrovascular constrictions. *Nature* 431:195-199.
- Murakami K, Koide M, Dumont TM, Russell SR, Tranmer BI, Wellman GC (2011) Subarachnoid Hemorrhage Induces Gliosis and Increased Expression of the Pro-inflammatory Cytokine High Mobility Group Box 1 Protein. *Transl Stroke Res* 2:72-79.
- Navarrete M, Araque A (2014) The Cajal school and the physiological role of astrocytes: a way of thinking. *Front Neuroanat* 8:33.

- Navarrete M, Perea G, Fernandez de SD, Gomez-Gonzalo M, Nunez A, Martin ED, Araque A (2012) Astrocytes mediate *in vivo* cholinergic-induced synaptic plasticity. PLoS Biol 10:e1001259.
- Navarrete M, Perea G, Maglio L, Pastor J, Garcia de SR, Araque A (2013) Astrocyte calcium signal and gliotransmission in human brain tissue. Cereb Cortex 23:1240-1246.
- Neary JT, Rathbone MP, Cattabeni F, Abbracchio MP, Burnstock G (1996) Trophic actions of extracellular nucleotides and nucleosides on glial and neuronal cells. Trends Neurosci 19:13-18.
- Nedergaard M (1994) Direct signaling from astrocytes to neurons in cultures of mammalian brain cells. Science 263:1768-1771.
- Nett WJ, Oloff SH, McCarthy KD (2002) Hippocampal astrocytes *in situ* exhibit calcium oscillations that occur independent of neuronal activity. J Neurophysiol 87:528-537.
- Newman EA (1984) Regional specialization of retinal glial cell membrane. Nature 309:155-157.
- Newman EA (1986) High potassium conductance in astrocyte endfeet. Science 233:453-454.
- Newman EA, Zahs KR (1997) Calcium waves in retinal glial cells. Science 275:844-847.
- Nishimura N, Rosidi NL, Iadecola C, Schaffer CB (2010) Limitations of collateral flow after occlusion of a single cortical penetrating arteriole. J Cereb Blood Flow Metab 30:1914-1927.
- Nizar K, et al. (2013) *In vivo* stimulus-induced vasodilation occurs without IP₃ receptor activation and may precede astrocytic calcium increase. J Neurosci 33:8411-8422.
- Nystoriak MA, O'Connor KP, Sonkusare SK, Brayden JE, Nelson MT, Wellman GC (2011) Fundamental increase in pressure-dependent constriction of brain parenchymal arterioles from subarachnoid hemorrhage model rats due to membrane depolarization. Am J Physiol Heart Circ Physiol 300:H803-H812.
- Ostergaard L, Aamand R, Karabegovic S, Tietze A, Blicher JU, Mikkelsen IK, Iversen NK, Secher N, Engedal TS, Anzabi M, Jimenez EG, Cai C, Koch KU, Naess-Schmidt ET, Obel A, Juul N, Rasmussen M, Sorensen JC (2013) The role of the microcirculation in delayed cerebral ischemia and chronic degenerative changes after subarachnoid hemorrhage. J Cereb Blood Flow Metab 33:1825-1837.

- Pannicke T, Fischer W, Biedermann B, Schadlich H, Grosche J, Faude F, Wiedemann P, Allgaier C, Illes P, Burnstock G, Reichenbach A (2000) P2X₇ receptors in Muller glial cells from the human retina. *J Neurosci* 20:5965-5972.
- Park IS, Meno JR, Witt CE, Chowdhary A, Nguyen TS, Winn HR, Ngai AC, Britz GW (2009) Impairment of intracerebral arteriole dilation responses after subarachnoid hemorrhage. Laboratory investigation. *J Neurosurg* 111:1008-1013.
- Parri HR, Crunelli V (2003) The role of Ca²⁺ in the generation of spontaneous astrocytic Ca²⁺ oscillations. *Neuroscience* 120:979-992.
- Parri HR, Gould TM, Crunelli V (2001) Spontaneous astrocytic Ca²⁺ oscillations *in situ* drive NMDAR-mediated neuronal excitation. *Nat Neurosci* 4:803-812.
- Pascual O, Ben AS, Rostaing P, Triller A, Bessis A (2012) Microglia activation triggers astrocyte-mediated modulation of excitatory neurotransmission. *Proc Natl Acad Sci U S A* 109:E197-E205.
- Passier PE, Visser-Meily JM, Rinkel GJ, Lindeman E, Post MW (2013) Determinants of health-related quality of life after aneurysmal subarachnoid hemorrhage: a systematic review. *Qual Life Res* 22:1027-1043.
- Paulson OB, Newman EA (1987) Does the release of potassium from astrocyte endfeet regulate cerebral blood flow? *Science* 237:896-898.
- Perea G, Araque A (2007) Astrocytes potentiate transmitter release at single hippocampal synapses. *Science* 317:1083-1086.
- Peters DG, Kassam AB, Feingold E, Heidrich-O'Hare E, Yonas H, Ferrell RE, Brufsky A (2001) Molecular anatomy of an intracranial aneurysm: coordinated expression of genes involved in wound healing and tissue remodeling. *Stroke* 32:1036-1042.
- Pluta RM, Hansen-Schwartz J, Dreier J, Vajkoczy P, Macdonald RL, Nishizawa S, Kasuya H, Wellman G, Keller E, Zauner A, Dorsch N, Clark J, Ono S, Kiris T, Leroux P, Zhang JH (2009) Cerebral vasospasm following subarachnoid hemorrhage: time for a new world of thought. *Neurol Res* 31:151-158.
- Porter JT, McCarthy KD (1996) Hippocampal astrocytes *in situ* respond to glutamate released from synaptic terminals. *J Neurosci* 16:5073-5081.
- Price DL, Ludwig JW, Mi H, Schwarz TL, Ellisman MH (2002) Distribution of *rSlo* Ca²⁺-activated K⁺ channels in rat astrocyte perivascular endfeet. *Brain Res* 956:183-193.
- Rabinstein AA, Weigand S, Atkinson JL, Wijdicks EF (2005) Patterns of cerebral infarction in aneurysmal subarachnoid hemorrhage. *Stroke* 36:992-997.

- Ralevic V, Burnstock G (1998) Receptors for purines and pyrimidines. *Pharmacol Rev* 50:413-492.
- Reinhard JF, Jr., Liebmann JE, Schlosberg AJ, Moskowitz MA (1979) Serotonin neurons project to small blood vessels in the brain. *Science* 206:85-87.
- Roy CS, Sherrington CS (1890) On the regulation of the blood-supply of the brain. *J Physiol* 11:85-158.
- Santello M, Bezzi P, Volterra A (2011) TNF α controls glutamatergic gliotransmission in the hippocampal dentate gyrus. *Neuron* 69:988-1001.
- Seidel KN, Derst C, Salzmann M, Holtje M, Priller J, Markgraf R, Heinemann SH, Heilmann H, Skatchkov SN, Eaton MJ, Veh RW, Pruss H (2011) Expression of the voltage- and Ca²⁺-dependent BK potassium channel subunits BK β 1 and BK β 4 in rodent astrocytes. *Glia* 59:893-902.
- Shao Y, McCarthy KD (1995) Receptor-mediated calcium signals in astroglia: multiple receptors, common stores and all-or-nothing responses. *Cell Calcium* 17:187-196.
- Shelton MK, McCarthy KD (1999) Mature hippocampal astrocytes exhibit functional metabotropic and ionotropic glutamate receptors *in situ*. *Glia* 26:1-11.
- Shelton MK, McCarthy KD (2000) Hippocampal astrocytes exhibit Ca²⁺-elevating muscarinic cholinergic and histaminergic receptors *in situ*. *J Neurochem* 74:555-563.
- Shigetomi E, Bushong EA, Haustein MD, Tong X, Jackson-Weaver O, Kracun S, Xu J, Sofroniew MV, Ellisman MH, Khakh BS (2013) Imaging calcium microdomains within entire astrocyte territories and endfeet with GCaMPs expressed using adeno-associated viruses. *J Gen Physiol* 141:633-647.
- Shirakawa H, Sakimoto S, Nakao K, Sugishita A, Konno M, Iida S, Kusano A, Hashimoto E, Nakagawa T, Kaneko S (2010) Transient receptor potential canonical 3 (TRPC3) mediates thrombin-induced astrocyte activation and upregulates its own expression in cortical astrocytes. *J Neurosci* 30:13116-13129.
- Simard M, Arcuino G, Takano T, Liu QS, Nedergaard M (2003) Signaling at the gliovascular interface. *J Neurosci* 23:9254-9262.
- Sofroniew MV (2009) Molecular dissection of reactive astrogliosis and glial scar formation. *Trends Neurosci* 32:638-647.
- Solomon RA, Antunes JL, Chen RY, Bland L, Chien S (1985) Decrease in cerebral blood flow in rats after experimental subarachnoid hemorrhage: a new animal model. *Stroke* 16:58-64.

- Srinivasan R, Huang BS, Venugopal S, Johnston AD, Chai H, Zeng H, Golshani P, Khakh BS (2015) Ca²⁺ signaling in astrocytes from IP₃R2^{-/-} mice in brain slices and during startle responses *in vivo*. *Nat Neurosci* 18:708-717.
- Straub SV, Bonev AD, Wilkerson MK, Nelson MT (2006) Dynamic inositol trisphosphate-mediated calcium signals within astrocytic endfeet underlie vasodilation of cerebral arterioles. *J Gen Physiol* 128:659-669.
- Takano T, Han X, Deane R, Zlokovic B, Nedergaard M (2007) Two-photon imaging of astrocytic Ca²⁺ signaling and the microvasculature in experimental mice models of Alzheimer's disease. *Ann N Y Acad Sci* 1097:40-50.
- Takano T, Tian GF, Peng W, Lou N, Libionka W, Han X, Nedergaard M (2006) Astrocyte-mediated control of cerebral blood flow. *Nat Neurosci* 9:260-267.
- Tian GF, Azmi H, Takano T, Xu Q, Peng W, Lin J, Oberheim N, Lou N, Wang X, Zielke HR, Kang J, Nedergaard M (2005) An astrocytic basis of epilepsy. *Nat Med* 11:973-981.
- Trachtenberg MC, Pollen DA (1970) Neuroglia: biophysical properties and physiologic function. *Science* 167:1248-1252.
- Vander Eecken HM, Adams RD (1953) The anatomy and functional significance of the meningeal arterial anastomoses of the human brain. *J Neuropathol Exp Neurol* 12:132-157.
- Vatter H, Weidauer S, Konczalla J, Dettmann E, Zimmermann M, Raabe A, Preibisch C, Zanella FE, Seifert V (2006) Time course in the development of cerebral vasospasm after experimental subarachnoid hemorrhage: clinical and neuroradiological assessment of the rat double hemorrhage model. *Neurosurgery* 58:1190-1197.
- Vaucher E, Hamel E (1995) Cholinergic basal forebrain neurons project to cortical microvessels in the rat: electron microscopic study with anterogradely transported *Phaseolus vulgaris* leucoagglutinin and choline acetyltransferase immunocytochemistry. *J Neurosci* 15:7427-7441.
- Verkhatsky A, Orkand RK, Kettenmann H (1998) Glial calcium: homeostasis and signaling function. *Physiol Rev* 78:99-141.
- Weidauer S, Vatter H, Beck J, Raabe A, Lanfermann H, Seifert V, Zanella F (2008) Focal laminar cortical infarcts following aneurysmal subarachnoid haemorrhage. *Neuroradiology* 50:1-8.
- Weir B, Grace M, Hansen J, Rothberg C (1978) Time course of vasospasm in man. *J Neurosurg* 48:173-178.

- Wetherington J, Serrano G, Dingledine R (2008) Astrocytes in the epileptic brain. *Neuron* 58:168-178.
- Winship IR, Plaa N, Murphy TH (2007) Rapid astrocyte calcium signals correlate with neuronal activity and onset of the hemodynamic response *in vivo*. *J Neurosci* 27:6268-6272.
- Zaritsky JJ, Eckman DM, Wellman GC, Nelson MT, Schwarz TL (2000) Targeted disruption of Kir2.1 and Kir2.2 genes reveals the essential role of the inwardly rectifying K⁺ current in K⁺-mediated vasodilation. *Circ Res* 87:160-166.
- Zhang Z, Chen G, Zhou W, Song A, Xu T, Luo Q, Wang W, Gu XS, Duan S (2007) Regulated ATP release from astrocytes through lysosome exocytosis. *Nat Cell Biol* 9:945-953.
- Zhou Q, Petersen CC, Nicoll RA (2000) Effects of reduced vesicular filling on synaptic transmission in rat hippocampal neurones. *J Physiol* 525 Pt 1:195-206.
- Zingesser LH, Schechter MM, Dexter J, Katzman R, Scheinberg LC (1968) On the significance of spasm associated with rupture of a cerebral aneurysm. The relationship between spasm as noted angiographically and regional blood flow determinations. *Arch Neurol* 18:520-528.
- Zonta M, Angulo MC, Gobbo S, Rosengarten B, Hossmann KA, Pozzan T, Carmignoto G (2003a) Neuron-to-astrocyte signaling is central to the dynamic control of brain microcirculation. *Nat Neurosci* 6:43-50.
- Zonta M, Sebelin A, Gobbo S, Fellin T, Pozzan T, Carmignoto G (2003b) Glutamate-mediated cytosolic calcium oscillations regulate a pulsatile prostaglandin release from cultured rat astrocytes. *J Physiol* 553:407-414.

Chapter 2: Astrocyte Ca²⁺ signaling drives inversion of neurovascular coupling after subarachnoid hemorrhage

Anthony C. Pappas¹, Masayo Koide¹, George C. Wellman^{1,2}

Departments of Pharmacology¹ and Surgery², Division of Neurosurgery, University of Vermont, 89 Beaumont Ave, Burlington, VT 05405-0068, USA

Abstract

Physiologically, neurovascular coupling (NVC) matches focal increases in neuronal activity with local arteriolar dilation. Astrocytes participate in NVC by sensing increased neurotransmission and releasing vasoactive agents (e.g. K^+) from perivascular endfeet surrounding parenchymal arterioles. Recently, we demonstrated an increase in the amplitude of spontaneous Ca^{2+} events in astrocyte endfeet and inversion of NVC from vasodilation to vasoconstriction in brain slices obtained from subarachnoid hemorrhage (SAH) model rats. However, the role of spontaneous astrocyte Ca^{2+} signaling in determining the polarity of the NVC response remains unclear. Here, we used two-photon imaging of Fluo-4-loaded rat brain slices to determine whether altered endfoot Ca^{2+} signaling underlies SAH-induced inversion of NVC. We report a time-dependent emergence of endfoot high-amplitude Ca^{2+} signals (eHACSs) after SAH that were not observed in endfeet from un-operated animals. Further, the percentage of endfeet with eHACS varied with time and paralleled the development of inversion of NVC. Endfeet with eHACS were present only around arterioles exhibiting inversion of NVC. Importantly, depletion of intracellular Ca^{2+} stores using cyclopiazonic acid abolished SAH-induced eHACS and restored arteriolar dilation in SAH brain slices to two mediators of NVC (a rise in endfoot Ca^{2+} and elevation of extracellular K^+). These data indicate a causal link between SAH-induced eHACS and inversion of NVC. Ultrastructural examination using transmission electron microscopy indicated that a similar proportion of endfeet exhibiting eHACS also exhibited asymmetrical enlargement. Our results demonstrate that subarachnoid blood causes a delayed increase

in the amplitude of spontaneous intracellular Ca^{2+} release events leading to inversion of NVC.

Introduction

Blood flow within the brain parenchyma is dynamically coupled to the ongoing pattern of neuronal activity. Under physiological conditions, stimulus-evoked increases in the frequency of neuronal action potentials elicit vasodilation of nearby parenchymal arterioles. This phenomenon, called functional hyperemia, or neurovascular coupling (NVC), supports brain health by spatially and temporally matching cerebral blood flow to local tissue metabolic demand (Iadecola, 1993; Anderson and Nedergaard, 2003). Astrocytes are key intermediaries in NVC—having projections to neuronal synapses as well as processes (endfeet) that encase parenchymal arterioles (Araque et al., 1999). In response to enhanced neurotransmission, astrocytes release vasoactive substances, including potassium ions (K^+), from their endfeet onto adjacent parenchymal arterioles (Zonta et al., 2003; Filosa et al., 2006). The majority of evidence supports a role for increased astrocyte endfoot Ca^{2+} in mediating neurally-evoked vasodilator release (Straub et al., 2006; Attwell et al., 2010; Srinivasan et al., 2015;).

In addition to nerve-stimulated increases in Ca^{2+} , spontaneous Ca^{2+} elevations (200-300 nM in amplitude) lasting several seconds occur in astrocyte endfeet (Koide et al., 2012; Shigetomi et al., 2013). In brain slices from healthy animals, these spontaneous events resulted from IP_3 -dependent endoplasmic reticulum (ER) Ca^{2+} release (Dunn et al., 2013). Presently, the ability of spontaneous Ca^{2+} signaling to influence NVC and/or the release of vasoactive substances into the restricted perivascular space between endfeet and parenchymal arterioles is unclear. However, we have recently demonstrated both an increase in the amplitude of spontaneous Ca^{2+} events in astrocyte endfeet and inversion

of the NVC response from vasodilation to vasoconstriction in brain slices obtained from subarachnoid hemorrhage (SAH) model rats (Koide et al., 2012; Koide and Wellman, 2015). Interestingly, although the NVC response switched from vasodilation to vasoconstriction, neurally-evoked changes in endfoot Ca^{2+} were not altered by SAH.

Strokes caused by cerebral aneurysm rupture and SAH are associated with a high incidence of morbidity and mortality that often manifest several days after the initial bleed (Al-Khindi et al., 2010; Ostergaard et al., 2013). The inversion of NVC may be an important contributor to delayed cerebral ischemia, development of neurological deficits and poor outcome frequently observed in SAH patients (Koide et al., 2013). The goal of the present study was to determine if altered spontaneous Ca^{2+} signaling in astrocyte endfeet plays a causal role in the inversion of NVC after SAH. Here, we report that the time-dependent emergence of high-amplitude spontaneous Ca^{2+} signals in astrocyte endfeet paralleled the occurrence of inversion of NVC in brain slices from SAH model rats. These endfoot high-amplitude Ca^{2+} signals (eHACSs) were only observed adjacent to arterioles exhibiting inversion of NVC. Importantly, normal arteriolar dilation was restored in brain slices from SAH animals when eHACSs were abolished by depletion of ER Ca^{2+} stores. These results indicate that subarachnoid blood causes an increase in the amplitude of spontaneous Ca^{2+} signaling events in astrocyte endfeet that leads to inversion of NVC. Further, this work signifies that pathological changes in astrocyte function can profoundly impact cerebral blood flow regulation.

Materials and Methods

Rat SAH model. To mimic aneurysmal SAH, isoflurane-anesthetized Sprague-Dawley rats (male, 10-12 week old, Charles River Laboratories) received two injections of autologous, unheparanized arterial blood (500 μ L drawn from tail artery) into the cisterna magna as previously described (Nystoriak et al., 2011; Koide et al., 2012). Blood injections were given 24 h apart with the exception of animals studied at the 4 h and 24 h time-points that received only one intracisternal injection. Sham-operated animals underwent identical procedures except that saline, rather than blood, was injected into the cisterna magna. All procedures were conducted in accordance with the Guide for the Care and Use of Laboratory Animals (eighth edition, 2011) and followed protocols approved by the Institutional Animal Care and Use Committee at the University of Vermont.

Simultaneous measurements of parenchymal arteriolar diameter and astrocyte endfoot Ca^{2+} in freshly prepared cortical brain slices.

Brain slice preparation: Animals were euthanized by decapitation while under deep anesthesia with pentobarbital (60 mg/kg) at the following time-points: 4 h, 24 h, and 2, 4, 7, and 14 d after SAH. Brains were removed from animals and placed in ice-cold, aerated (5% $CO_2/95\%$ O_2) artificial cerebrospinal fluid (ACSF) and coronal brain slices, 160 μ m in thickness, were cut from the middle cerebral artery (MCA) territory using a Leica VT1000S vibratome. Brain slices were then incubated with the fluorescent Ca^{2+} indicator dye, Fluo-4 AM (10 μ M) for 1.5 hr at 29°C in ACSF containing 0.04% pluronic acid. Using these parameters, Fluo-4 is preferentially loaded into astrocytes (Parri et al.,

2001; Kawamura and Kawamura, 2011). In a subset of brain slices, the caged- Ca^{2+} compound, 1-(4,5-dimethoxy-2-nitrophenyl)-1,2-diaminoethane-N,N,N',N'-tetraacetic acid, tetra(acetoxymethyl ester) (DMNP-EDTA AM, 10 μM) was included with the Fluo-4. Brain slices were then rinsed and maintained in aerated ACSF at room temperature until imaged.

Simultaneous measurements of arteriolar diameter and astrocyte endfoot Ca^{2+} : Infrared-differential interference contrast (IR-DIC) and fluorescent images were simultaneously recorded from brain slices using multiphoton imaging systems coupled to a Coherent Chameleon Ti-Sapphire laser. A BioRad Radiance multi-photon imaging system (excitation wavelength: 820 nm, fluorescent bandpass filter: 575/150 nm, sampling frequency ~ 1 Hz) with an Olympus XLUM PlanF1 20x objective (0.95 NA) was used for the majority of studies. For these experiments, image size was 512 x 512 pixels and pixel resolution was 0.12 $\mu\text{m}/\text{pixel}$. For studies requiring the photolysis of caged Ca^{2+} , a Zeiss LSM-7 multi-photon imaging system (excitation: 730 nm, fluorescent bandpass filter: 525/50 nm, sampling frequency ~ 2 Hz) was used with a Zeiss W Plan-APOCHROMAT 20x objective (1.0 NA). The image size for these experiments was 512 x 300 pixels, and pixel resolution was 0.17 $\mu\text{m}/\text{pixel}$. To study NVC, electrical field stimulation (EFS; 50 Hz, 0.3 ms alternating square pulse, 3 s duration) was applied using a pair of platinum wire electrodes (2 mm apart) to trigger neuronal action potentials (Koide et. al., 2012). To elevate astrocyte endfoot Ca^{2+} independent of neuronal activation, we used photolysis of caged- Ca^{2+} or “ Ca^{2+} uncaging” in DMNP-EDTA-loaded slices. Photolysis was achieved using a ~ 0.5 s laser pulse of approximately three times the average imaging power to uncage Ca^{2+} within a selected endfoot (excitation volume of $\sim 1 \mu\text{m}^3$).

Throughout all recordings, brain slices were continually superfused (≈ 2 mL/min) with ACSF (aerated with 5% CO₂/95% O₂, pH ~ 7.35 , 35-37°C) containing the thromboxane A₂ analog, 9,11 di-dideoxy-11 α ,9 α -epoxymethanoprostaglandin F_{2 α} (U46619, 100 nM) to induce a physiological level of arteriolar tone (Koide et al., 2012). Parenchymal arteriolar segments (diameter: 3-14 μ m before EFS) within the MCA territory, located at a depth of 50-250 μ m from the pial surface and surrounded by Fluo-4-loaded endfeet were chosen for this study. Intraluminal red blood cells were observed in the majority of recordings (89%) and their presence or absence did not correlate with a particular vascular response to EFS or uncaging. At the end of each experiment, brain slices were treated with ionomycin (10 μ M) and 20 mM CaCl₂ to obtain maximum fluorescence intensity.

Analysis of parenchymal arteriolar diameter: Using IR-DIC images, intraluminal parenchymal arteriolar diameter was measured at 3 evenly spaced points along a 10 μ m segment showing the greatest response to stimulation (EFS, Ca²⁺ uncaging or 10 mM K⁺ superfusion). Diameter change, expressed as percent increase or decrease from baseline diameter was determined from 10 s of recording prior to stimulation and then averaged for the three points of measurement. Diameter measurements were made manually using custom software, SparkAn, written by Dr. Adrian D. Bonev, at the University of Vermont (Burlington, VT).

Analysis of astrocyte endfoot Ca²⁺: A region of interest (ROI; 1.2 x 1.2 μ m) was placed within an astrocyte endfoot that was either (1) adjacent to an arteriolar segment used to measure diameter change after EFS or Ca²⁺ uncaging or (2) exhibiting spontaneous Ca²⁺ events in unstimulated brain slices. Baseline Ca²⁺ within a ROI was determined by

averaging 10 consecutive images prior to stimulation and/or exhibiting no spontaneous activity. The following criteria were used to define spontaneous Ca^{2+} events: (1) $\geq 30\%$ increase in fluorescence intensity for at least 2 consecutive images (~ 2 s) and (2) multiple events observed within a ROI during a 4 min recording. The maximal fluorescence method was used to estimate Ca^{2+} concentrations within a ROI (Maravall et al., 2000; Koide et al., 2012).

Ultrastructural analysis using electron microscopy.

Transmission electron microscopy (TEM) was used to examine brain parenchymal arterioles and surrounding astrocyte endfeet in cortical layer 2/3 of the MCA territory (i.e. the same region examined in brain slice studies). Specimens were prepared for TEM using standard procedures (Hayat, 1981). Briefly, un-operated control, 2 d sham-operated and 2 d SAH model rats were anesthetized with pentobarbital (60 mg/kg) and fixed by transcardial perfusion at an intravascular pressure of 75 mmHg using a solution containing 135 mM Sucrose, 0.085 mM NaH_2PO_4 , 0.5 mM CaCl_2 and 1% glutaraldehyde (pH 7.3). Brains were then dissected from animals and fixed in 1% glutaraldehyde for an additional 24 h. Cortical blocks were cut, rinsed in 0.1 M cacodylate buffer and immersed in 1% OsO_4 for 4 h at 4°C and then dehydrated using a series of graded ethanol and propylene oxide solutions, and embedded in Spurr's resin overnight at 60°C . Ultrathin (90 nm) sections obtained using an Ultracut microtome were contrasted with uranyl acetate and lead citrate. A Jeol 1400 Transmission Electron Microscope was used to obtain a series of non-overlapping images (magnification: 5000X) capturing the entire arteriolar circumference. Consistent with previous reports (Mathiisen et al., 2010; McCaslin et al., 2011) the cellular structures providing sheath-like coverage of the

abluminal surface of the arteriolar wall were identified as astrocyte endfeet. The distance between endfeet and arteriolar smooth muscle was considered as the perivascular space. Endfoot thickness and the perivascular space were measured at 10 random, equally-spaced points along the arteriolar circumference using ImageJ (NIH).

Statistical analysis.

Data are expressed as mean \pm SEM (n : the number of observations, N : the number of animals). Unpaired Student's two-tailed t test was used for comparisons between two groups. One-way analysis of variance (ANOVA) followed by either the Tukey or Bonferroni test were used for the *post hoc* comparison of multiple groups. Chi-squared analysis was used to determine dependence between variables.

Reagents.

U46619, cyclopiazonic acid (CPA), and ionomycin were obtained from Calbiochem (EMD Millipore, Chicago, IL). DMNP-EDTA AM was purchased from Interchim (Montluçon, France). Fluo-4 AM and pluronic acid were obtained from Invitrogen (Life Technologies, Eugene, OR). All other reagents were purchased from Sigma-Aldrich (St. Louis, MO). The composition of aCSF (in mM) was: 125 NaCl, 3 KCl, 18 NaHCO₃, 1.25 NaH₂PO₄, 1 MgCl₂, 2 CaCl₂, 5 glucose and 0.4 ascorbic acid. ACSF containing 10 mM K⁺ was made by iso-osmotic replacement of NaCl with KCl.

Results

The emergence of high-amplitude spontaneous Ca^{2+} events in astrocyte endfeet (eHACSSs) after SAH

To explore the relationship between the inversion of NVC and the occurrence of high-amplitude spontaneous Ca^{2+} signals in astrocyte endfeet, cortical brain slices from the MCA territory were studied from SAH model rats at six time-points following injection of blood into the subarachnoid space (4 h, 24 h, and 2, 4, 7, and 14 d). A subarachnoid blood clot was observed adjacent to the circle of Willis on the ventral surface of the brain between the 4 h and 4 d SAH time-points. However, at days 7 and 14 d post-SAH the clot was no longer visible. Although remote from the site of blood injection (i.e. cisterna magna), extravascular red blood cells have been observed around parenchymal arterioles from the MCA territory using this model of SAH (Koide et al., 2012). Spontaneous Ca^{2+} events were imaged using two-photon excitation microscopy and the fluorescent Ca^{2+} indicator, Fluo-4, in astrocyte endfeet surrounding parenchymal arterioles (Fig. 1A,B). Consistent with our previous observation (Koide et al., 2012), SAH led to a significant increase in the overall mean amplitude of spontaneous Ca^{2+} events following SAH ($F_{[6,523]} = 5.75$; ANOVA, $p < 0.0001$). *Post hoc* comparison of the means (Bonferroni) revealed significance at the 24 h, 2, 4, and 7 d SAH time-points ($p = 0.01$, $p = 0.0002$, $p = 0.004$, $p = 0.03$, respectively). With further analysis, we determined that the increased mean amplitudes were due to the emergence of a sub-population of high-amplitude Ca^{2+} events not observed in control animals. In brain slices from unoperated control animals, basal endfoot Ca^{2+} was 128 ± 4 nM and spontaneous elevations in endfoot Ca^{2+} did not exceed 500 nM (range: 179 nM to 496 nM; mean: 303 ± 10 nM; n

= 73 events from 13 endfeet). However, in brain slices from SAH animals, we often observed high-amplitude spontaneous events (peak Ca^{2+} , ≥ 500 nM; eHACSs) in addition to spontaneous Ca^{2+} increases that were similar in amplitude to those observed in unoperated animals (peak Ca^{2+} , < 500 nM; “control-like events”). Thus, after SAH, endfeet fell into one of two categories: (1) endfeet with spontaneous Ca^{2+} events that were all “control-like” in amplitude, i.e., peak Ca^{2+} < 500 nM, or (2) endfeet with a combination of eHACSs and “control-like” spontaneous Ca^{2+} events. χ^2 analysis indicates an association between the incidence of endfeet exhibiting eHACSs and time (4 h, 2 d, 4 d) post-SAH ($\chi^2 = 8.839$, $df = 2$, $p = 0.012$). For example, at the earliest time point (4 h SAH) only ~27% of endfeet had eHACSs, whereas ~83% of endfeet were eHACSs-positive in brain slices from 2 d SAH animals (Fig. 1C). The mean amplitude (~700 nM) and frequency of eHACSs were similar at all SAH time points ($F_{[5, 83]} = 0.81$; ANOVA, $p = 0.54$, and $F_{[5, 39]} = 1.80$; ANOVA, $p = 0.14$, respectively). When compared with events from control animals, *post hoc* comparison of the means (Bonferroni) demonstrated that there was no change in the amplitude of “control-like” spontaneous Ca^{2+} events at any time-points after SAH, irrespective of the presence or absence of eHACSs ($p > 0.05$ in each group, Table 1). These data demonstrate that SAH leads to the time-dependent emergence of high-amplitude spontaneous Ca^{2+} events (i.e. eHACSs) not observed in control animals.

The inversion of NVC parallels the emergence of eHACs after SAH

We next examined whether the inversion of NVC followed a similar time-dependent pattern of development as that of eHACs after SAH. In brain slices from control animals, EFS-evoked neuronal activation caused the anticipated NVC response: a rise in astrocyte endfoot Ca^{2+} followed by vasodilation of the adjacent arteriole (Fig. 2A; $n = 6$ arterioles, $N = 6$ animals). Similar vasodilatory NVC responses were observed in all brain slices obtained from 4 h SAH animals ($n = 6$ arterioles, $N = 5$ animals). However, EFS-induced vasoconstriction (i.e. inversion of NVC) was observed in brain slices from animals at later SAH time-points. Inversion of NVC peaked at 2 d SAH with 100% of brain slices ($n = 7$ arterioles, $N = 6$ animals) exhibiting EFS-induced vasoconstriction, then steadily declined at later time-points (Fig. 2B,C). One-way ANOVA demonstrated a main effect of time post-SAH on EFS-evoked changes in arteriolar diameter ($F_{[6, 40]} = 4.961$, $p = 0.0007$). *Post hoc* multiple comparisons of the means (Bonferroni) revealed significance at the 2 and 4 d SAH time-points ($p = 0.001$, 0.01 , respectively). Although SAH influenced the polarity of EFS-induced vascular responses, evoked increases in endfoot Ca^{2+} in brain slices from SAH animals were similar to those in the control group (Table 2, $F_{[6,39]} = 0.52$; ANOVA, $p = 0.79$). There also was no difference in the mean arteriolar diameter before EFS between groups ($F_{[6,40]} = 1.74$; ANOVA, $p = 0.14$). In two instances, one at the 24 h and one at the 7 d SAH time-points, we observed opposing vascular responses in brain slices from the same animal, suggesting that inversion of NVC develops and resolves non-uniformly throughout brain cortex. Consistent with our hypothesis that the emergence of eHACs dictates the polarity of the neurovascular response after SAH, the time course of

inversion of NVC was remarkably similar to the time course of the emergence of astrocyte endfeet exhibiting eHACSs (Fig. 2D).

To further explore causality between the emergence of eHACSs and inversion of NVC, we captured both phenomena in single continuous recordings (3 min recording of spontaneous activity followed by EFS) of brain slices obtained from 24 h SAH animals. Here, we chose to study the 24 h SAH time-point because approximately half of the brain slices from these animals exhibited normal NVC (EFS-induced vasodilation) while the remaining slices exhibited inversion of NVC (EFS-induced vasoconstriction). As anticipated, endfeet in brain slices from 24 h SAH animals displayed either only “control-like” spontaneous Ca^{2+} events (i.e. no eHACSs) or exhibited a combination of “control-like” events and eHACSs during the initial 3 min of recordings capturing spontaneous Ca^{2+} events (Fig. 3A). EFS-induced vasodilation ($12 \pm 4\%$ increase in diameter, $n = 4$ arterioles, $N = 4$ animals) occurred in all brain slices exhibiting only “control-like” spontaneous Ca^{2+} events (mean amplitude of spontaneous Ca^{2+} events: 284 ± 16 nM, range: 189-485 nM, 32 events in four brain slices from four animals, Fig. 3B). Conversely, inversion of NVC (EFS-induced vasoconstriction, $17 \pm 7\%$ decrease in diameter, $n = 5$ arterioles, $N = 5$ animals) was observed in all brain slices containing eHACSs-positive endfeet (71 events in 5 brain slices from 5 animals, Fig. 3B). The presence or absence of eHACSs did not impact EFS-evoked increases in astrocyte endfoot Ca^{2+} or the overall frequency of spontaneous Ca^{2+} events (Fig. 3C,D; $p = 0.46$; two-tailed t test, $p = 0.33$; two-tailed t test, respectively). In two cases, brain slices with endfeet exhibiting eHACSs also had endfeet where eHACSs were not observed along the

same arteriolar segment. These results are consistent with the emergence of eHACSs causing inversion of NVC after SAH.

Abolition of eHACSs restores vasodilatory responses in brain slices from SAH animals

Release of Ca^{2+} from the ER underlies the generation of spontaneous Ca^{2+} events in astrocyte endfeet of healthy animals (Dunn et al., 2013). To examine the role of ER Ca^{2+} release in the generation of eHACSs, cyclopiazonic acid (CPA), a selective sarco/endoplasmic reticulum Ca^{2+} -ATPase (SERCA) inhibitor, was used to deplete astrocyte ER Ca^{2+} stores. In brain slices from control animals, CPA treatment (30 μM , 25 min) abolished spontaneous endfoot Ca^{2+} events (Fig. 4A), as expected. Importantly, CPA also abolished all spontaneous Ca^{2+} signals, including eHACSs, in brain slices from 2 d SAH animals indicating that SAH-induced eHACSs are mediated via ER Ca^{2+} release (Fig. 4B).

Using CPA to deplete ER Ca^{2+} , we next examined whether the elimination of SAH-induced eHACS could restore vasodilatory responses typical of NVC. However, because EFS-evoked vasodilation is also dependent on astrocyte endfoot ER Ca^{2+} release (Straub et al., 2006), we targeted two elements downstream of neuronal activation in the NVC signaling cascade (increased endfoot Ca^{2+} and elevated perivascular K^+). First, two-photon photolysis of caged Ca^{2+} was used to induce a focal (excitation volume $\sim 1 \mu\text{m}^3$) rise in endfoot Ca^{2+} . Consistent with EFS-induced vascular responses (Fig. 2), uncaging Ca^{2+} in astrocyte endfeet in the absence of CPA caused a similar amplitude

endfoot Ca^{2+} transient in all brain slices (Control: 436 ± 35 nM; SAH: 417 ± 32 nM $p = 0.47$; two-tailed t test), but caused vasodilation in brain slices from control animals and vasoconstriction in brain slices from 2 d SAH animals. Treatment of brain slices from control animals with CPA did not affect vasodilation induced by photolysis of caged Ca^{2+} in astrocyte endfeet (Fig. 4C, $p = 0.243$; two-tailed t test). However, in brain slices from 2 d SAH animals, CPA treatment (i.e., abolishing eHACSs) reversed Ca^{2+} uncaging responses from constriction to dilation (Fig. 4D, $p < 0.0001$; two-tailed t test). In the presence of CPA, the amplitude of endfoot Ca^{2+} transients induced by uncaging Ca^{2+} were again similar between groups (Control: 365 ± 53 nM; SAH: 310 ± 50 nM, $p = 0.83$; two-tailed t test). These results indicate that abolishing eHACSs restored normal astrocyte-vascular signaling in brain slices from SAH animals (Fig. 4E).

Modest increases in the extracellular/perivascular K^+ concentration play an important role in astrocyte-to-smooth muscle communication during NVC (Filosa et al., 2006; Girouard et al., 2010). Typically, neurally-evoked increases in endfoot Ca^{2+} activate large-conductance Ca^{2+} -activated K^+ (BK) channels on astrocyte endfeet, causing an estimated 5-10 mM increase in perivascular K^+ and vasodilation via activation of smooth muscle strong inwardly rectifying K^+ (K_{IR}) channels (Filosa et al., 2006; Girouard et al., 2010). Previous studies have mimicked neurally-evoked endfoot K^+ efflux by increasing the K^+ concentration in the brain slice superfusate from 3 mM to 10 mM (Filosa et al., 2006; Girouard et al., 2010; Koide et al., 2012). Here, we examined the effect of K^+ -induced changes in arteriolar diameter in brain slices obtained from control and 2 d SAH animals in the presence and absence of endfoot spontaneous Ca^{2+} events. Similar to the inversion of NVC, increasing extracellular K^+ from 3 to 10 mM in brain

slices with intact astrocyte ER Ca^{2+} (i.e., endfeet exhibiting spontaneous Ca^{2+} events) caused arteriolar dilation in brain slices from un-operated animals and vasoconstriction in brain slices from 2 d SAH animals. As with Ca^{2+} uncaging, abolishing spontaneous Ca^{2+} events with CPA (30 μM , 25 min) restored arteriolar dilation in response to 10 mM extracellular K^+ in brain slices from 2 d SAH animals and had no effect on K^+ -induced vasodilation in brain slices from control animals (Fig. 4F, $p < 0.0001$; two-tailed t test, $p = 0.56$; two-tailed t test, respectively). Thus, abolishing eHACSs restored vasodilatory responses in brain slices after SAH.

Asymmetrical enlargement of perivascular astrocyte endfeet after SAH

Central nervous system (CNS) pathologies such as traumatic brain injury, ischemic stroke and SAH are associated with astrocyte hypertrophy and reactive gliosis (Murakami et al., 2011; Burda and Sofroniew, 2014). To explore the impact of SAH on the ultrastructure of the gliovascular interface (i.e., astrocyte endfeet and parenchymal arterioles), we used TEM to image brain cortex from control, 2 d sham-operated and 2 d SAH model animals. Astrocyte endfeet surrounding parenchymal arterioles from control and sham-operated animals exhibited a thin, uniform, sheath-like morphology (Fig. 5A). In contrast, perivascular endfeet of SAH animals exhibited regions of asymmetrical thickening that contained numerous subcellular organelles, including lysosomes (Fig. 5A). Lysosomes were observed in 12 of 16 endfeet after SAH, but were not observed in endfeet from control or sham-operated animals. Remarkably, in 2 d SAH animals, the percentage of endfeet exhibiting asymmetrical hypertrophy (~81%, 13/16 endfeet) was similar to the percentage of endfeet exhibiting eHACS (~83 %; Fig. 1D). Using a

threshold of 3-times the mean thickness of control endfeet (~690 nm), we determined that ~17% of the arteriolar circumference is surrounded by an enlarged endfoot after SAH (Fig. 5C, Tukey, $p < 0.0001$ vs control, $p = 0.0008$ vs sham). Interestingly, despite enlargement of endfoot processes, the distances measured between the endfeet and arteriolar smooth muscle (i.e., the perivascular space) in these samples were similar between groups (~70 nm, Fig. 5B, $F_{[2,627]} = 1.17$; ANOVA, $p = 0.31$). These results suggest a possible link between structural changes in perivascular endfeet after SAH and altered endfoot Ca^{2+} signaling (i.e. eHACSs).

Discussion

This study provides evidence that the emergence of high-amplitude spontaneous Ca^{2+} events within astrocyte endfeet underlies SAH-induced inversion of NVC. High-amplitude Ca^{2+} signals or “eHACSs” were absent in brain slices from un-operated control animals, and were present only in endfeet surrounding arterioles exhibiting inversion of NVC. Further, abolishing eHACSs through pharmacologic depletion of ER Ca^{2+} restored typical vasodilatory responses to two elements involved in the NVC signaling cascade — increased endfoot Ca^{2+} and modest elevation of extracellular K^+ . BK channels, localized to the endfoot membrane (Price et al., 2002), are the most likely Ca^{2+} sensor responsible for transducing eHACSs into a pathological vascular response. Astrocyte BK channels are an important component of neurovascular communication (Filosa et al., 2006; Girouard et al., 2010; Koide et al., 2012) and contain auxiliary β_4 subunits (Seidel et al., 2011) conferring a high level of Ca^{2+} -sensitivity to these channels (Horrigan and Aldrich, 2002; Bai et al., 2011). Thus, considering the Ca^{2+} -sensitivity and large single channel

conductance of BK channels, it is likely that SAH-induced eHACSs cause a substantial increase in BK-mediated K^+ efflux. As the restricted perivascular space between endfeet and arteriolar myocytes is estimated to be less than 100 nm (Nagelhus et al., 1999) (see also, Fig. 5B), relatively small changes in the number of K^+ ions would significantly impact the K^+ concentration within the micro-domain surrounding parenchymal arterioles (Girouard et al., 2010). Cerebral arteries are highly sensitive to changes in extracellular K^+ (Knot et al., 1996; Zaritsky et al., 2000). Modest increases in extracellular K^+ (≤ 20 mM) cause arteriolar dilation via activation of smooth muscle K_{IR} channels (Knot et al., 1996; Filosa et al., 2006; Girouard et al., 2010). However, larger increases (>20 mM) cause a depolarizing shift in the K^+ equilibrium potential of smooth muscle that leads to enhanced Ca^{2+} entry through L-type voltage-dependent Ca^{2+} channels and arteriolar constriction (Knot and Nelson, 1998). Our previous work indicates that SAH-induced inversion of NVC is a result of abnormally elevated basal perivascular K^+ that, when combined with neurally-evoked K^+ efflux, leads to smooth muscle membrane potential depolarization and a switch in the polarity of the vascular response from dilation to constriction (Koide et al., 2012). We now demonstrate that altered spontaneous Ca^{2+} signaling in the form of eHACSs dictates the polarity of NVC after SAH. These results are consistent with the concept that SAH-induced eHACSs enhance BK channel activity in the endfeet causing an increase in basal perivascular K^+ and inversion of NVC.

This work expands upon a growing body of research indicating that SAH-induced cortical infarcts and poor clinical outcome are due to disruption of blood flow within the brain micro-circulation (Dreier et al., 2002; Ishiguro et al., 2002; Rabinstein et al., 2005; Pluta et al., 2009; Nystoriak et al., 2011; Ostergaard et al., 2013). Microvasculature

dysfunction after SAH would be predicted to cause cerebral infarction in relatively small, spatially-defined regions due to the paucity of collaterals within the brain parenchyma (Nishimura et al., 2007). Roughly 60% of patients exhibit diffuse ischemic brain lesions following SAH (Hijdra et al., 1986). Further, it has been suggested that the mechanism underlying diffuse brain injury differs from that which causes cell death near the site of aneurysm rupture (Rabinstein et al., 2005). While neuronal viability was not directly examined in the current study, the inversion of NVC likely precedes substantial cell death or neuronal injury after SAH as EFS-evoked changes in endfoot Ca^{2+} were comparable in brain slices from control and SAH animals. Previous studies have also shown altered ion channel function and/or expression in vascular smooth muscle cells following exposure to the blood component, oxyhemoglobin (Ishiguro et al., 2005; Wellman, 2006; Link et al., 2008). Thus, it is possible that ischemic events following SAH result from the combined effects of inversion of NVC and other actions of SAH, including a direct increase in arteriolar smooth muscle contractility (Nystoriak et al., 2011). Future studies will be required to establish the contribution of pathological astrocyte Ca^{2+} signaling and inversion of NVC in the development of delayed cerebral ischemia following SAH.

Astrocytes typically respond to CNS perturbations (including SAH) by undergoing a characteristic hypertrophy known as reactive gliosis (Murakami et al., 2011; Burda and Sofroniew, 2014). Although the morphological and molecular changes associated with reactive gliosis are well-described (Sofroniew, 2009), the functional consequences remain unclear. Recent *in vivo* measurements of astrocyte Ca^{2+} signaling using a mouse model of familial Alzheimer's disease demonstrated a "hyperactive" Ca^{2+} signaling phenotype in reactive astrocytes (Delekate et al., 2014). Importantly, the

aberrant Ca^{2+} signals present in endfeet were associated with spontaneous vasoconstrictions of the neighboring arterioles. These data provide an interesting parallel between the phenomena we observe after SAH (i.e. emergence of endfeet exhibiting eHACSs, inversion of NVC, and asymmetrical endfoot hypertrophy) and the functional alterations observed in a mouse model of Alzheimer's disease.

The results from our TEM studies demonstrated asymmetrical enlargement of astrocyte endfeet following SAH. While endfoot swelling has been suggested to compress cerebral micro-vessels after SAH (Ostergaard et al., 2013), it is unlikely that the endfoot enlargement we are reporting directly causes arteriolar narrowing, as we detected no change in arteriolar diameter prior to EFS at any time-points after SAH (Table 2). Further, we found no change in the width of the perivascular space using TEM (Fig. 5). However, these static TEM measurements of the perivascular space were made using perfusion-fixed tissue susceptible to spacing artifacts. It is also important to consider that the perivascular space surrounding parenchymal arterioles provides a critical and dynamic conduit for the exchange of CSF with brain interstitial fluid (ISF) (Ilyff et al., 2012; Ilyff et al., 2013). Considering previous work showing that increased arousal decreases ISF-CSF fluid exchange (Xie et al., 2013), it is possible that increases in arteriolar diameter during vasodilatory NVC coincide with decreases in perivascular volume. Conversely, vasoconstrictive NVC would be predicted to increase perivascular volume and enhance ISF-CSF exchange. Thus, it is conceivable that the inversion of NVC after SAH represents an adaptive response promoting the clearance of bloody CSF.

Our data indicate that SAH-induced high-amplitude Ca^{2+} signaling events, in the form of eHACSs, result from increased Ca^{2+} release from subcellular ER stores (Fig. 4).

However, the cellular basis underlying the enhanced release of Ca^{2+} after SAH remains to be determined. An increase in ER Ca^{2+} load, or increased expression/sensitivity of IP_3 receptors could potentially contribute to the emergence of eHACSs after SAH. However, increased production of IP_3 could also underlie SAH-induced eHACSs. It is generally appreciated that endfoot Ca^{2+} signals result from activation of G_q -coupled receptors and the production of IP_3 (Fiacco and McCarthy, 2006; Straub et al., 2006). Astrocytes express a multitude of G_q -coupled receptors that could play a role in the generation of eHACSs. Previously, purinergic signaling was been implicated in the hyperactive Ca^{2+} signaling phenotype observed in reactive astrocytes in an Alzheimer's disease model (Delekate et al., 2014). Further, the G^q -coupled purinergic receptors, P2Y_2 and P2Y_4 , are expressed in astrocyte endfeet (Simard et al., 2003), and up-regulation of purinergic signaling has been implicated after SAH (Kasseckert et al., 2013). Interestingly, astrocyte lysosomes are capable of ATP release (Zhang et al., 2007) and we observed organelles appearing to be lysosomes in endfeet of SAH, but not control animals (Fig. 5A). There is strong evidence from Alzheimer's disease models that astrocyte lysosomes are involved in the clearance of β -amyloid plaques (Funato et al., 1998; Wyss-Coray et al., 2003). Considering the distribution of red blood cells and blood products along the parenchymal arteriolar walls after SAH (Koide et al., 2012), the presence of enlarged endfeet containing lysosomes in our TEM samples may indicate a role for astrocytes in the clearance of extravascular blood components. However, future studies are necessary to determine the role of reactive astrogliosis and purinergic signaling in the development of SAH-induced eHACSs and inversion of NVC.

In summary, our results indicate a causal link between the emergence of high-amplitude spontaneous Ca^{2+} events in astrocyte endfeet (i.e. eHACs) and SAH-induced inversion of NVC. These findings identify astrocytes as a key player in SAH-induced disruption of cortical blood flow. Further work targeting the impact of SAH on astrocyte function may lead to the development of new therapeutic strategies to treat brain pathologies such as hemorrhagic stroke.

References

- Al-Khindi T, Macdonald RL, Schweizer TA (2010) Cognitive and functional outcome after aneurysmal subarachnoid hemorrhage. *Stroke* 41:e519-e536.
- Anderson CM, Nedergaard M (2003) Astrocyte-mediated control of cerebral microcirculation. *Trends Neurosci* 26:340-344.
- Araque A, Parpura V, Sanzgiri RP, Haydon PG (1999) Tripartite synapses: glia, the unacknowledged partner. *Trends Neurosci* 22:208-215.
- Attwell D, Buchan AM, Chrapak S, Lauritzen M, Macvicar BA, Newman EA (2010) Glial and neuronal control of brain blood flow. *Nature* 468:232-243.
- Bai JP, Surguchev A, Navaratnam D (2011) β 4-subunit increases *Slo* responsiveness to physiological Ca^{2+} concentrations and together with β 1 reduces surface expression of *Slo* in hair cells. *Am J Physiol Cell Physiol* 300:C435-C446.
- Burda JE, Sofroniew MV (2014) Reactive gliosis and the multicellular response to CNS damage and disease. *Neuron* 81:229-248.
- Delekate A, Fuchtemeier M, Schumacher T, Ulbrich C, Foddis M, Petzold GC (2014) Metabotropic P2Y₁ receptor signalling mediates astrocytic hyperactivity *in vivo* in an Alzheimer's disease mouse model. *Nat Commun* 5:5422.
- Dreier JP, Sakowitz OW, Harder A, Zimmer C, Dirnagl U, Valdueza JM, Unterberg AW (2002) Focal laminar cortical MR signal abnormalities after subarachnoid hemorrhage. *Ann Neurol* 52:825-829.
- Dunn KM, Hill-Eubanks DC, Liedtke WB, Nelson MT (2013) TRPV4 channels stimulate Ca^{2+} -induced Ca^{2+} release in astrocytic endfeet and amplify neurovascular coupling responses. *Proc Natl Acad Sci U S A* 110:6157-6162.
- Fiacco TA, McCarthy KD (2006) Astrocyte calcium elevations: properties, propagation, and effects on brain signaling. *Glia* 54:676-690.
- Filosa JA, Bonev AD, Straub SV, Meredith AL, Wilkerson MK, Aldrich RW, Nelson MT (2006) Local potassium signaling couples neuronal activity to vasodilation in the brain. *Nat Neurosci* 9:1397-1403.
- Funato H, Yoshimura M, Yamazaki T, Saido TC, Ito Y, Yokofujita J, Okeda R, Ihara Y (1998) Astrocytes containing amyloid β -protein (A β)-positive granules are associated with A β 40-positive diffuse plaques in the aged human brain. *Am J Pathol* 152:983-992.

- Girouard H, Bonev AD, Hannah RM, Meredith A, Aldrich RW, Nelson MT (2010) Astrocytic endfoot Ca^{2+} and BK channels determine both arteriolar dilation and constriction. *Proc Natl Acad Sci U S A* 107:3811-3816.
- Hayat MA (1981) Fixation for electron microscopy. New York, New York: Academic Press, Inc.
- Hijdra A, van GJ, Stefanko S, Van Dongen KJ, Vermeulen M, Van CH (1986) Delayed cerebral ischemia after aneurysmal subarachnoid hemorrhage: clinicoanatomic correlations. *Neurology* 36:329-333.
- Horrigan FT, Aldrich RW (2002) Coupling between voltage sensor activation, Ca^{2+} binding and channel opening in large conductance (BK) potassium channels. *J Gen Physiol* 120:267-305.
- Iadecola C (1993) Regulation of the cerebral microcirculation during neural activity: is nitric oxide the missing link? *Trends Neurosci* 16:206-214.
- Ilf JJ, Wang M, Liao Y, Plog BA, Peng W, Gundersen GA, Benveniste H, Vates GE, Deane R, Goldman SA, Nagelhus EA, Nedergaard M (2012) A paravascular pathway facilitates CSF flow through the brain parenchyma and the clearance of interstitial solutes, including amyloid β . *Sci Transl Med* 4:147ra111.
- Ilf JJ, Wang M, Zeppenfeld DM, Venkataraman A, Plog BA, Liao Y, Deane R, Nedergaard M (2013) Cerebral arterial pulsation drives paravascular CSF-interstitial fluid exchange in the murine brain. *J Neurosci* 33:18190-18199.
- Ishiguro M, Puryear CB, Bisson E, Saundry CM, Nathan DJ, Russell SR, Tranmer BI, Wellman GC (2002) Enhanced myogenic tone in cerebral arteries from a rabbit model of subarachnoid hemorrhage. *Am J Physiol Heart Circ Physiol* 283:H2217-H2225.
- Ishiguro M, Wellman TL, Honda A, Russell SR, Tranmer BI, Wellman GC (2005) Emergence of a R-type Ca^{2+} channel ($\text{Cav} 2.3$) contributes to cerebral artery constriction after subarachnoid hemorrhage. *Circ Res* 96:419-426.
- Kasseckert SA, Shahzad T, Miqdad M, Stein M, Abdallah Y, Scharbrodt W, Oertel M (2013) The mechanisms of energy crisis in human astrocytes after subarachnoid hemorrhage. *Neurosurgery* 72:468-474.
- Kawamura M, Kawamura M (2011) Long-term facilitation of spontaneous calcium oscillations in astrocytes with endogenous adenosine in hippocampal slice cultures. *Cell Calcium* 49:249-258.

- Knot HJ, Nelson MT (1998) Regulation of arterial diameter and wall $[Ca^{2+}]$ in cerebral arteries of rat by membrane potential and intravascular pressure. *J Physiol* 508 (Pt 1):199-209.
- Knot HJ, Zimmermann PA, Nelson MT (1996) Extracellular K^+ -induced hyperpolarizations and dilatations of rat coronary and cerebral arteries involve inward rectifier K^+ channels. *J Physiol* 492 (Pt 2):419-430.
- Koide M, Bonev AD, Nelson MT, Wellman GC (2012) Inversion of neurovascular coupling by subarachnoid blood depends on large-conductance Ca^{2+} -activated K^+ (BK) channels. *Proc Natl Acad Sci U S A* 109:E1387-E1395.
- Koide M, Sukhotinsky I, Ayata C, Wellman GC (2013) Subarachnoid hemorrhage, spreading depolarizations and impaired neurovascular coupling. *Stroke Res Treat* 2013:819340.
- Koide M, Wellman GC (2015) Activation of TRPV4 channels does not mediate inversion of neurovascular coupling after SAH. *Acta Neurochir Suppl* 120:111-116.
- Link TE, Murakami K, Beem-Miller M, Tranmer BI, Wellman GC (2008) Oxyhemoglobin-induced expression of R-type Ca^{2+} channels in cerebral arteries. *Stroke* 39:2122-2128.
- Maravall M, Mainen ZF, Sabatini BL, Svoboda K (2000) Estimating intracellular calcium concentrations and buffering without wavelength ratioing. *Biophys J* 78:2655-2667.
- Mathiisen TM, Lehre KP, Danbolt NC, Ottersen OP (2010) The perivascular astroglial sheath provides a complete covering of the brain microvessels: an electron microscopic 3D reconstruction. *Glia* 58:1094-1103.
- McCaslin AF, Chen BR, Radosevich AJ, Cauli B, Hillman EM (2011) *In vivo* 3D morphology of astrocyte-vasculature interactions in the somatosensory cortex: implications for neurovascular coupling. *J Cereb Blood Flow Metab* 31:795-806.
- Murakami K, Koide M, Dumont TM, Russell SR, Tranmer BI, Wellman GC (2011) Subarachnoid Hemorrhage Induces Gliosis and Increased Expression of the Pro-inflammatory Cytokine High Mobility Group Box 1 Protein. *Transl Stroke Res* 2:72-79.
- Nagelhus EA, Horio Y, Inanobe A, Fujita A, Haug FM, Nielsen S, Kurachi Y, Ottersen OP (1999) Immunogold evidence suggests that coupling of K^+ siphoning and water transport in rat retinal Muller cells is mediated by a coenrichment of Kir4.1 and AQP4 in specific membrane domains. *Glia* 26:47-54.

- Nishimura N, Schaffer CB, Friedman B, Lyden PD, Kleinfeld D (2007) Penetrating arterioles are a bottleneck in the perfusion of neocortex. *Proc Natl Acad Sci U S A* 104:365-370.
- Nystoriak MA, O'Connor KP, Sonkusare SK, Brayden JE, Nelson MT, Wellman GC (2011) Fundamental increase in pressure-dependent constriction of brain parenchymal arterioles from subarachnoid hemorrhage model rats due to membrane depolarization. *Am J Physiol Heart Circ Physiol* 300:H803-H812.
- Ostergaard L, Aamand R, Karabegovic S, Tietze A, Blicher JU, Mikkelsen IK, Iversen NK, Secher N, Engedal TS, Anzabi M, Jimenez EG, Cai C, Koch KU, Naess-Schmidt ET, Obel A, Juul N, Rasmussen M, Sorensen JC (2013) The role of the microcirculation in delayed cerebral ischemia and chronic degenerative changes after subarachnoid hemorrhage. *J Cereb Blood Flow Metab* 33:1825-1837.
- Parri HR, Gould TM, Crunelli V (2001) Spontaneous astrocytic Ca^{2+} oscillations *in situ* drive NMDAR-mediated neuronal excitation. *Nat Neurosci* 4:803-812.
- Pluta RM, Hansen-Schwartz J, Dreier J, Vajkoczy P, Macdonald RL, Nishizawa S, Kasuya H, Wellman G, Keller E, Zauner A, Dorsch N, Clark J, Ono S, Kiris T, Leroux P, Zhang JH (2009) Cerebral vasospasm following subarachnoid hemorrhage: time for a new world of thought. *Neurol Res* 31:151-158.
- Price DL, Ludwig JW, Mi H, Schwarz TL, Ellisman MH (2002) Distribution of *rSlo* Ca^{2+} -activated K^{+} channels in rat astrocyte perivascular endfeet. *Brain Res* 956:183-193.
- Rabinstein AA, Weigand S, Atkinson JL, Wijdicks EF (2005) Patterns of cerebral infarction in aneurysmal subarachnoid hemorrhage. *Stroke* 36:992-997.
- Seidel KN, Derst C, Salzmann M, Holtje M, Priller J, Markgraf R, Heinemann SH, Heilmann H, Skatchkov SN, Eaton MJ, Veh RW, Pruss H (2011) Expression of the voltage- and Ca^{2+} -dependent BK potassium channel subunits BK β 1 and BK β 4 in rodent astrocytes. *Glia* 59:893-902.
- Shigetomi E, Bushong EA, Hausteiner MD, Tong X, Jackson-Weaver O, Kracun S, Xu J, Sofroniew MV, Ellisman MH, Khakh BS (2013) Imaging calcium microdomains within entire astrocyte territories and endfeet with GCaMPs expressed using adeno-associated viruses. *J Gen Physiol* 141:633-647.
- Simard M, Arcuino G, Takano T, Liu QS, Nedergaard M (2003) Signaling at the gliovascular interface. *J Neurosci* 23:9254-9262.

- Sofroniew MV (2009) Molecular dissection of reactive astrogliosis and glial scar formation. *Trends Neurosci* 32:638-647.
- Srinivasan R, Huang BS, Venugopal S, Johnston AD, Chai H, Zeng H, Golshani P, Khakh BS (2015) Ca²⁺ signaling in astrocytes from IP₃R2^{-/-} mice in brain slices and during startle responses *in vivo*. *Nat Neurosci* 18:708-717.
- Straub SV, Bonev AD, Wilkerson MK, Nelson MT (2006) Dynamic inositol trisphosphate-mediated calcium signals within astrocytic endfeet underlie vasodilation of cerebral arterioles. *J Gen Physiol* 128:659-669.
- Wellman GC (2006) Ion channels and calcium signaling in cerebral arteries following subarachnoid hemorrhage. *Neurol Res* 28:690-702.
- Wyss-Coray T, Loike JD, Brionne TC, Lu E, Anankov R, Yan F, Silverstein SC, Husemann J (2003) Adult mouse astrocytes degrade amyloid- β *in vitro* and *in situ*. *Nat Med* 9:453-457.
- Xie L, Kang H, Xu Q, Chen MJ, Liao Y, Thiyagarajan M, O'Donnell J, Christensen DJ, Nicholson C, Iliff JJ, Takano T, Deane R, Nedergaard M (2013) Sleep drives metabolite clearance from the adult brain. *Science* 342:373-377.
- Zaritsky JJ, Eckman DM, Wellman GC, Nelson MT, Schwarz TL (2000) Targeted disruption of Kir2.1 and Kir2.2 genes reveals the essential role of the inwardly rectifying K⁺ current in K⁺-mediated vasodilation. *Circ Res* 87:160-166.
- Zhang Z, Chen G, Zhou W, Song A, Xu T, Luo Q, Wang W, Gu XS, Duan S (2007) Regulated ATP release from astrocytes through lysosome exocytosis. *Nat Cell Biol* 9:945-953.
- Zonta M, Angulo MC, Gobbo S, Rosengarten B, Hossmann KA, Pozzan T, Carmignoto G (2003) Neuron-to-astrocyte signaling is central to the dynamic control of brain microcirculation. *Nat Neurosci* 6:43-50.

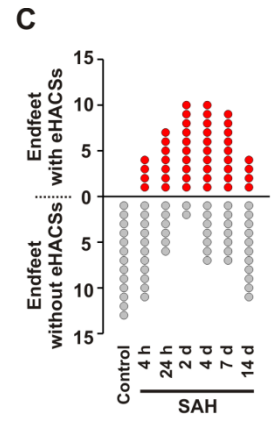
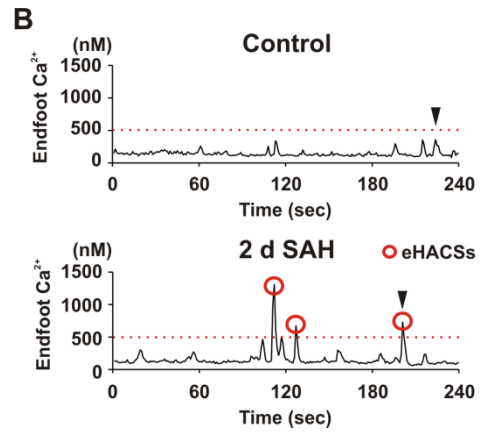
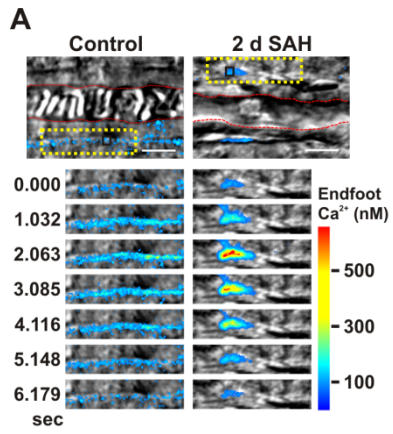


Figure 2-1. Emergence of endfoot high-amplitude Ca²⁺ signals (eHACS) following SAH

A, (Top) Images of parenchymal arterioles and surrounding astrocyte endfeet in brain slices obtained from control (left) and 2 d SAH model rats (right). The red dashed lines on grey-scale IR-DIC images depict intraluminal diameter. Overlapping pseudocolor-mapped fluorescent Ca²⁺ images of endfeet were simultaneously acquired using two-photon microscopy. Scale bars are 10 μ m. (Bottom) Time-lapse images from the area within the yellow dotted box in top panels. *B*, Spontaneous Ca²⁺ activity recorded from 1.2 x 1.2 μ m regions of interest shown in the black squares in panel *A*. Black arrowheads indicate the spontaneous Ca²⁺ events depicted in the time-lapse series of *A*. Red circles indicate eHACSs (peak Ca²⁺ levels \geq 500 nM). *C*, Number of endfeet with and without eHACSs (red and gray dots, respectively) observed in control ($N = 8$ animals) and SAH model animals ($N = 6-8$ animals per time point). χ^2 analysis indicates an association between the incidence of endfeet exhibiting eHACSs and time (4 h, 2 and 4 d) post-SAH ($\chi^2 = 8.839$, $df = 2$, $p = 0.012$).

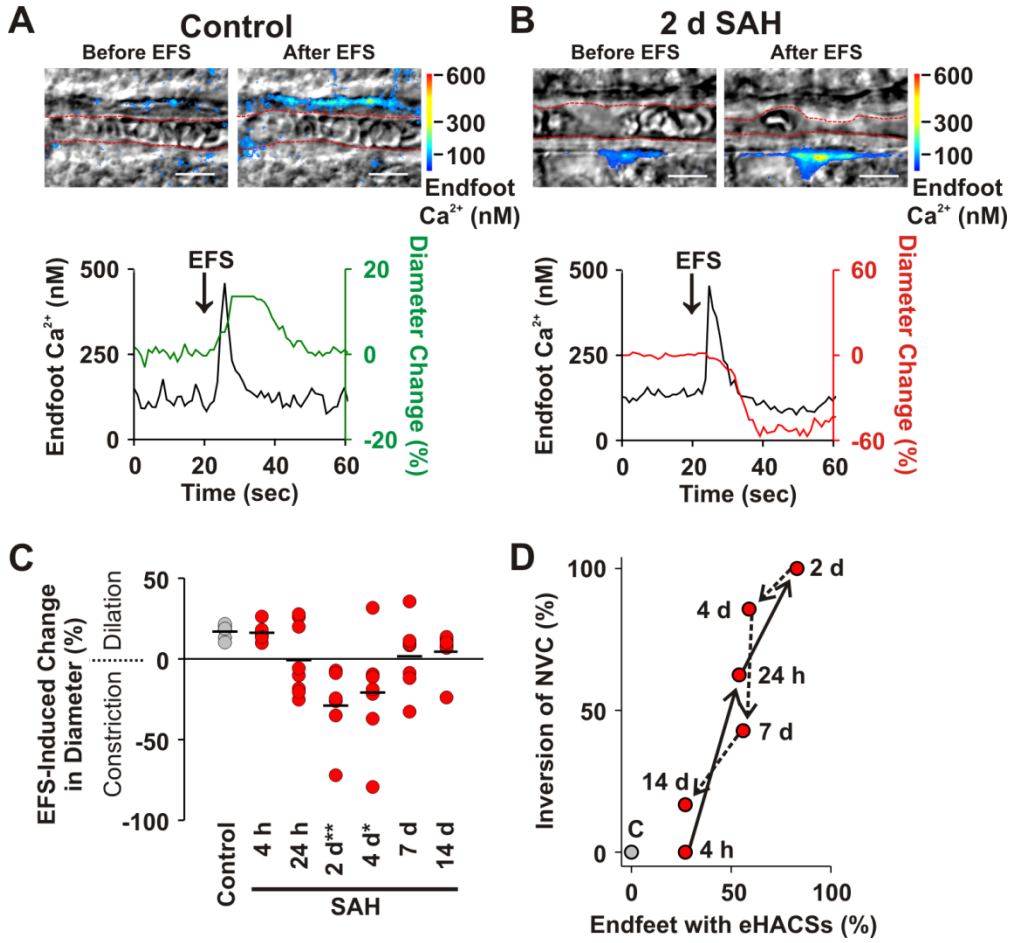


Figure 2-2. The inversion of NVC parallels the emergence of eHACs in brain slices from SAH model animals.

A, B, EFS-induced changes in arteriolar diameter and astrocyte endfoot Ca^{2+} in brain slices from control (*A*) and 2 d SAH animals (*B*). (Top) IR-DIC images with simultaneously acquired pseudo-colored Ca^{2+} fluorescence maps showing arteriolar diameter (depicted in red dashed line) and astrocyte endfoot Ca^{2+} before and after EFS. Scale bars are 10 μm . (Bottom) EFS-evoked changes in endfoot Ca^{2+} and arteriolar diameter corresponding to the above images. Although EFS caused a similar increase in astrocyte endfoot Ca^{2+} (black traces), it was associated vasodilation (green trace) in brain slices from control animals and vasoconstriction (red trace) in brain slices from 2 d SAH animals. *C*, Summary of EFS-induced arteriolar responses in brain slices from control and SAH model animals. Black lines represent the mean change in diameter per study group ($n = 6-8$ arterioles from 4-6 animals per group). $*p < 0.05$; $**p < 0.01$ (one-way ANOVA, followed by Bonferroni's *post hoc* test). *D*, Relationship between the percentage of endfeet with eHACs and percentage of arterioles exhibiting inversion of NVC at various time-points after induction of SAH. Arrows demonstrate the progression of time.

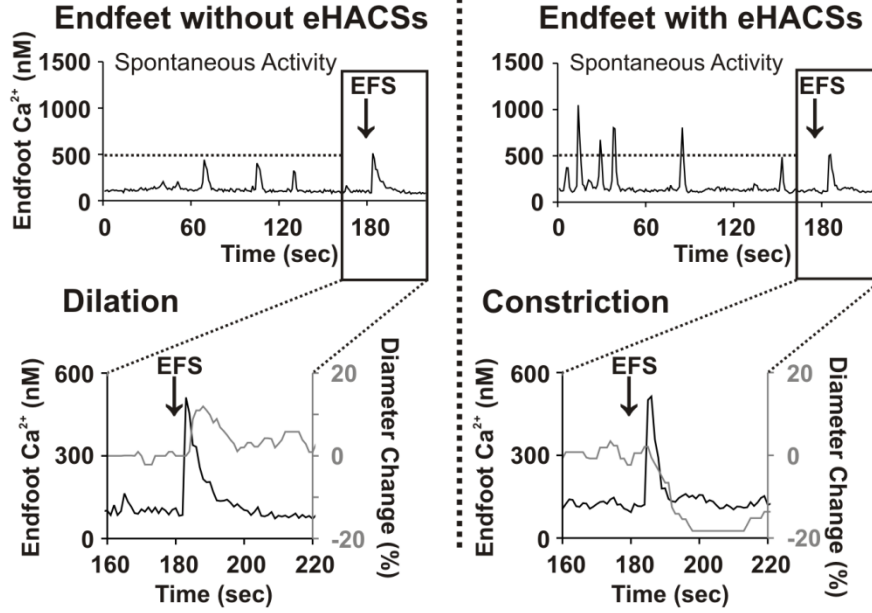
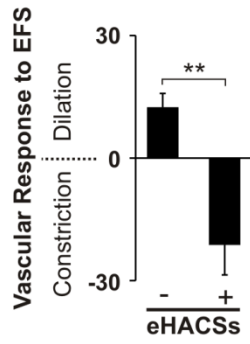
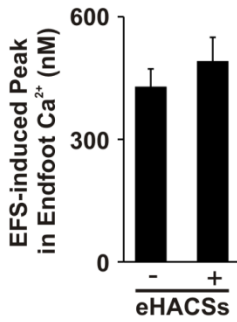
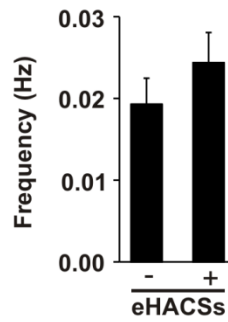
A**24 h SAH****B****C****D**

Figure 2-3. The presence of eHACSs is associated with inversion of NVC.

A, Continuous in tandem recordings of spontaneous Ca^{2+} events and EFS-evoked changes in arteriolar diameter and astrocyte endfoot Ca^{2+} from brain slices of 24 h SAH animals. In brain slices with endfeet lacking eHACSs (left), EFS triggered a rise in endfoot Ca^{2+} and vasodilation of the adjacent arteriole. However, when eHACSs were present in the surrounding endfeet (right), a similar EFS-evoked rise in endfoot Ca^{2+} elicited vasoconstriction (i.e., inversion of NVC). *B*, Summary of EFS-induced changes in arteriolar diameter in brains slices with and without endfeet exhibiting eHACSs ($n = 4$ or 5 arterioles, $N = 4$ or 5 animals). ** $p < 0.01$ (two-tailed t test). *C*, Summary of the EFS-induced rise in endfoot Ca^{2+} in brain slices with or without eHACSs ($n = 7-11$ endfeet, $N = 4-5$ animals). *D*, Summary of the frequency of spontaneous Ca^{2+} events in brain slices with or without eHACSs ($n = 7-11$ endfeet, $N = 4$ or 5 animals).

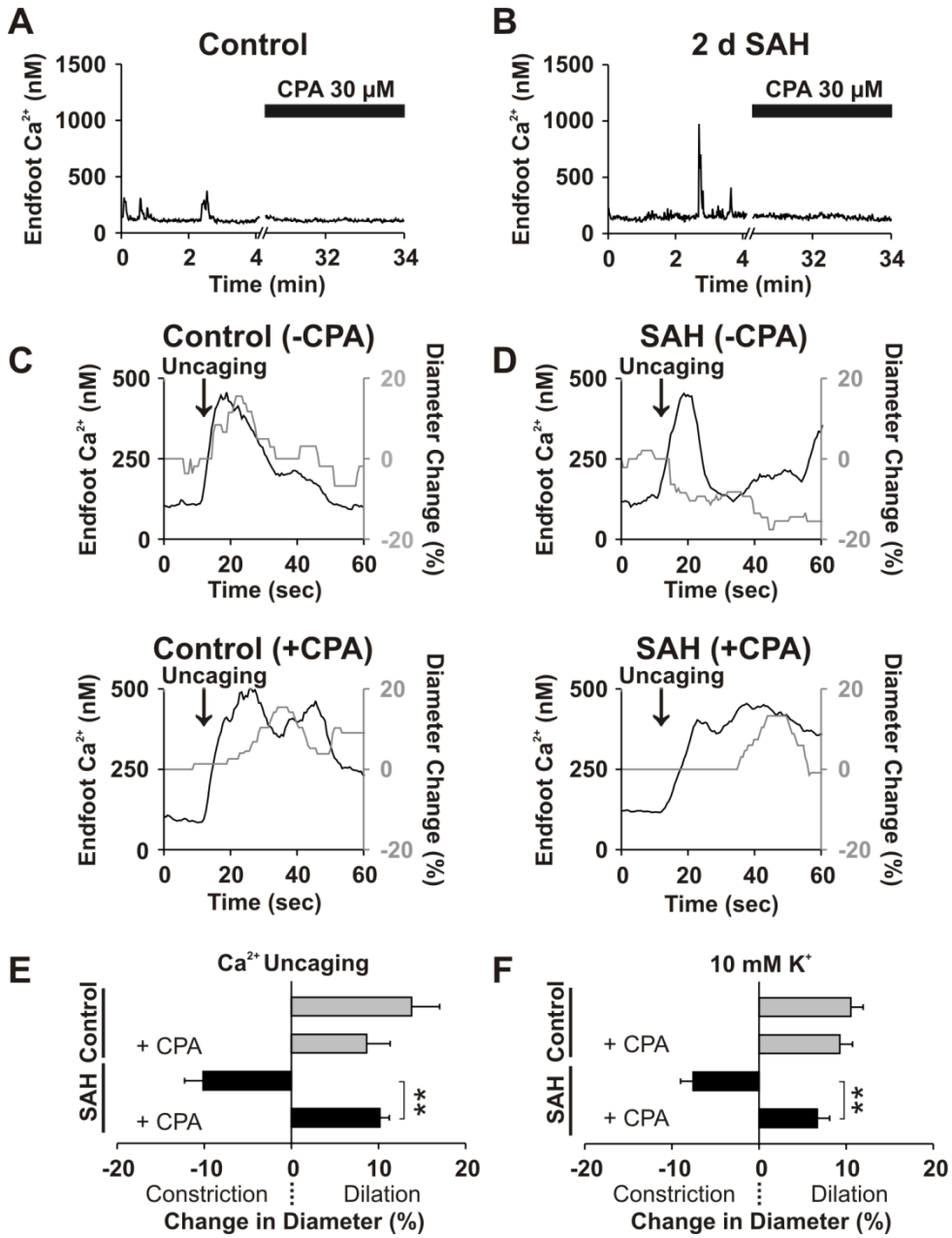


Figure 2-4. Abolishing eHACSs restores arteriolar dilation in brain slices from SAH animals

A,B, Depletion of intracellular Ca^{2+} stores with cyclopiazonic acid (CPA, 30 μM) treatment abolished spontaneous Ca^{2+} events in astrocyte endfeet from control and 2 d SAH animals ($n = 5-6$ endfeet per group, $N = 4$ animals per group). *C,D*, Changes in endfoot Ca^{2+} and arteriolar diameter evoked by photolysis (uncaging) of caged- Ca^{2+} in brain slices from control (*C*) and 2 d SAH animals (*D*), with (top) or without spontaneous Ca^{2+} signals (bottom), i.e., \pm CPA treatment. *E*, Summary data depicting percent change in arteriolar diameter induced by Ca^{2+} uncaging in the presence or absence of CPA ($n = 4$ arterioles per group, $N = 3-4$ animals per group). *F*, Summary data depicting percent change in diameter evoked by increasing extracellular K^+ in ACSF superfusate from 3 mM to 10 mM in the presence or absence of CPA ($n = 6-10$ arterioles per group, $N = 4-5$ animals per group). ** $p < 0.01$ (two-tailed t test).

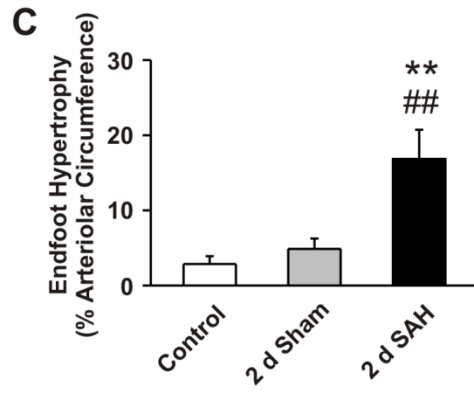
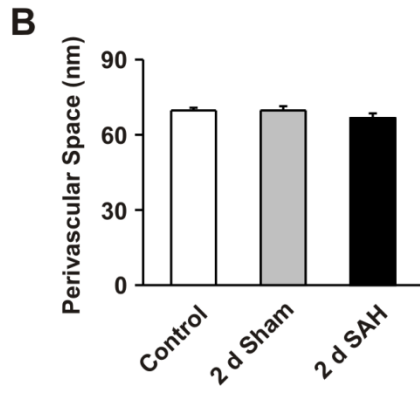
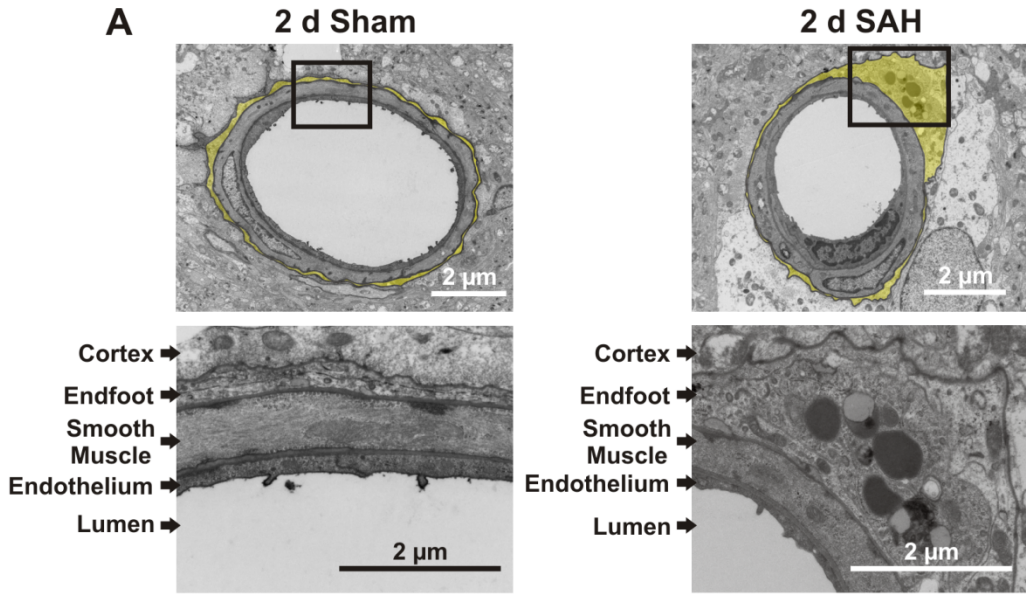


Figure 2-5. Astrocyte endfeet with asymmetrical hypertrophy encase parenchymal arterioles following SAH

A, (Top) Low-magnification TEM images of parenchymal arterioles in cerebral cortices obtained from 2 d sham-operated and 2 d SAH model animals. Astrocyte endfeet are highlighted in yellow. (Bottom) High-magnification images of the arteriolar wall (endothelial and smooth muscle cell layers) as well as the surrounding astrocyte endfoot from within the black boxes. Lysosomes (round electron dense structures) were only observed in areas of enlarged endfeet from SAH animals. *B*, Distance between astrocyte endfeet and arteriolar smooth muscle (i.e., width of the perivascular space) measured at 10 random equally spaced locations along the arteriolar circumference. ($n = 16-27$ arterioles per group, $N = 4-5$ animals per group). *C*, Summary of endfoot hypertrophy. Data are presented as the percentage of the arteriolar circumference surrounded by an enlarged endfoot (i.e., >3 times the mean thickness of control endfeet) ($n = 16-27$ arterioles per group, $N = 4-5$ animals per group). ** $p < 0.01$ vs control, ## $p < 0.01$ vs sham (one-way ANOVA, followed by the Tukey test).

Table 2-1. Impact of SAH on spontaneous Ca²⁺ events in astrocyte endfeet

	Control	4 h SAH	24 h SAH	2 d SAH	4 d SAH	7 d SAH	14 d SAH
Endfeet without eHACSSs							
Basal endfoot Ca ²⁺ (nM)	128 ± 4	121 ± 3 _{ns}	125 ± 7 _{ns}	134 ± 19 _{ns}	128 ± 7 _{ns}	121 ± 6 _{ns}	125 ± 4 _{ns}
Range of Ca ²⁺ event amplitudes (nM)	179 – 496	166 – 484	161 – 477	214 – 496	208 – 458	192 – 491	187 – 470
Mean amplitude (nM)	302 ± 10	270 ± 11 _{ns}	300 ± 17 _{ns}	348 ± 31 _{ns}	310 ± 14 _{ns}	313 ± 18 _{ns}	293 ± 11 _{ns}
Frequency of spontaneous Ca ²⁺ events (Hz)	0.024 ± 0.003	0.021 ± 0.004 _{ns}	0.022 ± 0.005 _{ns}	0.020 ± 0.011 _{ns}	0.017 ± 0.002 _{ns}	0.024 ± 0.003 _{ns}	0.019 ± 0.004 _{ns}
<i>n, N</i> (endfeet, animals)	13, 8	11, 4	6, 5	2, 7	7, 6	7, 5	11, 5
Endfeet with eHACSSs							
Basal endfoot Ca ²⁺ (nM)	-	124 ± 7	128 ± 3 _{NS}	127 ± 4 _{NS}	129 ± 4 _{NS}	131 ± 6 _{NS}	131 ± 4 _{NS}
Range of Ca ²⁺ event amplitudes (nM)	-	181 – 866	229 – 1618	182 – 1323	197 – 1141	195 – 1244	218 – 871
Mean amplitude of control-like events (nM)	-	294 ± 18	321 ± 16 _{NS}	312 ± 11 _{NS}	292 ± 14 _{NS}	289 ± 15 _{NS}	356 ± 24 _{NS}
Mean amplitude of eHACSSs (nM)	-	605 ± 43	738 ± 72 _{NS}	691 ± 40 _{NS}	769 ± 55 _{NS}	770 ± 73 _{NS}	758 ± 32 _{NS}
Frequency of spontaneous Ca ²⁺ events (Hz)	-	0.025 ± 0.005	0.024 ± 0.005 _{NS}	0.034 ± 0.004 _{NS}	0.019 ± 0.004 _{NS}	0.017 ± 0.002 _{NS}	0.019 ± 0.004 _{NS}
eHACSSs (percent of total events)	-	39.5 ± 12.6	41.0 ± 3.4 _{NS}	37.6 ± 8.5 _{NS}	46.6 ± 9.7 _{NS}	39.6 ± 8.6 _{NS}	32.7 ± 12.1 _{NS}
<i>n, N</i> (endfeet, animals)	0, 8	4, 4	7, 5	10, 7	10, 6	9, 5	4, 5

All Endfeet

Total spontaneous Ca ²⁺ events	73	81	72	94	78	63	70
--	----	----	----	----	----	----	----

One-way analysis of variance (ANOVA) followed by Bonferroni test were used for the *post hoc* comparison of multiple groups. ns: not statistically different ($p > 0.05$) compared to control group in endfeet without eHACs. NS: not statistically different ($p > 0.05$) compared to 4 h SAH group in endfeet with eHACs.

Table 2-2. Impact of SAH on NVC

	Control	4 h SAH	24 h SAH	2 d SAH	4 d SAH	7 d SAH	14 d SAH
Brain slices with intact NVC (i.e. arteriolar dilation)							
Arteriolar diameter before EFS (μm)	8.7 \pm 1.3	6.5 \pm 0.8	5.0 \pm 0.6	-	6.8	8.3 \pm 0.8	6.1 \pm 0.7
Endfoot Ca^{2+} before EFS (nM)	139 \pm 19	127 \pm 8	137 \pm 8	-	137	128 \pm 6	123 \pm 8
Endfoot Ca^{2+} after EFS (nM)	421 \pm 39	427 \pm 30	404 \pm 32	-	388	378 \pm 38	413 \pm 27
<i>n, N</i> (slices, animals)	6, 6	6, 5	3, 4	0, 5	1, 5	4, 6	5, 4
Brain slices with inversion of NVC (i.e. arteriolar constriction)							
Arteriolar diameter before EFS (μm)	-	-	5.7 \pm 0.8	7.2 \pm 1.5	9.2 \pm 1.6	5.1 \pm 1.0	4.2
Endfoot Ca^{2+} before EFS (nM)	-	-	128 \pm 6	128 \pm 4	135 \pm 3	122 \pm 5	122
Endfoot Ca^{2+} after EFS (nM)	-	-	361 \pm 16	377 \pm 24	394 \pm 37	440 \pm 15	361
<i>n, N</i> (slices, animals)	0, 6	0, 5	5, 4	7, 5	6, 5	3, 6	1, 4

Chapter 3: Purinergic signaling triggers endfoot high-amplitude Ca²⁺ signals and causes inversion of neurovascular coupling after subarachnoid hemorrhage

Anthony C. Pappas¹, Masayo Koide¹, George C. Wellman^{1,2}

Departments of Pharmacology¹ and Surgery², Division of Neurosurgery, University of Vermont, 89 Beaumont Ave, Burlington, VT 05405-0068, USA

Abstract

Neurovascular coupling (NVC) is the process whereby astrocytes match focal increases in neuronal activity with local arteriolar dilation by releasing vasoactive substances (e.g. K^+ ions) from perivascular endfeet. Previously, we demonstrated that an emergence of endfoot high-amplitude Ca^{2+} signals (eHACSs) after subarachnoid hemorrhage (SAH) caused a pathological shift in NVC from vasodilation to vasoconstriction. Extracellular purine nucleotides (e.g. ATP) can trigger astrocyte Ca^{2+} oscillations, and may be elevated following SAH. Here, we imaged Fluo-4-loaded rat brain slices using two-photon fluorescence microscopy to determine the role of purinergic signaling in the generation of SAH-induced eHACSs and inversion of NVC. We report that broad-spectrum inhibition of purinergic (P2) receptors using suramin selectively blocked eHACSs and restored vasodilatory NVC in brain slices from SAH animals. Importantly, eHACSs were selectively abolished using a cocktail of inhibitors targeting G_q -coupled P2Y receptors. Further, activation of P2Y receptors in brain slices from un-operated animals triggered high-amplitude Ca^{2+} events resembling eHACSs and disrupted NVC. Neither tetrodotoxin nor bafilomycin A1 had an effect on eHACSs suggesting that purine nucleotides are not released by ongoing neurotransmission after SAH. Together, these results indicate that purinergic signaling via P2Y receptors contributes to SAH-induced eHACSs and inversion of NVC.

Introduction

Aneurysmal subarachnoid hemorrhage (SAH) is associated with substantial morbidity and mortality against which current therapeutic options have limited efficacy¹. The development of multifocal cortical infarcts days to weeks after the initial bleed is a frequent complication jeopardizing the survival and long-term outcome of SAH patients²⁻⁴. Perfusion deficits within brain cortex are generally appreciated to contribute to the widespread ischemia following SAH^{5,6}. However, the signaling pathways linking SAH to micro-vascular dysfunction are not fully understood.

Intra-cerebral (parenchymal) arterioles represent a significant bottleneck to cortical perfusion, and are regulated extrinsically by surrounding astrocyte endfeet^{7,8}. In the healthy brain, increased neuronal activity triggers a rise in astrocyte endfoot Ca^{2+} causing the release of vasoactive substances (e.g. K^+ ions) into the restricted perivascular space and parenchymal arteriolar dilation⁹. This functional hyperemic response, also referred to as neurovascular coupling (NVC), ensures adequate delivery of O_2 and other nutrients to areas of the brain with increased metabolic demand. Previously, we demonstrated that an emergence of spontaneous endfoot high-amplitude Ca^{2+} signals (eHACSs) caused inversion of NVC from vasodilation to vasoconstriction in brain slices obtained from SAH model animals^{10,11}. A shift in NVC from vasodilation to vasoconstriction may contribute to the development of focal ischemia after SAH by restricting blood flow to active brain regions. However, the cellular basis underlying the generation of eHACSs after SAH has not been determined.

The goal of this study was to determine whether enhanced purinergic signaling underlies the generation of eHACSs and inversion of NVC after SAH. Astrocytes broadly express both ionotropic and metabotropic purinergic receptors that trigger a rise in intracellular Ca^{2+} when activated^{12, 13}. Increased signaling via extracellular purine nucleotides (e.g. ATP) is common after brain injury; including aneurysmal SAH^{12, 14} and studies have reported elevated levels of ATP in the cerebral spinal fluid (CSF) after SAH^{14, 15}. Interestingly, purinergic signaling has also been reported to cause aberrant astrocyte Ca^{2+} elevations that are associated with vascular instability and disrupted NVC in a mouse model of Alzheimer's disease^{16, 17}.

Here, using combined infrared-differential interference contrast (IR-DIC) and two-photon fluorescence microscopy, we report that inhibition of G_q -coupled P2Y purinergic receptors abolished eHACSs and restored vasodilatory NVC in brain slices obtained from SAH model animals. However, block of P2Y receptors did not affect astrocyte Ca^{2+} signaling in brain slices from control animals and inhibition of ionotropic P2X receptors did not alter Ca^{2+} signaling in either the control or SAH groups. Further, we show that activation of P2Y receptors in brain slices from control animals mimicked SAH by triggering high-amplitude endfoot Ca^{2+} events resembling eHACSs and disrupting NVC responses. This work identifies astrocyte P2Y receptors as an important component of SAH pathology and a novel potential therapeutic target in the treatment of micro-vascular dysfunction following cerebral aneurysm rupture.

Materials and Methods

Rat SAH model. The double-injection cisterna magna model was used to mimic aneurysmal SAH, as previously described^{10, 18}. Briefly, autologous, unheparanized arterial blood (0.5 mL drawn from the tail artery) was injected into the cisterna magna of isoflurane-anesthetized Sprague-Dawley rats (male, 10-12 weeks old, Charles River Laboratories). This surgical procedure was repeated following a 24 h recovery period. SAH model animals were euthanized at 2 d (48 h) following the first injection of subarachnoid blood. The 2 d SAH time point was chosen because we previously found that at this time point the vast majority of astrocyte endfeet (~80%) exhibit eHACSs; defined as spontaneous (i.e., non-stimulated) events with endfoot Ca^{2+} exceeding 500 nM¹¹. The 2 d SAH time-point also coincided with the highest percentage (100%) of brain slices exhibiting inversion of NVC. Un-operated animals served as the control group. All procedures were conducted in accordance with the Guide for the Care and Use of Laboratory Animals (eighth edition, 2011) and followed protocols approved by the Institutional Animal Care and Use Committee at the University of Vermont.

Simultaneous measurement of arteriolar diameter and astrocyte endfoot Ca^{2+} in cortical brain slices.

Brain slice preparation: Animals were euthanized by decapitation while under deep anesthesia with pentobarbital (60 mg/kg). Coronal brain slices (160 μm thick) were cut in ice-cold, aerated (5 % $\text{CO}_2/95$ % O_2) artificial cerebral spinal fluid (ACSF) using a Leica VT1000S vibratome. Brain slices were incubated with the fluorescent Ca^{2+} indicator, Fluo-4 AM (10 μM) for 1.5 h at 29 °C in aerated ACSF containing 0.04 %

pluronic acid. Under these conditions, Fluo-4 preferentially loads into astrocytes ¹⁹. After incubating with Fluo-4 AM, brain slices were rinsed and maintained in aerated ACSF at room temperature prior to imaging.

Simultaneous recordings of arteriolar diameter and endfoot Ca^{2+} : A BioRad Radiance multi-photon imaging system (excitation wavelength: 820 nm, fluorescent bandpass filter: 575/150 nm, sampling frequency ~1 Hz) coupled to a Coherent Chameleon Ti-Sapphire laser was used to simultaneously obtain infrared-differential interference contrast (IR-DIC) and fluorescent brain slices images. Arteriolar segments (cortical layer 2/3, middle cerebral artery territory) that were surrounded by fluo-4-loaded endfeet were chosen for study. Spontaneous endfoot Ca^{2+} signals were recorded in the absence of stimulation. NVC was initiated using electrical field stimulation (EFS; 50 Hz, 0.3 ms alternating square pulse, 3 s duration) to trigger neuronal action potentials ^{10, 11}. Throughout all recordings, brain slices were continually superfused with aerated ACSF (32-34 °C) containing the thromboxane A_2 analog, 9,11 di-dideoxy-11 α ,9 α -epoxymethanoprostaglandin $F_{2\alpha}$ (U46619, 100 nM) to induce an intermediate level of arteriolar tone. Ionomycin (10 μ M) and $CaCl_2$ (20 mM) were added to the bath at the end of each experiment to obtain maximal fluorescence.

Analysis of arteriolar diameter: Intraluminal arteriolar diameter was measured from IR-DIC images at 3 evenly spaced points along a 10 μ m length of segment exhibiting the greatest diameter change to EFS. Diameter change is expressed as the percent increase or decrease from baseline (determined from 10 s prior to EFS and averaged for the 3 points of measurement). Diameters were measured manually using custom software, SparkAn, written by Dr. Adrian D. Bonev, at the University of Vermont (Burlington, VT).

Analysis of endfoot Ca^{2+} : A region of interest (ROI, 1.2 μm x 1.2 μm) was placed within an endfoot that was either: 1) adjacent to the arteriolar segment used to measure diameter during EFS or 2) exhibiting spontaneous Ca^{2+} events in the absence of stimulation. Spontaneous Ca^{2+} events were defined by the following criteria: 1) $\geq 30\%$ increase in fluorescent intensity for at least 2 consecutive images, and 2) multiple events during a 4 min recording period¹¹. Endfoot Ca^{2+} concentrations were estimated using the maximal fluorescence method^{20,21}.

Statistical analysis: Data are expressed as mean \pm SEM (n : the number of observations, N : the number of animals). Student's two-tailed paired t test was used for comparisons between two groups.

Reagents: U46619 and ionomycin were obtained from Calbiochem (EMD Millipore, Chicago, IL). Fluo-4 AM and pluronic acid were obtained from Invitrogen (Life Technologies, Eugene, OR). All P2 receptor antagonists were obtained from Tocris (Bristol, United Kingdom). All other reagents were purchased from Sigma-Aldrich (St. Louis, MO). The composition of ACSF (in mM) was: 125 NaCl, 3 KCl, 18 NaHCO_3 , 1.25 NaH_2PO_4 , 1 MgCl_2 , 2 CaCl_2 , 5 glucose, and 0.4 ascorbic acid.

Results

Purinergic receptor inhibition abolishes SAH-induced eHACSs

The role of purinergic signaling in the SAH-induced generation of astrocyte endfoot high amplitude Ca^{2+} signals (eHACSs) was explored in brain slices using the broad-spectrum purinergic receptor antagonist, suramin (100 μM) (Fig. 1). In brain

slices from control animals, spontaneous Ca^{2+} signals with amplitudes of less than 500 nM were observed in Fluo-4-loaded endfeet using two-photon imaging. Suramin had no effect on the amplitude (Fig. 1A, B) or frequency (0.019 ± 0.002 Hz vs 0.018 ± 0.001 Hz, two-tailed paired t test, $p = 0.73$) of endfoot Ca^{2+} signals in control animals. In brain slices from SAH model animals, endfeet exhibited a mix of “control-like” Ca^{2+} signals (amplitudes < 500 nM) and high amplitude (> 500 nM) Ca^{2+} signals “eHACSs” as previously described^{10, 11}. Suramin treatment of brain slices from SAH animals nearly abolished eHACSs (Fig. 1B, C), but did not affect lower amplitude “control-like” events or the overall frequency of spontaneous Ca^{2+} signals (0.023 ± 0.005 Hz vs 0.025 ± 0.004 Hz, two-tailed paired t test, $p = 0.85$). In the presence of suramin, the mean amplitude of endfoot spontaneous Ca^{2+} signals was comparable between control and SAH groups (Fig. 1D). These results suggest that purinergic signaling is involved in SAH-induced eHACSs, but not “control-like” endfoot Ca^{2+} events.

Suramin restores vasodilatory NVC after SAH

As the emergence of eHACSs has been linked to inversion of NVC after SAH^{10, 11}, we examined whether disruption of eHACSs with suramin could restore vasodilatory NVC in brain slices from SAH animals. In the absence of suramin, generation of neuronal action potentials using EFS caused parenchymal arteriolar constriction in 100 % of SAH brain slices ($n = 7/7$, $N = 6$) (Fig. 2A). Remarkably, suramin restored arteriolar dilation to EFS in the majority of brain slices ($n = 6/7$, $N = 6$) (Fig. 2B). Suramin, however, did not alter the amplitude of EFS-evoked endfoot Ca^{2+} transients (Fig. 2C) or arteriolar diameter before EFS (6.5 ± 1.1 μm before suramin vs 6.2 ± 1.0 μm after

suramin, two-tailed paired *t* test, $p = 0.53$). These data demonstrate inversion of NVC after SAH is dependent upon purinergic signaling and the presence of eHACSs in astrocyte endfeet surrounding parenchymal arterioles.

P2Y receptors mediate SAH-induced eHACSs

Purinergic (P2) receptors are broadly divided into 2 classes: ligand-gated, Ca^{2+} -permeable ion channels (i.e., P2X receptors), and metabotropic G-protein coupled (P2Y) receptors²². P2X receptors and P2Y receptors can be distinguished using α , β methylene-ATP (α , β -meATP), an ATP analog that rapidly desensitizes P2X, but not P2Y receptors²³. To determine if Ca^{2+} influx through P2X receptors contributes to SAH-induced eHACSs, spontaneous endfoot Ca^{2+} signals were recorded in brain slices from SAH animals before and after a 25 minute application of α , β -meATP (10 μM). Treatment with α , β -meATP had no effect on the incidence of eHACSs or on the overall frequency of endfoot Ca^{2+} signals (Fig. 3A-C), suggesting that P2X receptors are not involved in the generation of eHACSs after SAH.

To examine the involvement of P2Y receptors in SAH-induced eHACSs, brain slices from SAH animals were treated with a cocktail of inhibitors targeting G_q -coupled P2Y receptors. The components of this mix of P2Y receptor inhibitors included selective: P2Y₁ (MRS 2179, 30 μM), P2Y₂ (AR-C 118925XX, 10 μM), P2Y₆ (MRS 2578, 30 μM), and P2Y₁₁ (NF 340, 30 μM) receptor antagonists²⁴⁻²⁶. This combination of P2Y inhibitors blocked eHACSs, but did not alter “control-like” events or the overall frequency of spontaneous Ca^{2+} signals (Fig. 3 D-F). Interestingly, treatment of SAH brain slices with the PLC inhibitor, U73122 (30 μM , 30 min) abolished both SAH-

induced eHACSs and all “control-like” events ($n = 5, N = 3$). Spontaneous endfoot Ca^{2+} signals were also abolished by U73122 in brain slices from un-operated control animals ($n = 7, N = 3$), however, the inactive analog, U73343 (30 μM , 30 min), was without effect ($n = 5, N = 4$). Together, these data indicate that G_q -coupled P2Y receptor signaling contributes to the generation of SAH-induced eHACSs and that non-purinergic G_q -coupled receptors mediate “control-like” endfoot Ca^{2+} signals.

Activation of P2Y receptors in brain slices from control animals mimics SAH

We next sought to determine whether pharmacologic activation of P2Y receptors could mimic SAH in brain slices from un-operated animals. To obviate the potentially confounding effects mediated by P2X receptors, brain slices were pre-treated with α, β -meATP (10 μM , 25 min) to desensitize P2X receptors. In the presence of α, β -meATP, Ca^{2+} signals in endfeet from control animals were unaltered (i.e., all peaks <500 nM). However, subsequent treatment of brain slices with the non-hydrolyzable ATP analog, ATP γ S (3 μM), to activate P2Y receptors triggered the emergence of high amplitude Ca^{2+} signals that were comparable to SAH-induced eHACSs (Fig. 4A-C). These data suggest that functional P2Y receptors are present on astrocyte endfeet in healthy control animals and that activating these receptors generates Ca^{2+} signals resembling SAH-induced eHACSs. Importantly, this pharmacological approach to activate P2Y receptors also caused a marked disruption of NVC in brain slices of control animals. In the presence of α, β -meATP (10 μM , 25 min), focal activation of neurons using EFS caused the anticipated arteriolar dilation in 100% of brain slices ($n = 5/5, N = 4$) (Fig. 4D). However, subsequent treatment with ATP γ S (3 μM , 10 min) to activate P2Y receptors,

caused inversion of NVC (i.e., EFS-induced vasoconstriction) in 2 of 5 brain slices and attenuated the vasodilatory responses in the other 3 brain slices (Fig. 4D). There was no effect of ATP γ S on the amplitude of the EFS-evoked endfoot Ca²⁺ transients (Fig. 4E), or on arteriolar diameter before EFS ($6.1 \pm 0.9 \mu\text{m}$ before ATP γ S vs $6.2 \pm 0.9 \mu\text{m}$ after ATP γ S, two-tailed paired *t* test, *p* = 0.64). These data indicate that P2Y receptor-mediated Ca²⁺ elevations in astrocyte endfeet can mimic SAH to disrupt NVC in brain slices from healthy control animals.

SAH-induced eHACSs occur independent of neurotransmitter release

Neuronal release is one potential source of extracellular purine nucleotides (e.g. ATP) that could impact endfoot Ca²⁺ signaling after SAH¹². To assess the contribution neurotransmitter release on eHACSs, tetrodotoxin (TTX, 3 μM , 20 min), an inhibitor of voltage-dependent Na⁺ channels, was used to block neuronal action potentials in brain slices from SAH animals¹⁰. Tetrodotoxin had no effect on the occurrence of eHACSs, the mean amplitude of Ca²⁺ events, or the frequency of Ca²⁺ events (Fig. 5A-C), suggesting that neuronal action potentials are not required for the generation of the P2Y receptor-mediated eHACSs. These results, however, do not rule out the possibility that quantal (i.e., action potential-independent) neurotransmitter release or vesicular-mediated gliotransmitter release underlies the emergence of eHACSs after SAH.

To determine whether vesicular release of purine nucleotides mediates SAH-induced eHACSs, brain slices from SAH animals were treated with bafilomycin A1 (4 μM), a vacuolar H⁺-ATPase inhibitor (Fig 5 D-G). Bafilomycin depletes both neuronal and astroglial vesicles of transmitter and has been shown to inhibit Ca²⁺ signals in the

fine processes of hippocampal astrocytes²⁷⁻²⁹. Brain slices were exposed to bafilomycin for 4 h at room temperature prior to imaging. Vehicle-treated (DMSO: 1:1000 dilution in ACSF) brain slices served as time controls for these experiments. Bafilomycin had no effect on eHACSs, the mean amplitude of events, or frequency of events compared to time controls (Fig. 5D-F). However, bafilomycin-treated slices failed to respond to EFS with a rise in endfoot Ca^{2+} (Fig. 5G) indicating that bafilomycin had successfully depleted vesicles of neurotransmitter. Together, these results suggest that neither local neurotransmission nor astroglial vesicular release underlie purinergic receptor activation leading to SAH-induced eHACSs.

Discussion

This study provides evidence that G_q -coupled P2Y purinergic receptor signaling underlies the emergence of endfoot high amplitude Ca^{2+} signals (eHACSs) and the inversion of NVC in brain slices from SAH animals. The following observations are consistent with this novel finding: 1) broad-spectrum inhibition of purinergic P2 receptors with suramin blocked eHACSs and restored vasodilatory NVC after SAH; 2) desensitization of Ca^{2+} -permeable P2X receptors had no effect on the incidence of eHACSs; 3) SAH-induced eHACSs were abolished using a combination of inhibitors targeting G_q -coupled P2Y₁, P2Y₂, P2Y₆ and P2Y₁₁ receptors; 4) activation of P2Y receptors in brain slices from un-operated control animals mimicked SAH by triggering high-amplitude endfoot Ca^{2+} events and disrupting NVC. These data identify astrocyte

purinergic receptor signaling as an important contributor to SAH-induced micro-vascular dysfunction and impaired NVC.

In brain slices from SAH animals, the emergence of high amplitude spontaneous Ca^{2+} signals in astrocyte endfeet has been linked to increased activity of endfoot large-conductance Ca^{2+} -activated (BK) K^+ channels, increased perivascular K^+ and inversion of NVC^{10, 11}. Here, we show activation of G_q -coupled P2Y receptors underlies the emergence of SAH-induced eHACSs. Astrocytes express a variety of P2Y receptor subtypes that can be activated by multiple ligands found in purine/pyrimidine catabolic pathways (e.g. ATP, ADP, UTP, UDP)^{12, 13}. As shown in figures 1 and 2, the broad-spectrum P2 receptor antagonist, suramin²², blocked eHACSs and restored NVC after SAH without affecting normal astrocyte Ca^{2+} signaling. Aside from acting as a purinergic antagonist, suramin has been shown to have a number of additional effects, including interference with receptor/G-protein coupling, inhibition of DNA and RNA polymerases and inhibition of growth factor binding^{22, 30}. Suramin has been used for nearly a century as a treatment for the initial phase of African trypanosomiasis, commonly referred to as sleeping sickness³¹ and has been studied as a treatment of high-grade glioma³² and prostate cancer³³. Our data using a combination of reagents targeting P2Y₁, P2Y₂, P2Y₆ and P2Y₁₁ receptors (Fig. 3) indicate that the beneficial effects of suramin after SAH (i.e., block of eHACSs and rescue of vasodilatory NVC) are due to inhibition of P2 receptors, rather than off-target effects. Interestingly, Naviaux et al. have recently reported that suramin, through actions on purinergic signaling, can alleviate autism-like behaviors in a mouse model of autism spectrum disorder³⁴. Further, P2Y receptor-mediated disruption of astrocyte Ca^{2+} signaling and impaired NVC have been observed in mouse models of

Alzheimer's disease^{16, 17}. Considering the dire need for better therapeutic options for patients following aneurysmal SAH^{1, 35}, future *in vivo* studies targeting P2Y receptors using SAH models are warranted.

P2Y receptors are activated by a number of endogenous ligands, including ATP. Consistent with a role of extracellular ATP in the generation of SAH-induced eHACSs, elevated levels of ATP have been reported in CSF after SAH^{14, 15}, and we have found that the non-hydrolyzable ATP analog, ATP γ S, mimicked SAH by triggering high-amplitude endfoot Ca²⁺ events and causing inversion of NVC brain slices from control animals (Fig. 4). A number of sources could potentially contribute to elevated levels of extracellular ATP in brain parenchyma after SAH. For example, both neurons and astrocytes are capable of releasing ATP through vesicular-mediated exocytosis^{27, 36}. However, it is unlikely that vesicular-mediated ATP release is involved in the generation of SAH-induced eHACSs, as neither tetrodotoxin nor bafilomycin impacted these events (Fig. 5). Astrocytes, considered to be a main source of extracellular ATP in the brain¹², can also release ATP through connexin-based hemi-channels that are enriched in perivascular astrocyte^{37, 38}. ATP can also be released from astrocytes via lysosomal-mediated exocytosis³⁹. Interestingly, our previous work demonstrated the presence of lysosomes within hypertrophic endfeet after SAH that could represent a supply of ATP¹¹.

Extravascular red blood cells (RBCs) represent another potential source of elevated purine nucleotides in brain parenchyma after SAH. ATP is maintained in relatively high abundance (> 1 mM) within intact RBCs⁴⁰. In addition, autopsy studies of SAH patients and work using experimental SAH models have both demonstrated RBCs deposited along the wall of brain parenchymal arterioles following SAH^{10, 41}.

Considering the relatively small volume of the restricted perivascular space between astrocyte endfeet and parenchymal arteriolar myocytes, it is conceivable that RBC lysis could cause relatively high local levels of ATP. However, the appearance of eHACSs within 24 hrs following the injection of whole blood into the subarachnoid space ¹¹ does not readily fit with the reported time course (3-7 days) for the lysis of RBCs in CSF after SAH ^{42, 43}. Thus, further study will be required to determine the identity and source of P2Y receptor ligands involved in the generation of SAH-induced eHACSs.

In summary, a growing body of evidence indicates that pathological changes in astrocyte Ca²⁺ signaling occur during disease states such as Alzheimer's disease, epilepsy and SAH ^{10, 11, 16, 17, 44}. Further, astrocyte Ca²⁺ signaling profoundly impacts cerebral blood flow regulation, including NVC ^{8, 45, 46}. Here, we expand upon this knowledge by identifying a causal link between the activity of G_q-coupled P2Y receptors and the emergence of SAH-induced eHACSs and the inversion of NVC. Our observations are consistent with previous reports of P2Y receptor-mediated disruption of astrocyte Ca²⁺ signaling and impaired NVC in mouse models of Alzheimer's disease ^{16, 17}. Moving forward, targeting purinergic signaling in astrocytes may improve cortical blood flow in patients after SAH and provide additional benefits to individuals with other brain pathologies.

References

- (1) Dabus G, Nogueira RG. Current options for the management of aneurysmal subarachnoid hemorrhage-induced cerebral vasospasm: a comprehensive review of the literature. *Interv Neurol* 2013 2:30-51.
- (2) Al-Khindi T, Macdonald RL, Schweizer TA. Cognitive and functional outcome after aneurysmal subarachnoid hemorrhage. *Stroke* 2010 41:e519-e536.
- (3) Rabinstein AA, Weigand S, Atkinson JL, Wijedicks EF. Patterns of cerebral infarction in aneurysmal subarachnoid hemorrhage. *Stroke* 2005 36:992-7.
- (4) Vergouwen MD, Ilodigwe D, Macdonald RL. Cerebral infarction after subarachnoid hemorrhage contributes to poor outcome by vasospasm-dependent and -independent effects. *Stroke* 2011 42:924-9.
- (5) Ostergaard L, Aamand R, Karabegovic S, Tietze A, Blicher JU, Mikkelsen IK, Iversen NK, Secher N, Engedal TS, Anzabi M, Jimenez EG, Cai C, Koch KU, Naess-Schmidt ET, Obel A, Juul N, Rasmussen M, Sorensen JC. The role of the microcirculation in delayed cerebral ischemia and chronic degenerative changes after subarachnoid hemorrhage. *J Cereb Blood Flow Metab* 2013 33:1825-37.
- (6) Terpolilli NA, Brem C, Buhler D, Plesnila N. Are We Barking Up the Wrong Vessels? Cerebral Microcirculation After Subarachnoid Hemorrhage. *Stroke* 2015 46:3014-9.
- (7) Nishimura N, Schaffer CB, Friedman B, Lyden PD, Kleinfeld D. Penetrating arterioles are a bottleneck in the perfusion of neocortex. *Proc Natl Acad Sci U S A* 2007 104:365-70.
- (8) Straub SV, Nelson MT. Astrocytic calcium signaling: the information currency coupling neuronal activity to the cerebral microcirculation. *Trends Cardiovasc Med* 2007 17:183-90.
- (9) Filosa JA, Bonev AD, Straub SV, Meredith AL, Wilkerson MK, Aldrich RW, Nelson MT. Local potassium signaling couples neuronal activity to vasodilation in the brain. *Nat Neurosci* 2006 9:1397-403.
- (10) Koide M, Bonev AD, Nelson MT, Wellman GC. Inversion of neurovascular coupling by subarachnoid blood depends on large-conductance Ca^{2+} -activated K^{+} (BK) channels. *Proc Natl Acad Sci U S A* 2012 109:E1387-E1395.
- (11) Pappas AC, Koide M, Wellman GC. Astrocyte Ca^{2+} Signaling Drives Inversion of Neurovascular Coupling after Subarachnoid Hemorrhage. *J Neurosci* 2015 35:13375-84.

- (12) Franke H, Verkhatsky A, Burnstock G, Illes P. Pathophysiology of astroglial purinergic signalling. *Purinergic Signal* 2012 8:629-57.
- (13) James G, Butt AM. P2Y and P2X purinoceptor mediated Ca^{2+} signalling in glial cell pathology in the central nervous system. *Eur J Pharmacol* 2002 447:247-60.
- (14) Kasseckert SA, Shahzad T, Miqdad M, Stein M, Abdallah Y, Scharbrodt W, Oertel M. The mechanisms of energy crisis in human astrocytes after subarachnoid hemorrhage. *Neurosurgery* 2013 72:468-74.
- (15) Macdonald RL, Weir BK, Marton LS, Zhang ZD, Sajdak M, Johns LM, Kowalczyk A, Borsody M. Role of adenosine 5'-triphosphate in vasospasm after subarachnoid hemorrhage: human investigations. *Neurosurgery* 2001 48:854-62.
- (16) Delekate A, Fuchtemeier M, Schumacher T, Ulbrich C, Foddis M, Petzold GC. Metabotropic P2Y₁ receptor signalling mediates astrocytic hyperactivity *in vivo* in an Alzheimer's disease mouse model. *Nat Commun* 2014 5:5422.
- (17) Takano T, Han X, Deane R, Zlokovic B, Nedergaard M. Two-photon imaging of astrocytic Ca^{2+} signaling and the microvasculature in experimental mice models of Alzheimer's disease. *Ann N Y Acad Sci* 2007 1097:40-50.
- (18) Nystoriak MA, O'Connor KP, Sonkusare SK, Brayden JE, Nelson MT, Wellman GC. Fundamental increase in pressure-dependent constriction of brain parenchymal arterioles from subarachnoid hemorrhage model rats due to membrane depolarization. *Am J Physiol Heart Circ Physiol* 2011 300:H803-H812.
- (19) Parri HR, Gould TM, Crunelli V. Spontaneous astrocytic Ca^{2+} oscillations *in situ* drive NMDAR-mediated neuronal excitation. *Nat Neurosci* 2001 4:803-12.
- (20) Girouard H, Bonev AD, Hannah RM, Meredith A, Aldrich RW, Nelson MT. Astrocytic endfoot Ca^{2+} and BK channels determine both arteriolar dilation and constriction. *Proc Natl Acad Sci U S A* 2010 107:3811-6.
- (21) Maravall M, Mainen ZF, Sabatini BL, Svoboda K. Estimating intracellular calcium concentrations and buffering without wavelength ratioing. *Biophys J* 2000 78:2655-67.
- (22) Ralevic V, Burnstock G. Receptors for purines and pyrimidines. *Pharmacol Rev* 1998 50:413-92.
- (23) Heppner TJ, Bonev AD, Nelson MT. Elementary purinergic Ca^{2+} transients evoked by nerve stimulation in rat urinary bladder smooth muscle. *J Physiol* 2005 564:201-12.

- (24) Barragan-Iglesias P, Pineda-Farias JB, Cervantes-Duran C, Bravo-Hernandez M, Rocha-Gonzalez HI, Murbartian J, Granados-Soto V. Role of spinal P2Y₆ and P2Y₁₁ receptors in neuropathic pain in rats: possible involvement of glial cells. *Mol Pain* 2014 10:1744-8069.
- (25) Kawamura M, Gachet C, Inoue K, Kato F. Direct excitation of inhibitory interneurons by extracellular ATP mediated by P2Y₁ receptors in the hippocampal slice. *J Neurosci* 2004 24:10835-45.
- (26) Kim B, Jeong HK, Kim JH, Lee SY, Jou I, Joe EH. Uridine 5'-diphosphate induces chemokine expression in microglia and astrocytes through activation of the P2Y₆ receptor. *J Immunol* 2011 186:3701-9.
- (27) Bowser DN, Khakh BS. Vesicular ATP is the predominant cause of intercellular calcium waves in astrocytes. *J Gen Physiol* 2007 129:485-91.
- (28) Sun MY, Devaraju P, Xie AX, Holman I, Samones E, Murphy TR, Fiocco TA. Astrocyte calcium microdomains are inhibited by bafilomycin A1 and cannot be replicated by low-level Schaffer collateral stimulation *in situ*. *Cell Calcium* 2014 55:1-16.
- (29) Zhou Q, Petersen CC, Nicoll RA. Effects of reduced vesicular filling on synaptic transmission in rat hippocampal neurones. *J Physiol* 2000 1:195-206.
- (30) Michel MC, Seifert R. Selectivity of pharmacological tools: implications for use in cell physiology. A review in the theme: Cell signaling: proteins, pathways and mechanisms. *Am J Physiol Cell Physiol* 2015 308:C505-C520.
- (31) Neuberger A, Meltzer E, Leshem E, Dickstein Y, Stienlauf S, Schwartz E. The changing epidemiology of human African trypanosomiasis among patients from nonendemic countries--1902-2012. *PLoS One* 2014 9:e88647.
- (32) Grossman SA, Phuphanich S, Lesser G, Rozental J, Grochow LB, Fisher J, Piantadosi S. Toxicity, efficacy, and pharmacology of suramin in adults with recurrent high-grade gliomas. *J Clin Oncol* 2001 19:3260-6.
- (33) Ahles TA, Herndon JE, Small EJ, Vogelzang NJ, Kornblith AB, Ratain MJ, Stadler W, Palchak D, Marshall ME, Wilding G, Petrylak D, Holland JC. Quality of life impact of three different doses of suramin in patients with metastatic hormone-refractory prostate carcinoma: results of Intergroup O159/Cancer and Leukemia Group B 9480. *Cancer* 2004 101:2202-8.

- (34) Naviaux JC, Schuchbauer MA, Li K, Wang L, Risbrough VB, Powell SB, Naviaux RK. Reversal of autism-like behaviors and metabolism in adult mice with single-dose antipurinergic therapy. *Transl Psychiatry* 2014 4:400.
- (35) Pluta RM, Hansen-Schwartz J, Dreier J, Vajkoczy P, Macdonald RL, Nishizawa S, Kasuya H, Wellman G, Keller E, Zauner A, Dorsch N, Clark J, Ono S, Kiris T, Leroux P, Zhang JH. Cerebral vasospasm following subarachnoid hemorrhage: time for a new world of thought. *Neurol Res* 2009 31:151-8.
- (36) Unsworth CD, Johnson RG. Acetylcholine and ATP are coreleased from the electromotor nerve terminals of *Narcine brasiliensis* by an exocytotic mechanism. *Proc Natl Acad Sci U S A* 1990 87:553-7.
- (37) Cotrina ML, Lin JH, Alves-Rodrigues A, Liu S, Li J, Azmi-Ghadimi H, Kang J, Naus CC, Nedergaard M. Connexins regulate calcium signaling by controlling ATP release. *Proc Natl Acad Sci U S A* 1998 95:15735-40.
- (38) Simard M, Arcuino G, Takano T, Liu QS, Nedergaard M. Signaling at the gliovascular interface. *J Neurosci* 2003 23:9254-62.
- (39) Zhang Z, Chen G, Zhou W, Song A, Xu T, Luo Q, Wang W, Gu XS, Duan S. Regulated ATP release from astrocytes through lysosome exocytosis. *Nat Cell Biol* 2007 9:945-53.
- (40) Miseta A, Bogner P, Berenyi E, Kellermayer M, Galambos C, Wheatley DN, Cameron IL. Relationship between cellular ATP, potassium, sodium and magnesium concentrations in mammalian and avian erythrocytes. *Biochim Biophys Acta* 1993 1175:133-9.
- (41) Crompton MR. The Pathogenesis of cerebral infarction following the rupture of berry aneurysms. *Brain* 1964 87:491-510.
- (42) Konno Y, Sato T, Suzuki K, Matsumoto M, Sasaki T, Kodama N. Sequential changes of oxyhemoglobin in drained fluid of cisternal irrigation therapy--reference to the effect of ascorbic acid. *Acta Neurochir Suppl* 2001;77:167-9.:167-9.
- (43) Pluta RM, Afshar JK, Boock RJ, Oldfield EH. Temporal changes in perivascular concentrations of oxyhemoglobin, deoxyhemoglobin, and methemoglobin after subarachnoid hemorrhage. *J Neurosurg* 1998 88:557-61.
- (44) Tian GF, Azmi H, Takano T, Xu Q, Peng W, Lin J, Oberheim N, Lou N, Wang X, Zielke HR, Kang J, Nedergaard M. An astrocytic basis of epilepsy. *Nat Med* 2005 11:973-81.

- (45) Anderson CM, Nedergaard M. Astrocyte-mediated control of cerebral microcirculation. *Trends Neurosci* 2003 26:340-4.
- (46) Attwell D, Buchan AM, Charpak S, Lauritzen M, Macvicar BA, Newman EA. Glial and neuronal control of brain blood flow. *Nature* 2010 468:232-43.

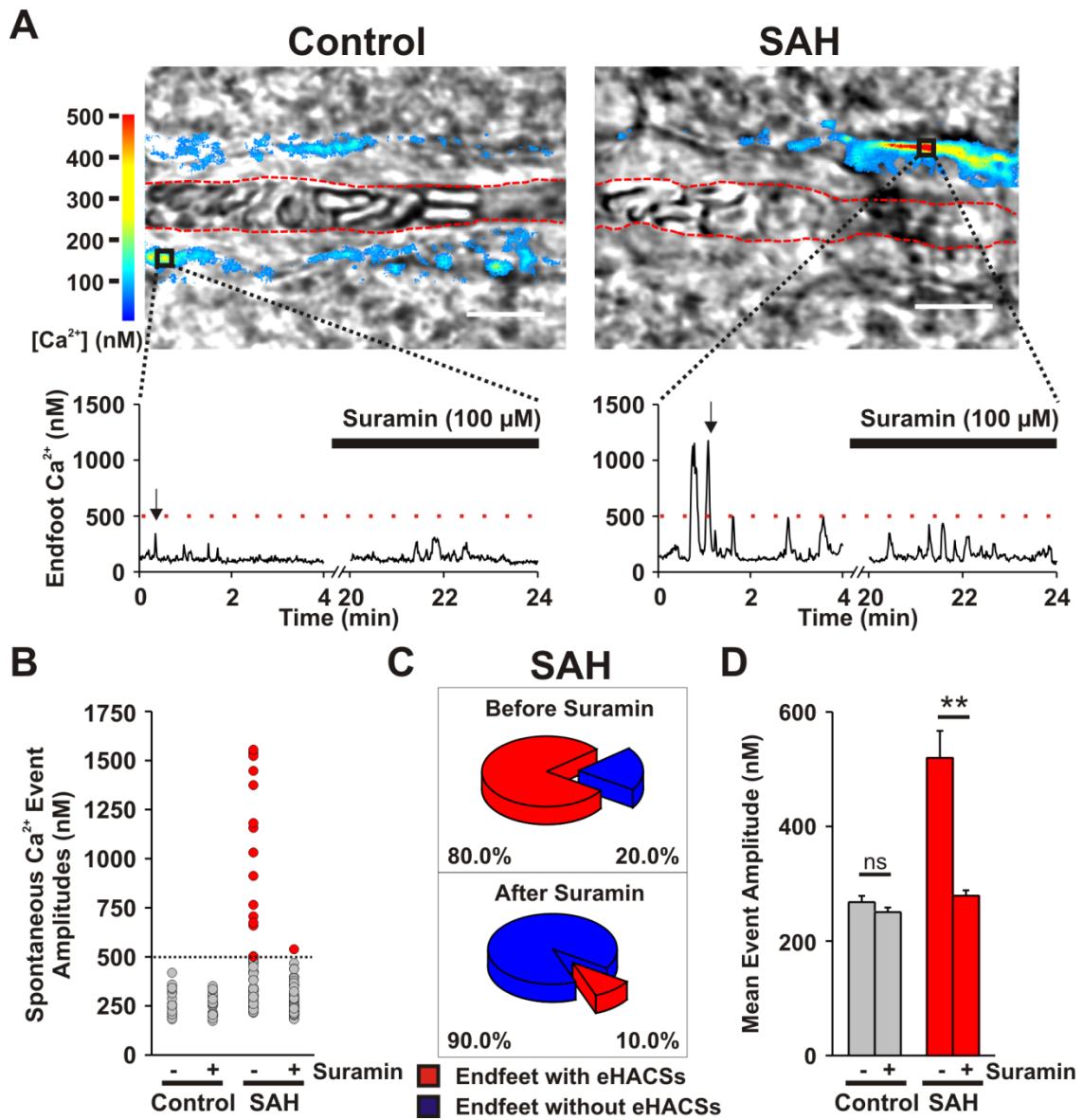


Figure 3-1. Inhibition of purinergic signaling with suramin selectively blocks SAH-induced eHACSs

(A) Images of control and SAH parenchymal arterioles with overlapping pseudocolor-mapped fluorescent Ca^{2+} levels in surrounding astrocyte endfeet obtained using simultaneous IR-DIC and 2 photon microscopy (top). Red-dashed lines depict arteriolar lumen. Scale bar is 10 μm . Traces demonstrating spontaneous fluctuations in intracellular Ca^{2+} (i.e. spontaneous Ca^{2+} events) recorded within the regions corresponding to the black boxes in the above images before and after treatment with suramin (bottom). The moments in the trace directly beneath the arrows are depicted in the frames above. These frames capture peak Ca^{2+} levels during a typical “control-like” event (<500 nM, left) and during an eHACS (≥ 500 nM, right) (B) Distribution of all spontaneous Ca^{2+} event amplitudes recorded in brain slices from control and SAH model animals before and after treatment with suramin. Note that eHACSs (red dots, peaks ≥ 500 nM) are almost completely abolished in SAH brain slices treated with suramin. (C) Summary pie chart indicating the incidence of endfeet with eHACSs before and after treatment with suramin. These data only represent endfeet in brain slices from SAH animals. eHACSs were not observed in brain slices from control animals. (D) Summary data showing the effect of suramin on the mean amplitudes of all spontaneous endfoot Ca^{2+} events in brain slices from control and SAH model animals. Two-tailed paired t test, $**p < 0.01$.

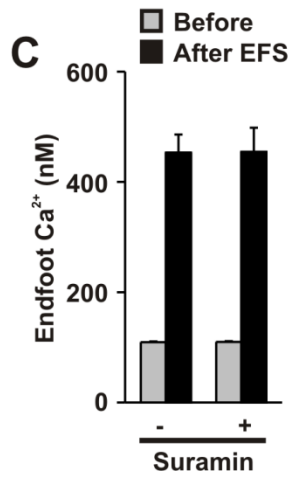
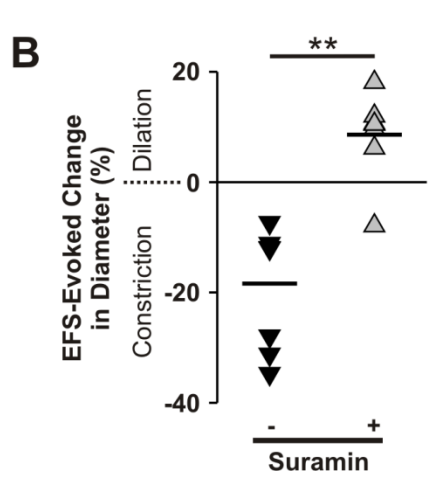
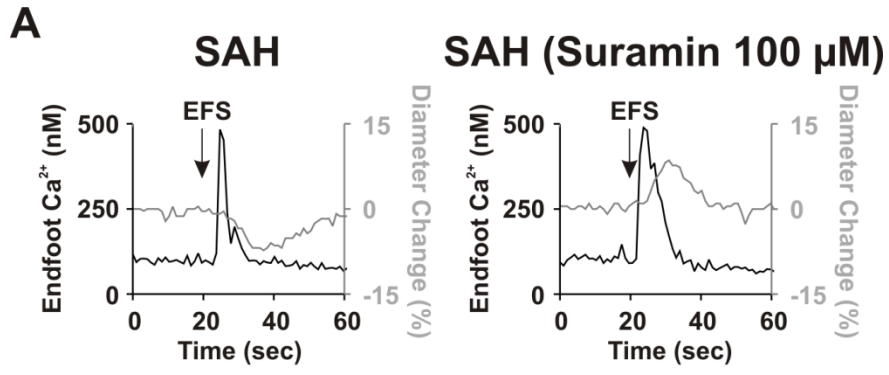


Figure 3-2. Blocking eHACs restores vasodilatory NVC after SAH

(A) Representative traces showing EFS-induced elevation of endfoot Ca^{2+} (black lines) and subsequent changes in arteriolar diameter (gray lines). (B) Summary scatter plot demonstrating EFS-evoked changes in arteriolar diameter before (black triangles) and after (gray triangles) treatment with suramin. Two-tailed paired t test, $**p < 0.01$. (C) Summary data showing EFS-evoked changes in endfoot Ca^{2+} in SAH brain slices before and after treatment with suramin.

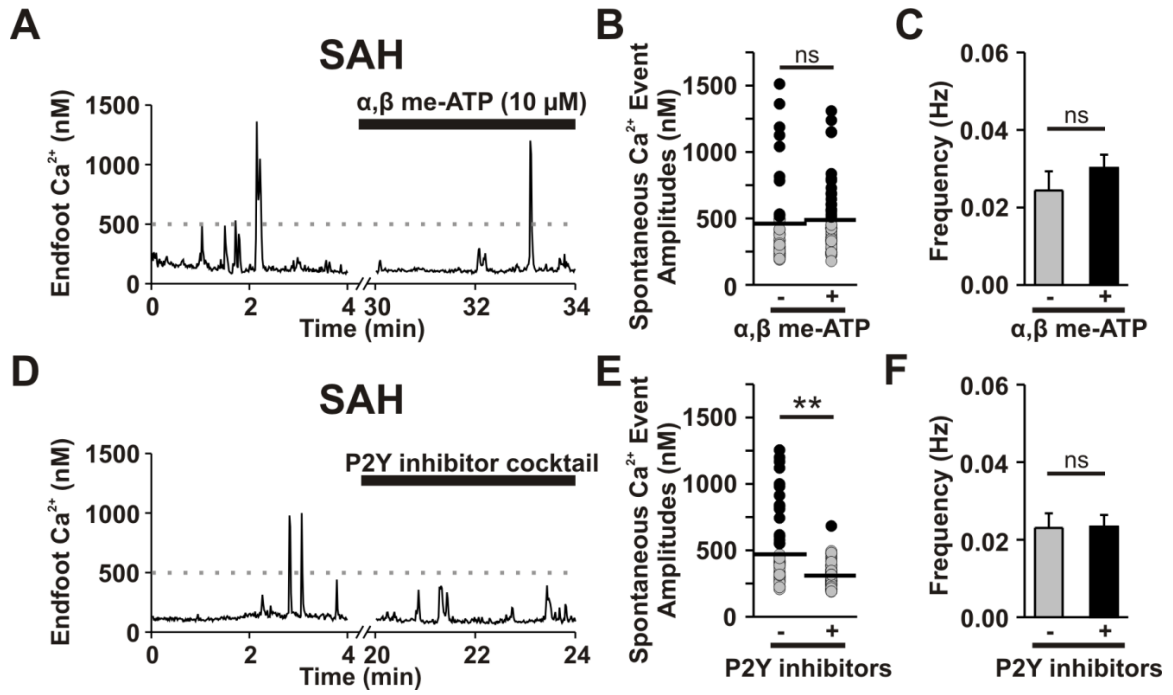


Figure 3-3. P2Y receptors mediate SAH-induced eHACSs

(A) Representative trace depicting spontaneous Ca^{2+} activity recorded from a SAH brain slice before and after treatment with, α,β -meATP, an ATP analogue that rapidly desensitizes P2X receptors. (B) Distribution of all spontaneous Ca^{2+} event amplitudes recorded in brain slices from SAH animals before and after treatment with α,β -meATP. eHACSs (black dots) were still present following desensitization of P2X receptors. Horizontal black lines indicate the mean amplitudes of all events. (C) Summary data showing the frequency of endfoot Ca^{2+} events in the presence or absence of α,β -meATP. (D) Representative trace of spontaneous Ca^{2+} activity recorded from a SAH brain slice before and after treatment with a P2Y inhibitor cocktail containing selective P2Y₁ (MRS 2179, 30 μM), P2Y₂ (AR-C 118925XX, 10 μM), P2Y₆ (MRS 2578, 30 μM), and P2Y₁₁ (NF 340, 30 μM) antagonists. (E) Distribution of all spontaneous Ca^{2+} event amplitudes recorded from SAH animals before and after treatment with the P2Y inhibitor cocktail. Note that the P2Y inhibitor cocktail selectively abolished eHACSs (black dots). Horizontal black lines indicate the mean amplitudes of all events. Two-tailed paired *t* test, $**p < 0.01$. (F) Summary data showing the frequency of spontaneous endfoot Ca^{2+} events in the presence or absence of the P2Y inhibitor cocktail.

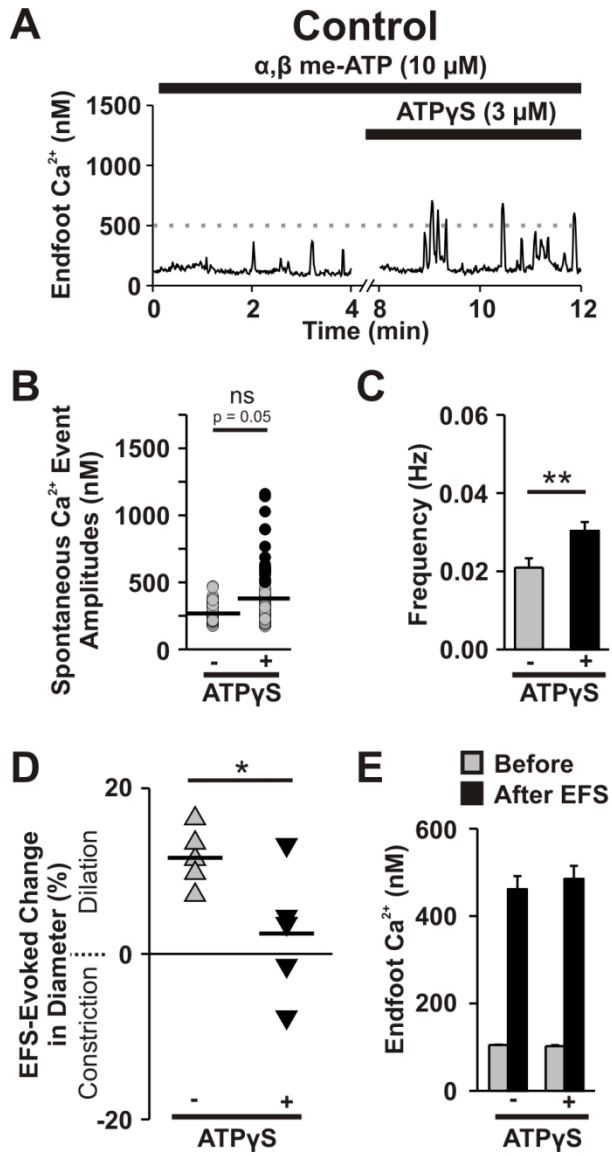


Figure 3-4. Activation of P2Y receptors in brain slices from control animals mimics SAH

(A) Representative trace showing the effect of ATP γ S, a non-hydrolyzable ATP analog, on spontaneous Ca²⁺ activity in a brain slice obtained from a healthy control animal. In these experiments, α,β -meATP was included in the superfusate to desensitize P2X receptors. (B) Distribution of all spontaneous Ca²⁺ event amplitudes recorded in brain slices from control animals before and after treatment with ATP γ S. Note that events mimicking SAH-induced eHACSs (black dots, peak Ca²⁺ \geq 500 nM) emerged following treatment with ATP γ S. Horizontal black lines indicate the mean amplitudes of all events. Two-tailed paired *t* test, n.s. $p = 0.05$. (C) Summary data showing the frequency of endfoot Ca²⁺ events in the presence or absence of ATP γ S. Two-tailed paired *t* test, ** $p < 0.01$. (D) Summary scatter plot demonstrating EFS-evoked changes in arteriolar diameter in brain slices from healthy control animals before and after treatment with ATP γ S. Two-tailed paired *t* test, * $p < 0.05$. (E) Summary data showing EFS-evoked changes in endfoot Ca²⁺ before and after treatment with ATP γ S. For studies examining NVC, α,β -meATP was also included in the slice superfusate.

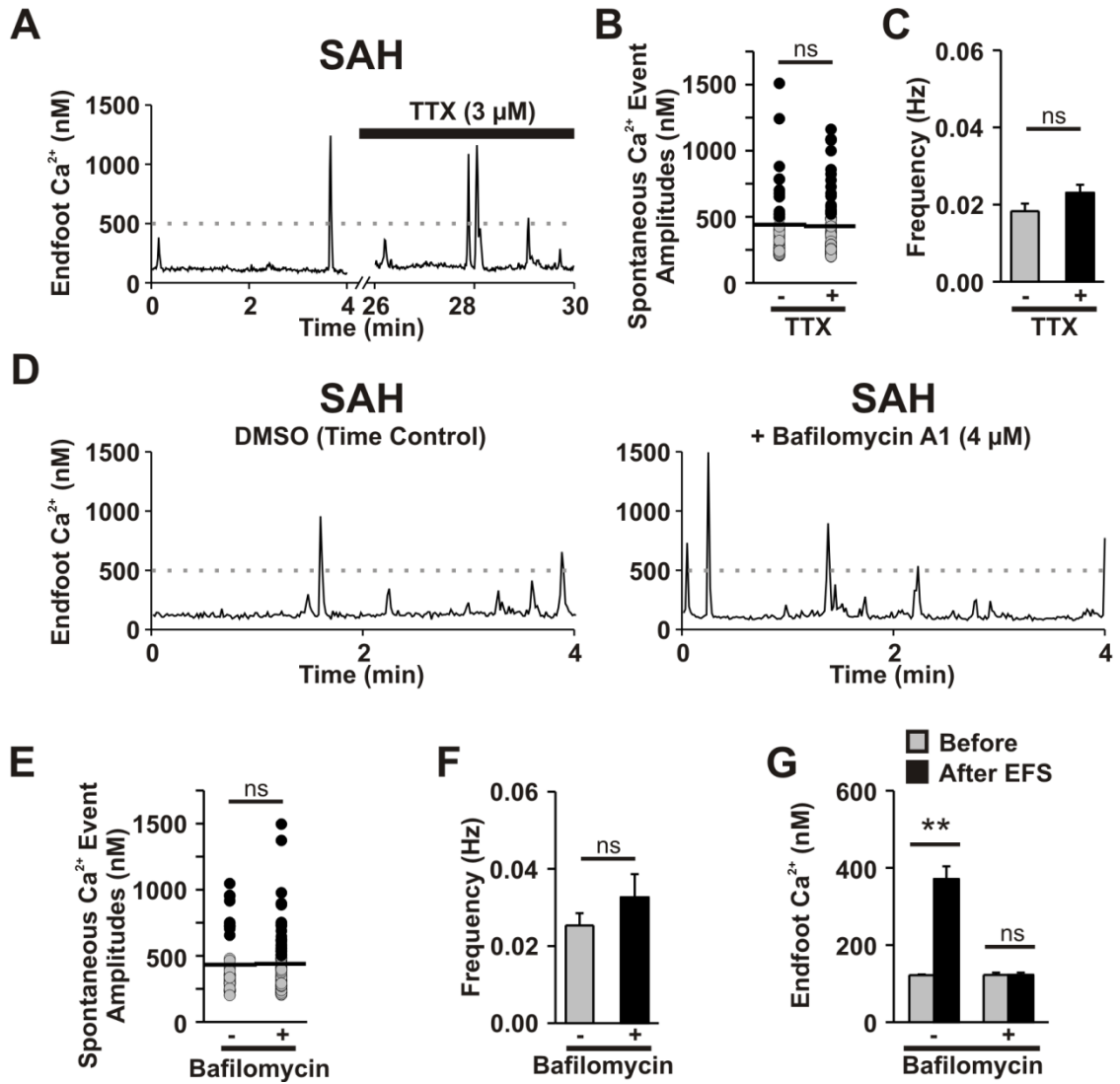


Figure 3-5. Local neurotransmission is not involved in the generation of eHACSS after SAH

(A) Representative trace of spontaneous Ca^{2+} activity recorded from a SAH brain slice before and after treatment with tetrodotoxin (TTX), a fast Na^+ channel inhibitor that blocks neuronal action potentials. (B) Distribution of all spontaneous Ca^{2+} event amplitudes recorded in SAH brain slices before and after treatment with TTX. Note that eHACSSs (black dots, peak $\text{Ca}^{2+} \geq 500$ nM) are still present following treatment with TTX. Horizontal black lines indicate the mean amplitudes of all events. (C) Summary data showing the frequency of endfoot Ca^{2+} events in the presence or absence of TTX. (D) Representative traces of spontaneous Ca^{2+} activity recorded from SAH brain slices from either the vehicle-treated time control (left), or bafilomycin A1-treated (right) groups. Bafilomycin A1 depletes vesicles of neurotransmitter by inhibiting the vacuolar H^+ -ATPase. (E) Distribution of all spontaneous Ca^{2+} event amplitudes recorded in SAH brain slices from the vehicle-treated time control (- bafilomycin), or bafilomycin A1-treated groups. Note eHACSSs were not abolished in bafilomycin-treated SAH brain slices. (F) Summary data showing the frequency of endfoot Ca^{2+} events in vehicle-treated time control, or bafilomycin A1-treated SAH brain slices. (G) Summary data showing EFS-evoked changes in endfoot Ca^{2+} recorded from vehicle-treated time control, or bafilomycin A1-treated SAH brain slices. Note EFS failed to elevate endfoot Ca^{2+} in bafilomycin A1-treated SAH brain slices. Two-tailed paired t test, $**p < 0.01$, n.s. $p > 0.05$.

Chapter 4: Discussion and Future Directions

The studies included in this dissertation were designed to address two specific aims: (1) to determine whether altered astrocyte Ca^{2+} signaling, in the form of eHACSs, is causally linked to the inversion of neurovascular coupling after SAH and (2) to elucidate the cellular basis underlying the generation of eHACSs. Our data provide substantial evidence that SAH-induced eHACSs cause a pathological shift in neurovascular coupling from vasodilation to vasoconstriction. Both phenomena, eHACSs and inversion of neurovascular coupling, followed a similar time-dependent pattern of development. Further, depleting ER Ca^{2+} stores or selectively blocking eHACSs restored vasodilatory responses in SAH brain slices. Together, these data indicate that eHACSs drive inversion of neurovascular coupling after SAH. Moreover, our results identify perivascular astrocytes as a contributing element to the parenchymal arteriolar dysfunction and impaired cerebral hemodynamics commonly observed following aneurysmal SAH.

Our data provide evidence that purinergic signaling via G_q -coupled P2Y receptors underlies the generation of eHACSs after SAH. Treating SAH brain slices with the broad-spectrum purinergic receptor antagonist, suramin, selectively blocked eHACSs and restored vasodilatory neurovascular coupling. The fact that a purinergic signaling pathway triggers a pathological change in astrocyte Ca^{2+} signaling after SAH is not surprising. Extracellular purine nucleotides, such as ATP, are commonly elevated in the brain following injury (Franke et al., 2012). Kasseckert et al. (2013) measured a 400-fold increase in the concentration of ATP in the cerebrospinal fluid (CSF) of SAH patients

compared to non-SAH controls. Importantly, the investigators found that exposing cultured human astrocytes to the bloody CSF triggered a steep elevation of intra-cellular Ca^{2+} that was prevented by either suramin, or the IP_3R antagonist, xestospongin D. In the live rodent, evidence suggests that arterial pulsation drives the flow of CSF into the brain, alongside parenchymal arterioles in between astrocyte endfeet and vascular smooth muscle (Iloff et al., 2012; Iliff et al., 2013). This flow pattern would be expected to deliver CSF with elevated ATP levels directly into the perivascular space where it could alter endfoot Ca^{2+} dynamics leading to the emergence of eHACSSs.

The above description details one way in which SAH could trigger P2Y receptor-mediated eHACSSs. However, there are unresolved issues that argue against this possibility. Mainly, in the acute brain slice preparation the flow of CSF has typically been stopped for hours before imaging. Even if ATP levels within the perivascular space were elevated at the time the animal was euthanized, ectonucleotidases would likely degrade ATP prior to the start of the experiment. Under physiologic conditions, the concentration of extracellular purine nucleotides is regulated by the activity of ectonucleoside triphosphate diphosphohydrolases (E-NTPDases). Astrocytes express several members of the E-NTPDase family, with E-NTPDase 2, being the enzyme most responsible for ATPase activity (Wink et al., 2006). Astrocytes also express ecto-5'-nucleotidase/CD73 allowing them to convert AMP to adenosine (Wink et al., 2003). Thus, the full compliment of enzymes expressed by astrocytes would allow them to fully degrade ATP trapped within the perivascular space after SAH. It is important to mention here that blood vessels also express E-NTPDases, with E-NTPDase 1 being the

predominant enzyme in the brain vasculature (Braun et al., 2000). Thus, CSF-derived ATP seems unlikely to trigger eHACSs in the *ex vivo* brain slice preparation.

The multiple reports linking SAH to increased levels of ATP in the CSF have suggested that lysed erythrocytes (i.e., red blood cells) are the source of ATP after SAH (Macdonald et al., 2001; Yin et al., 2002; Kasseckert et al., 2013). Given the flow of CSF into the brain parenchyma, one would expect extravasated red blood cells to invade the brain cortex alongside parenchymal arterioles. In fact, the accumulation of extravascular red blood cells in human SAH patients was already described over 50 years ago (Crompton, 1964). Using the double injection cisterna magna SAH model, Koide et al. (2012) observed red blood cells adjacent to the parenchymal arteriolar wall, up to 1 mm from the cortical surface within 10 min of SAH. Extravascular red blood cells were also observed along parenchymal arterioles up to 7 d post-SAH using the acute brain slice preparation (Pappas et al., 2015). It could be argued that the slow and gradual breakdown of perivascular red blood cells after SAH leads to a localized elevation of ATP independent of the ATP levels in circulating CSF. Thus, the presence extravascular debris may be linked to the emergence of P2Y receptor-mediated eHACSs after SAH. Careful studies must be designed to determine whether breakdown of extravascular red blood cells generates SAH-induced eHACSs. A simple first step would be to inject a comparable volume of hemolysate into the cisterna magna of anesthetized animals and determine whether their brain slices exhibit eHACSs or inversion of neurovascular coupling at 2 d post-SAH. Lysing the red blood cells before delivery into the subarachnoid space, would remove the possibility of the cells accumulating along the arterioles and gradually releasing their contents into the extracellular milieu. Although

the injected hemolysate would contain high levels of ATP, endogenous ectonucleotidases would be expected to degrade the nucleotides relatively quickly.

Another possibility is that reactive gliosis is involved in the release of extracellular purine nucleotides after SAH. Inflammatory perturbations to the CNS, including SAH, cause nearby microglia to shift from a dormant state to an activated state (Murakami et al., 2011; Plog et al., 2014). In a recent study, Pascual et al. (2012) demonstrated that the activation of brain microglia resulted in the release of ATP onto nearby astrocytes. Importantly, the resultant activation of astrocyte P2Y₁ receptors triggered additional ATP release from the astrocytes, thereby causing an amplification of the purinergic signal. In addition to stimulating the release of gliotransmitters, activation of P2Y₁ receptors has been linked to the development of reactive astrogliosis (Franke et al., 2001). There is strong evidence, such as increased expression of glial fibrillary acidic protein (GFAP) and S100 β , that reactive astrogliosis occurs following SAH (Yokota et al., 1994; Murakami et al., 2011). Presently, we demonstrate a hypertrophic morphology of astrocyte endfeet, a clear indication of reactive astrogliosis, in tissue obtained from 2 d SAH animals (see Fig. 2-5). Our time course data show a gradual emergence of endfeet exhibiting eHACSSs, reaching a peak at 2 d post-SAH, and then slowly declining at later time-points (see Fig. 2-1). The prevailing thought is that the inflammatory component to reactive gliosis occurs early following injury (between 0 and 7 d post-insult) and subsequently shifts to a phase of cell proliferation and tissue remodeling (Burda and Sofroniew, 2014). Interestingly, the time course in which the inflammatory response is suggested to occur appears to coincide with the emergence of eHACSSs and development of inversion of neurovascular coupling. Future studies will be necessary to determine the

relationship between these phenomena. For example, one could use immunohistochemistry to determine if SAH-induced activated microglia are in close enough proximity to initiate ATP release from perivascular astrocytes. To date, the vast majority of work suggests that astrocyte ATP release mechanisms involve either: (1) Ca^{2+} -dependent exocytosis of ATP-containing vesicles (Montana et al., 2006; Bowser and Khakh, 2007), (2) ATP efflux through plasmalemmal hemichannels formed by connexins and pannexins (Kang et al., 2008), or (3) ATP release via lysosomes (Zhang et al., 2007). Functional studies targeting the above mechanisms could also be used to determine whether eHACSs after SAH are the result of a paracrine/autocrine astrocyte purinergic signaling pathway.

Our data demonstrate that suramin selectively blocked eHACSs and restored vasodilatory neurovascular coupling after SAH. Although suramin is recognized as a broad-spectrum purinergic (P2) receptor antagonist (Ralevic and Burnstock, 1998), it has also been suggested to have many off-target effects including: disruption of growth factor receptor signaling (Coffey et al., 1987), uncoupling of G-protein coupled receptors (Beindl et al., 1996), and activation of skeletal muscle ryanodine receptors (Hohenegger et al., 1996). Despite the widespread actions of suramin, the positive effects we observed in SAH brain slices are most likely due to block of P2Y receptor signaling. Most importantly, we observed a similar block of SAH-induced eHACSs in brain slices treated with a cocktail of inhibitors targeting G_q -coupled P2Y receptors (Fig. 3-3). These data argue against potential off-target effects, such as disruption of growth factor receptor signaling. Currently, there is a lack of evidence supporting functional expression of ryanodine receptors (i.e., ER Ca^{2+} release channels) in astrocytes *in situ* (Straub et al.,

2006). If suramin were activating astrocyte ryanodine receptors, then one would predict that suramin would cause an increased amplitude and frequency of endfoot Ca^{2+} events. Instead, we observed a selective blockade of SAH-induced eHACSs and no change in Ca^{2+} event frequency in control or SAH brain slices following treatment with suramin (Fig. 3-1). Our results also argue against an uncoupling of G-protein coupled receptors. The endfoot Ca^{2+} transients evoked by EFS are sensitive to phospholipase C inhibition indicating that G_q -coupled receptors mediate neuronal activity-dependent elevation of endfoot Ca^{2+} (Straub et al., 2006). We observed no change in the amplitude of the EFS-evoked endfoot Ca^{2+} transients in brain slices treated with suramin (Fig. 3-2). Further, the vasoconstrictor, U46619, is a G_q -coupled receptor agonist. If suramin were uncoupling G-protein coupled receptors, then one would predict that suramin would abolish arteriolar tone. However, we observed no change in parenchymal arteriolar diameter following treatment with suramin. Thus, despite suramin's potential off-target effects, the most likely explanation for our results is that suramin is disrupting SAH-induced eHACSs by blocking astrocyte P2Y receptors.

Suramin is a well-tolerated FDA-approved drug that has been used previously to treat high-grade glioma (Grossman et al., 2001). This is significant as it identifies a signaling pathway that could be targeted therapeutically in the management of SAH patients. Current therapeutic options are limited and often have poor efficacy. Experimental evidence using a canine SAH model has already provided evidence that *in vivo* treatment with suramin reduces the severity of SAH-induced vasospasm; although the investigators claim the effects were due to inhibition of tyrosine kinase activity (Kimura et al., 2002). Future studies will be necessary to determine (1) if inversion of

neurovascular coupling occurs in SAH animals *in vivo*, and (2) if suramin can restore or improve vasodilatory neurovascular coupling after SAH.

Our data provide strong evidence that SAH-induced eHACSs are mediated by the activity of G_q-coupled P2Y receptors. Astrocytes express most P2Y receptor subtypes and immunohistochemical examination has already revealed expression of the G_q-coupled receptors P2Y₁, P2Y₂ and P2Y₄ on perivascular endfeet (Franke et al., 2012; Simard et al., 2013). There have been no studies examining the localization of other astrocyte G_q-coupled P2Y receptors in relation to the intra-cerebral vasculature. It is possible that multiple P2Y receptor subtypes are responsible for the generation of eHACSs after SAH. P2Y receptors can exist as homodimers or heterodimers with other P2 receptors, or P1 (i.e., adenosine) receptors (Tonazzini et al., 2008; Koles et al., 2011). Further, if extracellular purine and/or pyrimidine nucleotides are driving the generation of eHACSs after SAH, then it stands to reason that one P2Y receptor could be involved in triggering a Ca²⁺ event in response to ATP, while another receptor responds to ATP's degradation product, ADP. Accordingly, the same would be expected for the pyrimidines UTP and UDP. Thus, it seems that a broad-spectrum purinergic receptor antagonist, such as suramin, would be the most useful approach to block P2Y receptor-mediated eHACSs after SAH. Future studies using a combination of qPCR/western blotting and immunohistochemistry could be useful to determine if SAH leads to an increased expression of G_q-coupled P2Y receptors in perivascular astrocytes. This may aid in narrowing down the exact mechanism by which extracellular purine and/or pyrimidine nucleotides trigger eHACSs.

To conclude, the studies presented in this dissertation demonstrate that the inversion of neurovascular coupling after SAH is due to a pathological change in astrocyte endfoot Ca^{2+} signaling (i.e., eHACSs). Our results provide clear evidence that perivascular astrocytes play a pivotal role in mediating SAH-induced vascular dysfunction. Importantly, our data indicate a role for extracellular purine and/or pyrimidine nucleotides in the generation of eHACSs after SAH. We report that inhibition of G_q -coupled P2Y receptors selectively blocked eHACSs and restored vasodilatory neurovascular coupling in brain slices obtained from SAH animals. Moving forward, it will be important to determine the link between SAH and enhanced purinergic signaling. Further, it will be necessary to consider the role of perivascular astrocytes in the development of neurological deficits following aneurysmal SAH.

References

- Beindl W, Mitterauer T, Hohenegger M, Ijzerman AP, Nanoff C, Freissmuth M (1996) Inhibition of receptor/G protein coupling by suramin analogues. *Mol Pharmacol* 50:415-423.
- Bowser DN, Khakh BS (2007) Vesicular ATP is the predominant cause of intercellular calcium waves in astrocytes. *J Gen Physiol* 129:485-491.
- Braun N, Sevigny J, Robson SC, Enjoji K, Guckelberger O, Hammer K, Di VF, Zimmermann H (2000) Assignment of ecto-nucleoside triphosphate diphosphohydrolase-1/cd39 expression to microglia and vasculature of the brain. *Eur J Neurosci* 12:4357-4366.
- Burda JE, Sofroniew MV (2014) Reactive gliosis and the multicellular response to CNS damage and disease. *Neuron* 81:229-248.
- Coffey RJ, Jr., Leof EB, Shipley GD, Moses HL (1987) Suramin inhibition of growth factor receptor binding and mitogenicity in AKR-2B cells. *J Cell Physiol* 132:143-148.
- Crompton MR (1964) The pathogenesis of cerebral infarction following the rupture of cerebral berry aneurysms. *Brain* 87:491-510.
- Franke H, Krugel U, Schmidt R, Grosche J, Reichenbach A, Illes P (2001) P2 receptor-types involved in astrogliosis *in vivo*. *Br J Pharmacol* 134:1180-1189.
- Franke H, Verkhratsky A, Burnstock G, Illes P (2012) Pathophysiology of astroglial purinergic signalling. *Purinergic Signal* 8:629-657.
- Grossman SA, Phuphanich S, Lesser G, Rozental J, Grochow LB, Fisher J, Piantadosi S (2001) Toxicity, efficacy, and pharmacology of suramin in adults with recurrent high-grade gliomas. *J Clin Oncol* 19:3260-3266.
- Hohenegger M, Matyash M, Poussu K, Herrmann-Frank A, Sarkozi S, Lehmann-Horn F, Freissmuth M (1996) Activation of the skeletal muscle ryanodine receptor by suramin and suramin analogs. *Mol Pharmacol* 50:1443-1453.
- Illiff JJ, Wang M, Liao Y, Plogg BA, Peng W, Gundersen GA, Benveniste H, Vates GE, Deane R, Goldman SA, Nagelhus EA, Nedergaard M (2012) A paravascular pathway facilitates CSF flow through the brain parenchyma and the clearance of interstitial solutes, including amyloid β . *Sci Transl Med* 4:147ra111.

- Illiff JJ, Wang M, Zeppenfeld DM, Venkataraman A, Plog BA, Liao Y, Deane R, Nedergaard M (2013) Cerebral arterial pulsation drives paravascular CSF-interstitial fluid exchange in the murine brain. *J Neurosci* 33:18190-18199.
- Kang J, Kang N, Lovatt D, Torres A, Zhao Z, Lin J, Nedergaard M (2008) Connexin 43 hemichannels are permeable to ATP. *J Neurosci* 28:4702-4711.
- Kasseckert SA, Shahzad T, Miqdad M, Stein M, Abdallah Y, Scharbrodt W, Oertel M (2013) The mechanisms of energy crisis in human astrocytes after subarachnoid hemorrhage. *Neurosurgery* 72:468-474.
- Kimura H, Meguro T, Badr A, Zhang JH (2002) Suramin-induced reversal of chronic cerebral vasospasm in experimental subarachnoid hemorrhage. *J Neurosurg* 97:129-135.
- Koide M, Bonev AD, Nelson MT, Wellman GC (2012) Inversion of neurovascular coupling by subarachnoid blood depends on large-conductance Ca^{2+} -activated K^{+} (BK) channels. *Proc Natl Acad Sci USA* 109:E1387-E1395.
- Koles L, Leichsenring A, Rubini P, Illes P (2011) P2 receptor signaling in neurons and glial cells of the central nervous system. *Adv Pharmacol* 61:441-493.
- Macdonald RL, Weir BK, Marton LS, Zhang ZD, Sajdak M, Johns LM, Kowalczyk A, Borsody M (2001) Role of adenosine 5'-triphosphate in vasospasm after subarachnoid hemorrhage: human investigations. *Neurosurgery* 48:854-862.
- Montana V, Malarkey EB, Verderio C, Matteoli M, Parpura V (2006) Vesicular transmitter release from astrocytes. *Glia* 54:700-715.
- Murakami K, Koide M, Dumont TM, Russell SR, Tranmer BI, Wellman GC (2011) Subarachnoid hemorrhage induces gliosis and increased expression of the pro-inflammatory cytokine high mobility group box 1 protein. *Transl Stroke Res* 2:72-79.
- Pappas AC, Koide M, Wellman GC (2015) Astrocyte Ca^{2+} signaling drives inversion of neurovascular coupling after subarachnoid hemorrhage. *J Neurosci* 35:13375-13384.
- Pascual O, Ben AS, Rostaing P, Triller A, Bessis A (2012) Microglia activation triggers astrocyte-mediated modulation of excitatory neurotransmission. *Proc Natl Acad Sci USA* 109:E197-E205.
- Plog BA, Moll KM, Kang H, Illiff JJ, Dashnaw ML, Nedergaard M, Vates GE (2014) A novel technique for morphometric quantification of subarachnoid hemorrhage-induced microglia activation. *J Neurosci Methods* 229:44-52.

- Ralevic V, Burnstock G (1998) Receptors for purines and pyrimidines. *Pharmacol Rev* 50:413-492.
- Simard M, Arcuino G, Takano T, Liu QS, Nedergaard M (2003) Signaling at the gliovascular interface. *J Neurosci* 23:9254-9262.
- Straub SV, Bonev AD, Wilkerson MK, Nelson MT (2006) Dynamic inositol trisphosphate-mediated calcium signals within astrocytic endfeet underlie vasodilation of cerebral arterioles. *J Gen Physiol* 128:659-669.
- Tonazzini I, Trincavelli ML, Montali M, Martini C (2008) Regulation of A1 adenosine receptor functioning induced by P2Y₁ purinergic receptor activation in human astroglial cells. *J Neurosci Res* 86:2857-2866.
- Wink MR, Braganhol E, Tamajusuku AS, Casali EA, Karl J, Barreto-Chaves ML, Sarkis JJ, Battastini AM (2003) Extracellular adenine nucleotides metabolism in astrocyte cultures from different brain regions. *Neurochem Int* 43:621-628.
- Wink MR, Braganhol E, Tamajusuku AS, Lenz G, Zerbini LF, Libermann TA, Sevigny J, Battastini AM, Robson SC (2006) Nucleoside triphosphate diphosphohydrolase-2 (NTPDase2/CD39L1) is the dominant ectonucleotidase expressed by rat astrocytes. *Neuroscience* 138:421-432.
- Yin W, Tibbs R, Tang J, Badr A, Zhang J (2002) Haemoglobin and ATP levels in CSF from a dog model of vasospasm. *J Clin Neurosci* 9:425-428.
- Yokota M, Peterson JW, Tani E, Yamaura I (1994) The immunohistochemical distribution of protein kinase C isozymes is altered in the canine brain and basilar artery after subarachnoid hemorrhage. *Neurosci Lett* 180:171-174.
- Zhang Z, Chen G, Zhou W, Song A, Xu T, Luo Q, Wang W, Gu XS, Duan S (2007) Regulated ATP release from astrocytes through lysosome exocytosis. *Nat Cell Biol* 9:945-953.

Comprehensive Bibliography

- Abbracchio MP, Brambilla R, Ceruti S, Cattabeni F (1999) Signalling mechanisms involved in P2Y receptor-mediated reactive astrogliosis. *Prog Brain Res* 120:333-342.
- Agulhon C, Sun MY, Murphy T, Myers T, Lauderdale K, Fiacco TA (2012) Calcium signaling and gliotransmission in normal vs. reactive astrocytes. *Front Pharmacol* 3:139.
- Ahles TA, Herndon JE, Small EJ, Vogelzang NJ, Kornblith AB, Ratain MJ, Stadler W, Palchak D, Marshall ME, Wilding G, Petrylak D, Holland JC (2004) Quality of life impact of three different doses of suramin in patients with metastatic hormone-refractory prostate carcinoma: results of Intergroup O159/Cancer and Leukemia Group B 9480. *Cancer* 101:2202-8.
- Ajiboye N, Chalouhi N, Starke RM, Zanaty M, Bell R (2015) Unruptured cerebral aneurysms: evaluation and management. *Scientific World Journal* 2015:954954.
- Al-Khindi T, Macdonald RL, Schweizer TA (2010) Cognitive and functional outcome after aneurysmal subarachnoid hemorrhage. *Stroke* 41:e519-e536.
- Alkayed NJ, Birks EK, Narayanan J, Petrie KA, Kohler-Cabot AE, Harder DR (1997) Role of P-450 arachidonic acid epoxygenase in the response of cerebral blood flow to glutamate in rats. *Stroke* 28:1066-1072.
- Alkayed NJ, Narayanan J, Gebremedhin D, Medhora M, Roman RJ, Harder DR (1996) Molecular characterization of an arachidonic acid epoxygenase in rat brain astrocytes. *Stroke* 27:971-979.
- Anderson CM, Nedergaard M (2003) Astrocyte-mediated control of cerebral microcirculation. *Trends Neurosci* 26:340-344.
- Angulo MC, Kozlov AS, Charpak S, Audinat E (2004) Glutamate released from glial cells synchronizes neuronal activity in the hippocampus. *J Neurosci* 24:6920-6927.
- Araque A, Parpura V, Sanzgiri RP, Haydon PG (1999) Tripartite synapses: glia, the unacknowledged partner. *Trends Neurosci* 22:208-215.
- Attwell D, Buchan AM, Charpak S, Lauritzen M, MacVicar BA, Newman EA (2010) Glial and neuronal control of brain blood flow. *Nature* 468:232-243.

- Baeres FM, Moller M (2004) Origin of PACAP-immunoreactive nerve fibers innervating the subarachnoidal blood vessels of the rat brain. *J Cereb Blood Flow Metab* 24:628-635.
- Bai JP, Surguchev A, Navaratnam D (2011) β 4-subunit increases *Slo* responsiveness to physiological Ca^{2+} concentrations and together with β 1 reduces surface expression of *Slo* in hair cells. *Am J Physiol Cell Physiol* 300:C435-C446.
- Barragan-Iglesias P, Pineda-Farias JB, Cervantes-Duran C, Bravo-Hernandez M, Rocha-Gonzalez HI, Murbartian J, Granados-Soto V (2014) Role of spinal P2Y₆ and P2Y₁₁ receptors in neuropathic pain in rats: possible involvement of glial cells. *Mol Pain* 10:1744-8069.
- Bayliss WM (1902) On the local reactions of the arterial wall to changes of internal pressure. *J Physiol* 28:220-231.
- Begley DJ, Brightman MW (2003) Structural and functional aspects of the blood-brain barrier. *Prog Drug Res* 61:39-78.
- Beindl W, Mitterauer T, Hohenegger M, Ijzerman AP, Nanoff C, Freissmuth M (1996) Inhibition of receptor/G protein coupling by suramin analogues. *Mol Pharmacol* 50:415-423.
- Benfenati V, Amiry-Moghaddam M, Caprini M, Mylonakou MN, Rapisarda C, Ottersen OP, Ferroni S (2007) Expression and functional characterization of transient receptor potential vanilloid-related channel 4 (TRPV4) in rat cortical astrocytes. *Neuroscience* 148:876-892.
- Bennett DA, Krishnamurthi RV, Barker-Collo S, Forouzanfar MH, Naghavi M, Connor M, Lawes CM, Moran AE, Anderson LM, Roth GA, Mensah GA, Ezzati M, Murray CJ, Feigin VL (2014) The global burden of ischemic stroke: findings of the GBD 2010 study. *Glob Heart* 9:107-112.
- Bonder DE, McCarthy KD (2014) Astrocytic G_q-GPCR-linked IP₃R-dependent Ca^{2+} signaling does not mediate neurovascular coupling in mouse visual cortex *in vivo*. *J Neurosci* 34:13139-13150.
- Bowser DN, Khakh BS (2007) Vesicular ATP is the predominant cause of intercellular calcium waves in astrocytes. *J Gen Physiol* 129:485-491.
- Brambilla R, Burnstock G, Bonazzi A, Ceruti S, Cattabeni F, Abbracchio MP (1999) Cyclo-oxygenase-2 mediates P2Y receptor-induced reactive astrogliosis. *Br J Pharmacol* 126:563-567.
- Braun N, Sevigny J, Robson SC, Enyoji K, Guckelberger O, Hammer K, Di VF, Zimmermann H (2000) Assignment of ecto-nucleoside triphosphate

- diphosphohydrolase-1/cd39 expression to microglia and vasculature of the brain. *Eur J Neurosci* 12:4357-4366.
- Brayden JE, Li Y, Tavares MJ (2013) Purinergic receptors regulate myogenic tone in cerebral parenchymal arterioles. *J Cereb Blood Flow Metab* 33:293-299.
- Burda JE, Sofroniew MV (2014) Reactive gliosis and the multicellular response to CNS damage and disease. *Neuron* 81:229-248.
- Carmignoto G, Pasti L, Pozzan T (1998) On the role of voltage-dependent calcium channels in calcium signaling of astrocytes *in situ*. *J Neurosci* 18:4637-4645.
- Chen BR, Kozberg MG, Bouchard MB, Shaik MA, Hillman EM (2014) A critical role for the vascular endothelium in functional neurovascular coupling in the brain. *J Am Heart Assoc* 3:e000787.
- Chen J, Tan Z, Zeng L, Zhang X, He Y, Gao W, Wu X, Li Y, Bu B, Wang W, Duan S (2013) Heterosynaptic long-term depression mediated by ATP released from astrocytes. *Glia* 61:178-191.
- Cipolla MJ (2009) *The Cerebral Circulation*.
- Cipolla MJ, Li R, Vitullo L (2004) Perivascular innervation of penetrating brain parenchymal arterioles. *J Cardiovasc Pharmacol* 44:1-8.
- Coffey RJ, Jr., Leof EB, Shipley GD, Moses HL (1987) Suramin inhibition of growth factor receptor binding and mitogenicity in AKR-2B cells. *J Cell Physiol* 132:143-148.
- Cornell-Bell AH, Finkbeiner SM, Cooper MS, Smith SJ (1990) Glutamate induces calcium waves in cultured astrocytes: long-range glial signaling. *Science* 247:470-473.
- Cotrina ML, Lin JH, Alves-Rodrigues A, Liu S, Li J, Azmi-Ghadimi H, Kang J, Naus CC, Nedergaard M (1998) Connexins regulate calcium signaling by controlling ATP release. *Proc Natl Acad Sci U S A* 95:15735-40.
- Crompton MR (1964) The pathogenesis of cerebral infarction following the rupture of cerebral berry aneurysms. *Brain* 87:491-510.
- Dabertrand F, Hannah RM, Pearson JM, Hill-Eubanks DC, Brayden JE, Nelson MT (2013) Prostaglandin E₂, a postulated astrocyte-derived neurovascular coupling agent, constricts rather than dilates parenchymal arterioles. *J Cereb Blood Flow Metab* 33:479-482.

- Dabus G, Nogueira RG (2013) Current options for the management of aneurysmal subarachnoid hemorrhage-induced cerebral vasospasm: a comprehensive review of the literature. *Interv Neurol* 2:30-51.
- Davis J, Xu F, Deane R, Romanov G, Previti ML, Zeigler K, Zlokovic BV, Van Nostrand WE (2004) Early-onset and robust cerebral microvascular accumulation of amyloid β -protein in transgenic mice expressing low levels of a vasculotropic Dutch/Iowa mutant form of amyloid beta-protein precursor. *J Biol Chem* 279:20296-20306.
- Delekate A, Fuchtemeier M, Schumacher T, Ulbrich C, Foddis M, Petzold GC (2014) Metabotropic P2Y₁ receptor signalling mediates astrocytic hyperactivity *in vivo* in an Alzheimer's disease mouse model. *Nat Commun* 5:5422.
- Dreier JP, Major S, Manning A, Woitzik J, Drenckhahn C, Steinbrink J, Tolias C, Oliveira-Ferreira AI, Fabricius M, Hartings JA, Vajkoczy P, Lauritzen M, Dirnagl U, Bohner G, Strong AJ (2009) Cortical spreading ischaemia is a novel process involved in ischaemic damage in patients with aneurysmal subarachnoid haemorrhage. *Brain* 132:1866-1881.
- Dreier JP, Sakowitz OW, Harder A, Zimmer C, Dirnagl U, Valdueza JM, Unterberg AW (2002) Focal laminar cortical MR signal abnormalities after subarachnoid hemorrhage. *Ann Neurol* 52:825-829.
- Drury AN, Szent-Gyorgyi A (1929) The physiological activity of adenine compounds with especial reference to their action upon the mammalian heart. *J Physiol* 68:213-237.
- Duan S, Anderson CM, Keung EC, Chen Y, Chen Y, Swanson RA (2003) P2X7 receptor-mediated release of excitatory amino acids from astrocytes. *J Neurosci* 23:1320-1328.
- Dunn KM, Hill-Eubanks DC, Liedtke WB, Nelson MT (2013) TRPV4 channels stimulate Ca²⁺-induced Ca²⁺ release in astrocytic endfeet and amplify neurovascular coupling responses. *Proc Natl Acad Sci USA* 110:6157-6162.
- Faraci FM, Heistad DD (1990) Regulation of large cerebral arteries and cerebral microvascular pressure. *Circ Res* 66:8-17.
- Farkas E, Luiten PG (2001) Cerebral microvascular pathology in aging and Alzheimer's disease. *Prog Neurobiol* 64:575-611.
- Fatatis A, Russell JT (1992) Spontaneous changes in intracellular calcium concentration in type I astrocytes from rat cerebral cortex in primary culture. *Glia* 5:95-104.

- Feigin VL, Lawes CM, Bennett DA, Barker-Collo SL, Parag V (2009) Worldwide stroke incidence and early case fatality reported in 56 population-based studies: a systematic review. *Lancet Neurol* 8:355-369.
- Fiacco TA, McCarthy KD (2004) Intracellular astrocyte calcium waves *in situ* increase the frequency of spontaneous AMPA receptor currents in CA1 pyramidal neurons. *J Neurosci* 24:722-732.
- Fiacco TA, McCarthy KD (2006) Astrocyte calcium elevations: properties, propagation, and effects on brain signaling. *Glia* 54:676-690.
- Filosa JA, Bonev AD, Straub SV, Meredith AL, Wilkerson MK, Aldrich RW, Nelson MT (2006) Local potassium signaling couples neuronal activity to vasodilation in the brain. *Nat Neurosci* 9:1397-1403.
- Filosa JA, Morrison HW, Iddings JA, Du W, Kim KJ (2015) Beyond neurovascular coupling, role of astrocytes in the regulation of vascular tone. *Neuroscience*.
- Franke H, Krugel U, Schmidt R, Grosche J, Reichenbach A, Illes P (2001) P2 receptor-types involved in astrogliosis *in vivo*. *Br J Pharmacol* 134:1180-1189.
- Franke H, Verkhratsky A, Burnstock G, Illes P (2012) Pathophysiology of astroglial purinergic signalling. *Purinergic Signal* 8:629-657.
- Funato H, Yoshimura M, Yamazaki T, Saido TC, Ito Y, Yokofujita J, Okeda R, Ihara Y (1998) Astrocytes containing amyloid β -protein (A β)-positive granules are associated with A β 40-positive diffuse plaques in the aged human brain. *Am J Pathol* 152:983-992.
- Gebremedhin D, Ma YH, Falck JR, Roman RJ, VanRollins M, Harder DR (1992) Mechanism of action of cerebral epoxyeicosatrienoic acids on cerebral arterial smooth muscle. *Am J Physiol* 263:H519-H525.
- Gillespie JH (1934) The biological significance of the linkages in adenosine triphosphoric acid. *J Physiol* 80:345-359.
- Girouard H, Bonev AD, Hannah RM, Meredith A, Aldrich RW, Nelson MT (2010) Astrocytic endfoot Ca²⁺ and BK channels determine both arteriolar dilation and constriction. *Proc Natl Acad Sci USA* 107:3811-3816.
- Grossman SA, Phuphanich S, Lesser G, Rozental J, Grochow LB, Fisher J, Piantadosi S (2001) Toxicity, efficacy, and pharmacology of suramin in adults with recurrent high-grade gliomas. *J Clin Oncol* 19:3260-3266.
- Hamel E (2006) Perivascular nerves and the regulation of cerebrovascular tone. *J Appl Physiol* (1985) 100:1059-1064.

- Harder DR, Gebremedhin D, Narayanan J, Jefcoat C, Falck JR, Campbell WB, Roman R (1994) Formation and action of a P-450 4A metabolite of arachidonic acid in cat cerebral microvessels. *Am J Physiol* 266:H2098-H2107.
- Hayat MA (1981) Fixation for electron microscopy. New York, New York: Academic Press, Inc.
- Haydon PG, Carmignoto G (2006) Astrocyte control of synaptic transmission and neurovascular coupling. *Physiol Rev* 86:1009-1031.
- Heilbrun MP, Olesen J, Lassen NA (1972) Regional cerebral blood flow studies in subarachnoid hemorrhage. *J Neurosurg* 37:36-44.
- Heneka MT, Sastre M, Dumitrescu-Ozimek L, Dewachter I, Walter J, Klockgether T, Van LF (2005) Focal glial activation coincides with increased BACE1 activation and precedes amyloid plaque deposition in APP[V717I] transgenic mice. *J Neuroinflammation* 2:22.
- Henneberger C, Papouin T, Oliet SH, Rusakov DA (2010) Long-term potentiation depends on release of D-serine from astrocytes. *Nature* 463:232-236.
- Heppner TJ, Bonev AD, Nelson MT (2005) Elementary purinergic Ca^{2+} transients evoked by nerve stimulation in rat urinary bladder smooth muscle. *J Physiol* 564:201-12.
- Hijdra A, van GJ, Stefanko S, Van Dongen KJ, Vermeulen M, Van CH (1986) Delayed cerebral ischemia after aneurysmal subarachnoid hemorrhage: clinicoanatomic correlations. *Neurology* 36:329-333.
- Hirst WD, Young KA, Newton R, Allport VC, Marriott DR, Wilkin GP (1999) Expression of COX-2 by normal and reactive astrocytes in the adult rat central nervous system. *Mol Cell Neurosci* 13:57-68.
- Hohenegger M, Matyash M, Poussu K, Herrmann-Frank A, Sarkozi S, Lehmann-Horn F, Freissmuth M (1996) Activation of the skeletal muscle ryanodine receptor by suramin and suramin analogs. *Mol Pharmacol* 50:1443-1453.
- Horrigan FT, Aldrich RW (2002) Coupling between voltage sensor activation, Ca^{2+} binding and channel opening in large conductance (BK) potassium channels. *J Gen Physiol* 120:267-305.
- Iadecola C (1993) Regulation of the cerebral microcirculation during neural activity: is nitric oxide the missing link? *Trends Neurosci* 16:206-214.
- Iloff JJ, Wang M, Liao Y, Plogg BA, Peng W, Gundersen GA, Benveniste H, Vates GE, Deane R, Goldman SA, Nagelhus EA, Nedergaard M (2012) A paravascular

pathway facilitates CSF flow through the brain parenchyma and the clearance of interstitial solutes, including amyloid β . *Sci Transl Med* 4:147ra111.

Iloff JJ, Wang M, Zeppenfeld DM, Venkataraman A, Plog BA, Liao Y, Deane R, Nedergaard M (2013) Cerebral arterial pulsation drives paravascular CSF-interstitial fluid exchange in the murine brain. *J Neurosci* 33:18190-18199.

Illes P, Alexandre RJ (2004) Molecular physiology of P2 receptors in the central nervous system. *Eur J Pharmacol* 483:5-17.

Ishiguro M, Puryear CB, Bisson E, Saundry CM, Nathan DJ, Russell SR, Tranmer BI, Wellman GC (2002) Enhanced myogenic tone in cerebral arteries from a rabbit model of subarachnoid hemorrhage. *Am J Physiol Heart Circ Physiol* 283:H2217-H2225.

Ishiguro M, Wellman TL, Honda A, Russell SR, Tranmer BI, Wellman GC (2005) Emergence of a R-type Ca^{2+} channel ($\text{Cav} 2.3$) contributes to cerebral artery constriction after subarachnoid hemorrhage. *Circ Res* 96:419-426.

Ishiguro M, Morielli AD, Zvarova K, Tranmer BI, Penar PL, Wellman GC (2006) Oxyhemoglobin-induced suppression of voltage-dependent K^+ channels in cerebral arteries by enhanced tyrosine kinase activity. *Circ Res* 99:1252-1260.

Jakubowski J, Kendall B (1978) Coincidental aneurysms with tumours of pituitary origin. *J Neurol Neurosurg Psychiatry* 41:972-979.

James G, Butt AM (2002) P2Y and P2X purinoceptor mediated Ca^{2+} signalling in glial cell pathology in the central nervous system. *Eur J Pharmacol* 447:247-60.

Kang J, Kang N, Lovatt D, Torres A, Zhao Z, Lin J, Nedergaard M (2008) Connexin 43 hemichannels are permeable to ATP. *J Neurosci* 28:4702-4711.

Kasseckert SA, Shahzad T, Miqdad M, Stein M, Abdallah Y, Scharbrodt W, Oertel M (2013) The mechanisms of energy crisis in human astrocytes after subarachnoid hemorrhage. *Neurosurgery* 72:468-474.

Kawamura M, Gachet C, Inoue K, Kato F (2004) Direct excitation of inhibitory interneurons by extracellular ATP mediated by P2Y₁ receptors in the hippocampal slice. *J Neurosci* 24:10835-45.

Kawamura M, Kawamura M (2011) Long-term facilitation of spontaneous calcium oscillations in astrocytes with endogenous adenosine in hippocampal slice cultures. *Cell Calcium* 49:249-258.

- Kim B, Jeong HK, Kim JH, Lee SY, Jou I, Joe EH (2011) Uridine 5'-diphosphate induces chemokine expression in microglia and astrocytes through activation of the P2Y₆ receptor. *J Immunol* 2011 186:3701-9.
- Kim KJ, Iddings JA, Stern JE, Blanco VM, Croom D, Kirov SA, Filosa JA (2015) Astrocyte contributions to flow/pressure-evoked parenchymal arteriole vasoconstriction. *J Neurosci* 35:8245-8257.
- Kimura H, Meguro T, Badr A, Zhang JH (2002) Suramin-induced reversal of chronic cerebral vasospasm in experimental subarachnoid hemorrhage. *J Neurosurg* 97:129-135.
- Kirischuk S, Moller T, Voitenko N, Kettenmann H, Verkhratsky A (1995) ATP-induced cytoplasmic calcium mobilization in Bergmann glial cells. *J Neurosci* 15:7861-7871.
- Knot HJ, Zimmermann PA, Nelson MT (1996) Extracellular K⁺-induced hyperpolarizations and dilatations of rat coronary and cerebral arteries involve inward rectifier K⁺ channels. *J Physiol* 492 (Pt 2):419-430.
- Knot HJ, Nelson MT (1998) Regulation of arterial diameter and wall [Ca²⁺] in cerebral arteries of rat by membrane potential and intravascular pressure. *J Physiol* 508 (Pt 1):199-209.
- Koehler RC, Roman RJ, Harder DR (2009) Astrocytes and the regulation of cerebral blood flow. *Trends Neurosci* 32:160-169.
- Koide M, Bonev AD, Nelson MT, Wellman GC (2012) Inversion of neurovascular coupling by subarachnoid blood depends on large-conductance Ca²⁺-activated K⁺ (BK) channels. *Proc Natl Acad Sci USA* 109:E1387-E1395.
- Koide M, Penar PL, Tranmer BI, Wellman GC (2007) Heparin-binding EGF-like growth factor mediates oxyhemoglobin-induced suppression of voltage-dependent potassium channels in rabbit cerebral artery myocytes. *Am J Physiol Heart Circ Physiol* 293:H1750-H1759.
- Koide M, Wellman GC (2013) SAH-induced suppression of voltage-gated K⁺ (K_v) channel currents in parenchymal arteriolar myocytes involves activation of the HB-EGF/EGFR pathway. *Acta Neurochir Suppl* 115:179-184.
- Koide M, Sukhotinsky I, Ayata C, Wellman GC (2013) Subarachnoid hemorrhage, spreading depolarizations and impaired neurovascular coupling. *Stroke Res Treat* 2013:819340.
- Koide M, Wellman GC (2015) Activation of TRPV4 channels does not mediate inversion of neurovascular coupling after SAH. *Acta Neurochir Suppl* 120:111-116.

- Koles L, Leichsenring A, Rubini P, Illes P (2011) P2 receptor signaling in neurons and glial cells of the central nervous system. *Adv Pharmacol* 61:441-493.
- Konno Y, Sato T, Suzuki K, Matsumoto M, Sasaki T, Kodama N (2001) Sequential changes of oxyhemoglobin in drained fluid of cisternal irrigation therapy--reference to the effect of ascorbic acid. *Acta Neurochir Suppl* 77:167-9.:167-9.
- Krimer LS, Muly EC, III, Williams GV, Goldman-Rakic PS (1998) Dopaminergic regulation of cerebral cortical microcirculation. *Nat Neurosci* 1:286-289.
- Krishnamurthi RV, Moran AE, Forouzanfar MH, Bennett DA, Mensah GA, Lawes CM, Barker-Collo S, Connor M, Roth GA, Sacco R, Ezzati M, Naghavi M, Murray CJ, Feigin VL (2014) The global burden of hemorrhagic stroke: a summary of findings from the GBD 2010 study. *Glob Heart* 9:101-106.
- Latour I, Hamid J, Beedle AM, Zamponi GW, MacVicar BA (2003) Expression of voltage-gated Ca²⁺ channel subtypes in cultured astrocytes. *Glia* 41:347-353.
- Li Y, Baylie RL, Tavares MJ, Brayden JE (2014) TRPM4 channels couple purinergic receptor mechanoactivation and myogenic tone development in cerebral parenchymal arterioles. *J Cereb Blood Flow Metab* 34:1706-1714.
- Link TE, Murakami K, Beem-Miller M, Tranmer BI, Wellman GC (2008) Oxyhemoglobin-induced expression of R-type Ca²⁺ channels in cerebral arteries. *Stroke* 39:2122-2128.
- Longden TA, Nelson MT (2015) Vascular inward rectifier K⁺ channels as external K⁺ sensors in the control of cerebral blood flow. *Microcirculation* 22:183-196.
- Macdonald RL, Higashida RT, Keller E, Mayer SA, Molyneux A, Raabe A, Vajkoczy P, Wanke I, Bach D, Frey A, Marr A, Roux S, Kassell N (2011) Clazosentan, an endothelin receptor antagonist, in patients with aneurysmal subarachnoid haemorrhage undergoing surgical clipping: a randomised, double-blind, placebo-controlled phase 3 trial (CONSCIOUS-2). *Lancet Neurol* 10:618-625.
- Macdonald RL, Higashida RT, Keller E, Mayer SA, Molyneux A, Raabe A, Vajkoczy P, Wanke I, Bach D, Frey A, Nowbakht P, Roux S, Kassell N (2012) Randomized trial of clazosentan in patients with aneurysmal subarachnoid hemorrhage undergoing endovascular coiling. *Stroke* 43:1463-1469.
- Macdonald RL, Weir BK, Marton LS, Zhang ZD, Sajdak M, Johns LM, Kowalczyk A, Borsody M (2001) Role of adenosine 5'-triphosphate in vasospasm after subarachnoid hemorrhage: human investigations. *Neurosurgery* 48:854-862.
- MacVicar BA (1984) Voltage-dependent calcium channels in glial cells. *Science* 226:1345-1347.

- MacVicar BA, Hochman D, Delay MJ, Weiss S (1991) Modulation of intracellular Ca^{2+} in cultured astrocytes by influx through voltage-activated Ca^{2+} channels. *Glia* 4:448-455.
- Maravall M, Mainen ZF, Sabatini BL, Svoboda K (2000) Estimating intracellular calcium concentrations and buffering without wavelength ratioing. *Biophys J* 78:2655-2667.
- Mathiisen TM, Lehre KP, Danbolt NC, Ottersen OP (2010) The perivascular astroglial sheath provides a complete covering of the brain microvessels: an electron microscopic 3D reconstruction. *Glia* 58:1094-1103.
- McCaslin AF, Chen BR, Radosevich AJ, Cauli B, Hillman EM (2011) *In vivo* 3D morphology of astrocyte-vasculature interactions in the somatosensory cortex: implications for neurovascular coupling. *J Cereb Blood Flow Metab* 31:795-806.
- Michel MC, Seifert R (2015) Selectivity of pharmacological tools: implications for use in cell physiology. A review in the theme: Cell signaling: proteins, pathways and mechanisms. *Am J Physiol Cell Physiol* 308:C505-C520.
- Miseta A, Bogner P, Berenyi E, Kellermayer M, Galambos C, Wheatley DN, Cameron IL (1993) Relationship between cellular ATP, potassium, sodium and magnesium concentrations in mammalian and avian erythrocytes. *Biochim Biophys Acta* 1175:133-9.
- Mocco J, Komotar RJ, Lavine SD, Meyers PM, Connolly ES, Solomon RA (2004) The natural history of unruptured intracranial aneurysms. *Neurosurg Focus* 17:E3.
- Montana V, Malarkey EB, Verderio C, Matteoli M, Parpura V (2006) Vesicular transmitter release from astrocytes. *Glia* 54:700-715.
- Mulligan SJ, MacVicar BA (2004) Calcium transients in astrocyte endfeet cause cerebrovascular constrictions. *Nature* 431:195-199.
- Murakami K, Koide M, Dumont TM, Russell SR, Tranmer BI, Wellman GC (2011) Subarachnoid Hemorrhage Induces Gliosis and Increased Expression of the Pro-inflammatory Cytokine High Mobility Group Box 1 Protein. *Transl Stroke Res* 2:72-79.
- Nagelhus EA, Horio Y, Inanobe A, Fujita A, Haug FM, Nielsen S, Kurachi Y, Ottersen OP (1999) Immunogold evidence suggests that coupling of K^+ siphoning and water transport in rat retinal Muller cells is mediated by a coenrichment of Kir4.1 and AQP4 in specific membrane domains. *Glia* 26:47-54.
- Navarrete M, Araque A (2014) The Cajal school and the physiological role of astrocytes: a way of thinking. *Front Neuroanat* 8:33.

- Navarrete M, Perea G, Fernandez de SD, Gomez-Gonzalo M, Nunez A, Martin ED, Araque A (2012) Astrocytes mediate *in vivo* cholinergic-induced synaptic plasticity. *PLoS Biol* 10:e1001259.
- Navarrete M, Perea G, Maglio L, Pastor J, Garcia de SR, Araque A (2013) Astrocyte calcium signal and gliotransmission in human brain tissue. *Cereb Cortex* 23:1240-1246.
- Naviaux JC, Schuchbauer MA, Li K, Wang L, Risbrough VB, Powell SB, Naviaux RK (2014) Reversal of autism-like behaviors and metabolism in adult mice with single-dose antipurinergic therapy. *Transl Psychiatry* 4:400.
- Neary JT, Rathbone MP, Cattabeni F, Abbracchio MP, Burnstock G (1996) Trophic actions of extracellular nucleotides and nucleosides on glial and neuronal cells. *Trends Neurosci* 19:13-18.
- Nedergaard M (1994) Direct signaling from astrocytes to neurons in cultures of mammalian brain cells. *Science* 263:1768-1771.
- Nett WJ, Oloff SH, McCarthy KD (2002) Hippocampal astrocytes *in situ* exhibit calcium oscillations that occur independent of neuronal activity. *J Neurophysiol* 87:528-537.
- Neuberger A, Meltzer E, Leshem E, Dickstein Y, Stienlauf S, Schwartz E (2014) The changing epidemiology of human African trypanosomiasis among patients from nonendemic countries--1902-2012. *PLoS One* 9:e88647.
- Newman EA (1984) Regional specialization of retinal glial cell membrane. *Nature* 309:155-157.
- Newman EA (1986) High potassium conductance in astrocyte endfeet. *Science* 233:453-454.
- Newman EA, Zahs KR (1997) Calcium waves in retinal glial cells. *Science* 275:844-847.
- Nishimura N, Rosidi NL, Iadecola C, Schaffer CB (2010) Limitations of collateral flow after occlusion of a single cortical penetrating arteriole. *J Cereb Blood Flow Metab* 30:1914-1927.
- Nishimura N, Schaffer CB, Friedman B, Lyden PD, Kleinfeld D (2007) Penetrating arterioles are a bottleneck in the perfusion of neocortex. *Proc Natl Acad Sci USA* 104:365-370.
- Nizar K, et al. (2013) *In vivo* stimulus-induced vasodilation occurs without IP3 receptor activation and may precede astrocytic calcium increase. *J Neurosci* 33:8411-8422.

- Nystoriak MA, O'Connor KP, Sonkusare SK, Brayden JE, Nelson MT, Wellman GC (2011) Fundamental increase in pressure-dependent constriction of brain parenchymal arterioles from subarachnoid hemorrhage model rats due to membrane depolarization. *Am J Physiol Heart Circ Physiol* 300:H803-H812.
- Ostergaard L, Aamand R, Karabegovic S, Tietze A, Blicher JU, Mikkelsen IK, Iversen NK, Secher N, Engedal TS, Anzabi M, Jimenez EG, Cai C, Koch KU, Naess-Schmidt ET, Obel A, Juul N, Rasmussen M, Sorensen JC (2013) The role of the microcirculation in delayed cerebral ischemia and chronic degenerative changes after subarachnoid hemorrhage. *J Cereb Blood Flow Metab* 33:1825-1837.
- Pannicke T, Fischer W, Biedermann B, Schadlich H, Grosche J, Faude F, Wiedemann P, Allgaier C, Illes P, Burnstock G, Reichenbach A (2000) P2X7 receptors in Muller glial cells from the human retina. *J Neurosci* 20:5965-5972.
- Pappas AC, Koide M, Wellman GC (2015) Astrocyte Ca^{2+} signaling drives inversion of neurovascular coupling after subarachnoid hemorrhage. *J Neurosci* 35:13375-13384.
- Park IS, Meno JR, Witt CE, Chowdhary A, Nguyen TS, Winn HR, Ngai AC, Britz GW (2009) Impairment of intracerebral arteriole dilation responses after subarachnoid hemorrhage. Laboratory investigation. *J Neurosurg* 111:1008-1013.
- Parri HR, Crunelli V (2003) The role of Ca^{2+} in the generation of spontaneous astrocytic Ca^{2+} oscillations. *Neuroscience* 120:979-992.
- Parri HR, Gould TM, Crunelli V (2001) Spontaneous astrocytic Ca^{2+} oscillations *in situ* drive NMDAR-mediated neuronal excitation. *Nat Neurosci* 4:803-812.
- Pascual O, Ben AS, Rostaing P, Triller A, Bessis A (2012) Microglia activation triggers astrocyte-mediated modulation of excitatory neurotransmission. *Proc Natl Acad Sci USA* 109:E197-E205.
- Passier PE, Visser-Meily JM, Rinkel GJ, Lindeman E, Post MW (2013) Determinants of health-related quality of life after aneurysmal subarachnoid hemorrhage: a systematic review. *Qual Life Res* 22:1027-1043.
- Paulson OB, Newman EA (1987) Does the release of potassium from astrocyte endfeet regulate cerebral blood flow? *Science* 237:896-898.
- Perea G, Araque A (2007) Astrocytes potentiate transmitter release at single hippocampal synapses. *Science* 317:1083-1086.
- Peters DG, Kassam AB, Feingold E, Heidrich-O'Hare E, Yonas H, Ferrell RE, Brufsky A (2001) Molecular anatomy of an intracranial aneurysm: coordinated expression of genes involved in wound healing and tissue remodeling. *Stroke* 32:1036-1042.

- Plog BA, Moll KM, Kang H, Iliff JJ, Dashnaw ML, Nedergaard M, Vates GE (2014) A novel technique for morphometric quantification of subarachnoid hemorrhage-induced microglia activation. *J Neurosci Methods* 229:44-52.
- Pluta RM, Afshar JK, Boock RJ, Oldfield EH (1998) Temporal changes in perivascular concentrations of oxyhemoglobin, deoxyhemoglobin, and methemoglobin after subarachnoid hemorrhage. *J Neurosurg* 88:557-61.
- Pluta RM, Hansen-Schwartz J, Dreier J, Vajkoczy P, Macdonald RL, Nishizawa S, Kasuya H, Wellman G, Keller E, Zauner A, Dorsch N, Clark J, Ono S, Kiris T, Leroux P, Zhang JH (2009) Cerebral vasospasm following subarachnoid hemorrhage: time for a new world of thought. *Neurol Res* 31:151-158.
- Porter JT, McCarthy KD (1996) Hippocampal astrocytes *in situ* respond to glutamate released from synaptic terminals. *J Neurosci* 16:5073-5081.
- Price DL, Ludwig JW, Mi H, Schwarz TL, Ellisman MH (2002) Distribution of *rSlo* Ca²⁺-activated K⁺ channels in rat astrocyte perivascular endfeet. *Brain Res* 956:183-193.
- Rabinstein AA, Weigand S, Atkinson JL, Wijdicks EF (2005) Patterns of cerebral infarction in aneurysmal subarachnoid hemorrhage. *Stroke* 36:992-997.
- Ralevic V, Burnstock G (1998) Receptors for purines and pyrimidines. *Pharmacol Rev* 50:413-492.
- Reinhard JF, Jr., Liebmann JE, Schlosberg AJ, Moskowitz MA (1979) Serotonin neurons project to small blood vessels in the brain. *Science* 206:85-87.
- Roy CS, Sherrington CS (1890) On the regulation of the blood-supply of the brain. *J Physiol* 11:85-158.
- Santello M, Bezzi P, Volterra A (2011) TNF α controls glutamatergic gliotransmission in the hippocampal dentate gyrus. *Neuron* 69:988-1001.
- Seidel KN, Derst C, Salzmann M, Holtje M, Priller J, Markgraf R, Heinemann SH, Heilmann H, Skatchkov SN, Eaton MJ, Veh RW, Pruss H (2011) Expression of the voltage- and Ca²⁺-dependent BK potassium channel subunits BK β 1 and BK β 4 in rodent astrocytes. *Glia* 59:893-902.
- Shao Y, McCarthy KD (1995) Receptor-mediated calcium signals in astroglia: multiple receptors, common stores and all-or-nothing responses. *Cell Calcium* 17:187-196.
- Shelton MK, McCarthy KD (1999) Mature hippocampal astrocytes exhibit functional metabotropic and ionotropic glutamate receptors *in situ*. *Glia* 26:1-11.

- Shelton MK, McCarthy KD (2000) Hippocampal astrocytes exhibit Ca²⁺-elevating muscarinic cholinergic and histaminergic receptors *in situ*. *J Neurochem* 74:555-563.
- Shigetomi E, Bushong EA, Hausteiner MD, Tong X, Jackson-Weaver O, Kracun S, Xu J, Sofroniew MV, Ellisman MH, Khakh BS (2013) Imaging calcium microdomains within entire astrocyte territories and endfeet with GCaMPs expressed using adeno-associated viruses. *J Gen Physiol* 141:633-647.
- Shirakawa H, Sakimoto S, Nakao K, Sugishita A, Konno M, Iida S, Kusano A, Hashimoto E, Nakagawa T, Kaneko S (2010) Transient receptor potential canonical 3 (TRPC3) mediates thrombin-induced astrocyte activation and upregulates its own expression in cortical astrocytes. *J Neurosci* 30:13116-13129.
- Simard M, Arcuino G, Takano T, Liu QS, Nedergaard M (2003) Signaling at the gliovascular interface. *J Neurosci* 23:9254-9262.
- Sofroniew MV (2009) Molecular dissection of reactive astrogliosis and glial scar formation. *Trends Neurosci* 32:638-647.
- Solomon RA, Antunes JL, Chen RY, Bland L, Chien S (1985) Decrease in cerebral blood flow in rats after experimental subarachnoid hemorrhage: a new animal model. *Stroke* 16:58-64.
- Srinivasan R, Huang BS, Venugopal S, Johnston AD, Chai H, Zeng H, Golshani P, Khakh BS (2015) Ca²⁺ signaling in astrocytes from IP₃R2^{-/-} mice in brain slices and during startle responses *in vivo*. *Nat Neurosci* 18:708-717.
- Straub SV, Bonev AD, Wilkerson MK, Nelson MT (2006) Dynamic inositol trisphosphate-mediated calcium signals within astrocytic endfeet underlie vasodilation of cerebral arterioles. *J Gen Physiol* 128:659-669.
- Straub SV, Nelson MT (2007) Astrocytic calcium signaling: the information currency coupling neuronal activity to the cerebral microcirculation. *Trends Cardiovasc Med* 17:183-190.
- Sun MY, Devaraju P, Xie AX, Holman I, Samones E, Murphy TR, Fiocco TA (2014) Astrocyte calcium microdomains are inhibited by bafilomycin A1 and cannot be replicated by low-level Schaffer collateral stimulation *in situ*. *Cell Calcium* 55:1-16.
- Takano T, Han X, Deane R, Zlokovic B, Nedergaard M (2007) Two-photon imaging of astrocytic Ca²⁺ signaling and the microvasculature in experimental mice models of Alzheimer's disease. *Ann N Y Acad Sci* 1097:40-50.

- Takano T, Tian GF, Peng W, Lou N, Libionka W, Han X, Nedergaard M (2006) Astrocyte-mediated control of cerebral blood flow. *Nat Neurosci* 9:260-267.
- Terpolilli NA, Brem C, Buhler D, Plesnila N. Are We Barking Up the Wrong Vessels? Cerebral Microcirculation After Subarachnoid Hemorrhage. *Stroke* 2015 46:3014-9.
- Tian GF, Azmi H, Takano T, Xu Q, Peng W, Lin J, Oberheim N, Lou N, Wang X, Zielke HR, Kang J, Nedergaard M (2005) An astrocytic basis of epilepsy. *Nat Med* 11:973-981.
- Tonazzini I, Trincavelli ML, Montali M, Martini C (2008) Regulation of A1 adenosine receptor functioning induced by P2Y₁ purinergic receptor activation in human astroglial cells. *J Neurosci Res* 86:2857-2866.
- Trachtenberg MC, Pollen DA (1970) Neuroglia: biophysical properties and physiologic function. *Science* 167:1248-1252.
- Unsworth CD, Johnson RG (1990) Acetylcholine and ATP are coreleased from the electromotor nerve terminals of *Narcine brasiliensis* by an exocytotic mechanism. *Proc Natl Acad Sci U S A* 87:553-7.
- Vander Eecken HM, Adams RD (1953) The anatomy and functional significance of the meningeal arterial anastomoses of the human brain. *J Neuropathol Exp Neurol* 12:132-157.
- Vatter H, Weidauer S, Konczalla J, Dettmann E, Zimmermann M, Raabe A, Preibisch C, Zanella FE, Seifert V (2006) Time course in the development of cerebral vasospasm after experimental subarachnoid hemorrhage: clinical and neuroradiological assessment of the rat double hemorrhage model. *Neurosurgery* 58:1190-1197.
- Vaucher E, Hamel E (1995) Cholinergic basal forebrain neurons project to cortical microvessels in the rat: electron microscopic study with anterogradely transported *Phaseolus vulgaris* leucoagglutinin and choline acetyltransferase immunocytochemistry. *J Neurosci* 15:7427-7441.
- Vergouwen MD, Ilodigwe D, Macdonald RL. Cerebral infarction after subarachnoid hemorrhage contributes to poor outcome by vasospasm-dependent and -independent effects. *Stroke* 2011 42:924-9.
- Verkhratsky A, Orkand RK, Kettenmann H (1998) Glial calcium: homeostasis and signaling function. *Physiol Rev* 78:99-141.

- Weidauer S, Vatter H, Beck J, Raabe A, Lanfermann H, Seifert V, Zanella F (2008) Focal laminar cortical infarcts following aneurysmal subarachnoid haemorrhage. *Neuroradiology* 50:1-8.
- Weir B, Grace M, Hansen J, Rothberg C (1978) Time course of vasospasm in man. *J Neurosurg* 48:173-178.
- Wellman GC (2006) Ion channels and calcium signaling in cerebral arteries following subarachnoid hemorrhage. *Neurol Res* 28:690-702.
- Wetherington J, Serrano G, Dingledine R (2008) Astrocytes in the epileptic brain. *Neuron* 58:168-178.
- Wink MR, Braganhol E, Tamajusuku AS, Casali EA, Karl J, Barreto-Chaves ML, Sarkis JJ, Battastini AM (2003) Extracellular adenine nucleotides metabolism in astrocyte cultures from different brain regions. *Neurochem Int* 43:621-628.
- Wink MR, Braganhol E, Tamajusuku AS, Lenz G, Zerbini LF, Libermann TA, Sevigny J, Battastini AM, Robson SC (2006) Nucleoside triphosphate diphosphohydrolase-2 (NTPDase2/CD39L1) is the dominant ectonucleotidase expressed by rat astrocytes. *Neuroscience* 138:421-432.
- Winship IR, Plaa N, Murphy TH (2007) Rapid astrocyte calcium signals correlate with neuronal activity and onset of the hemodynamic response *in vivo*. *J Neurosci* 27:6268-6272.
- Wyss-Coray T, Loike JD, Brionne TC, Lu E, Anankov R, Yan F, Silverstein SC, Husemann J (2003) Adult mouse astrocytes degrade amyloid- β *in vitro* and *in situ*. *Nat Med* 9:453-457.
- Xie L, Kang H, Xu Q, Chen MJ, Liao Y, Thiyagarajan M, O'Donnell J, Christensen DJ, Nicholson C, Iliff JJ, Takano T, Deane R, Nedergaard M (2013) Sleep drives metabolite clearance from the adult brain. *Science* 342:373-377.
- Yin W, Tibbs R, Tang J, Badr A, Zhang J (2002) Haemoglobin and ATP levels in CSF from a dog model of vasospasm. *J Clin Neurosci* 9:425-428.
- Yokota M, Peterson JW, Tani E, Yamaura I (1994) The immunohistochemical distribution of protein kinase C isozymes is altered in the canine brain and basilar artery after subarachnoid hemorrhage. *Neurosci Lett* 180:171-174.
- Zaritsky JJ, Eckman DM, Wellman GC, Nelson MT, Schwarz TL (2000) Targeted disruption of Kir2.1 and Kir2.2 genes reveals the essential role of the inwardly rectifying K⁺ current in K⁺-mediated vasodilation. *Circ Res* 87:160-166.

- Zhang Z, Chen G, Zhou W, Song A, Xu T, Luo Q, Wang W, Gu XS, Duan S (2007) Regulated ATP release from astrocytes through lysosome exocytosis. *Nat Cell Biol* 9:945-953.
- Zhou Q, Petersen CC, Nicoll RA (2000) Effects of reduced vesicular filling on synaptic transmission in rat hippocampal neurones. *J Physiol* 525 Pt 1:195-206.
- Zingesser LH, Schechter MM, Dexter J, Katzman R, Scheinberg LC (1968) On the significance of spasm associated with rupture of a cerebral aneurysm. The relationship between spasm as noted angiographically and regional blood flow determinations. *Arch Neurol* 18:520-528.
- Zonta M, Angulo MC, Gobbo S, Rosengarten B, Hossmann KA, Pozzan T, Carmignoto G (2003a) Neuron-to-astrocyte signaling is central to the dynamic control of brain microcirculation. *Nat Neurosci* 6:43-50.
- Zonta M, Sebelin A, Gobbo S, Fellin T, Pozzan T, Carmignoto G (2003b) Glutamate-mediated cytosolic calcium oscillations regulate a pulsatile prostaglandin release from cultured rat astrocytes. *J Physiol* 553:407-414.